ACID LEACHING OF STANNITES

by

HAKURU BADDALAGE MALIYASENA B.Sc. (Cey)

A thesis submitted for the degree of Doctor of Philosophy of the University of London

August, 1975

To Thatha

ABSTRACT

Four forms of stannite were prepared. Cubic stannite and α - and β -stannites (both tetragonal) were obtained as thermal transformation products of the primary substance normal stannite, $Cu_{2.07}Fe_{1.02}SnS_{3.99}$, which was synthesised from the elements. The phase changes were established by high temperature X-ray diffraction and by quenching experiments.

A crystal structure for cubic stannite is proposed and the manner in which it may be derived from that of normal stannite is discussed.

Samples of all the four forms were leached in acidic ferric chloride solutions in the temperature range 65°C to 95°C. The effect of temperature, Fe^{+3} concentration; particle size, stirring speed and sample weight on the rate of leaching of normal stannite was studied. Normal stannite and α -stannite were also leached in acidic hydrogen peroxide.

The solid leach residues have been examined by X-ray diffraction, electron probe microanalysis, optical and scanning electron microscopy.

No phase change or structural change were noticed during leaching.

The rate determining step was found to be a surface reaction between the ferric ions adsorbed on the surface and the mineral.

All the four forms of stannite leached according to the same mechanism.

CONTENTS

ABSTRACT 3

INTRODUCTION 7

SECTION 1- LITERATURE SURVEY

1.1 Leaching of Copper Sulphides 10

1.1.1 Leaching of Covellite 10

1.1.2 Leaching of Chalcocite 14

1.1.3 Leaching of Chalcopyrite 18

1.1.4 Leaching of Bornite 28

1.2 Solid State Diffusion in Sulphides 38

1.3 Previous Work on the Leaching of Stannite 47

1.4 Structures of Stannite 58

1.5 Phase Relations 80

1.5.1 Stannite series of Minerals 80

1.5.2 The System Fe - Sn - S 90

1.5.3 The System Cu - Sn - S 92

1.5.4 Some Binary Systems 94

1.6 Previous Work on the Synthesis of Stannite 97

SECTION 2- EXPERIMENTAL PROCEDURES

2.1 Synthesis of Normal Stannite 100

2.2 Leaching Apparatus and Experimental Procedure 107

2.3 Analysis of Solutions 111

2.4 Analysis of Solids

2.4.1 Atomic Absorption Spectrophotometry 114

2.4.2 Microscopic Analysis 115

2.4.3 Electron Probe Microanalysis 116

2.4.4 X-Ray Diffraction

2.4.4.1 Guinier-DeWolf Camera 117

2.4.4.2 High Temperature Camera 120

2.4.4.3 Diffractometer Techniques 122

2.5 Purity of Materials 126

SECTION 3- THERMAL TRANSFORMATIONS OF STANNITES -RESULTS AND DISCUSSION

3.1 Normal Stannite 130

3.2 Cubic Stannite 136

3.3 α- and β- Stannites 145

SECTION 4- LEACHING OF NORMAL STANNITE - RESULTS AND DISCUSSION

4.1 Ferric Chloride Leaching - General 153

4.1.1 Effect of Temperature 161

4.1.2 Effect of Particle Size 167

4.1.3 Effect of Ferric Ion Concentration 171

4.1.4 Effect of Sample Weight 174

4.1.5 Effect of Stirring Speed 176

4.2 Hydrogen Peroxide Leaching 178

4.3 Analysis of Leach Residues

4.3.1 Atomic Absorption Spectrophotometry and Electron Probe Microanalysis 182

4.3.2 X-Ray Diffraction 184

4.4 Optical and Scanning Electron Microscopy 195

4.5 Hydrochloric Acid Leaching 204

SECTION 5- LEACHING OF CUBIC STANNITE, α - AND β -STANNITES - RESULTS AND DISCUSSION

5.1 Ferric Chloride Leaching 209

5.2 Effect of Storage Time on Leaching 211

5.3 Hydrogen Peroxide Leaching 213

5.4 X-Ray Diffraction of Leach Residues 216

SECTION 6- GENERAL DISCUSSION 219

SECTION 7- CONCLUSIONS

7.1 Summary of Results 228

7.2 Comparison with Previous Work 230

APPENDIX A AN ATTEMPT TO USE ELECTRON MICROSCOPY TO STUDY THE LEACHING OF COPPER SULPHIDES 232

APPENDIX B KINETIC RESULTS 234

APPENDIX C X-RAY DIFFRACTION DATA 258

ACKNOWLEDGEMENTS 262

REFERENCES 263

INTRODUCTION

A sizeable proportion of present day copper supplies comes from the leaching of copper sulphide ores which mostly contain chalcopyrite, bornite and covellite. Understandably a great effort is being made to rationalize their leaching behaviour.

By 1972 the Hydrometallurgy Group at Imperial College had studied the last three of these and found that bornite and chalcopyrite which have crystal structures related to that of sphalerite leach differently. To further the knowledge of this behaviour, how a 'foreign' element influences the leaching of a host mineral was considered. The first step of this was to study the leaching of synthetic bornite with substantial quantities of silver in the lattice. This was not successful however because the bornite lattice did not accept silver in excess of 1.2% . The leaching behaviour of this 'silver doped bornite' was essentially the same as that of bornite.

A copper-iron sulphide with a crystal structure similar to chalcopyrite (or bornite) and having a fourth metal had to be sought.

Stannite Cu_2FeSnS_4 has a crystal stucture very similar to calcopyrite. Therefore this was chosen for the present study.

Ferric chloride was chosen as the oxidant, because it is known to produce higher reaction rates than the more commonly used ferric sulphate.

A literature survey covering the leaching of covellite, chalcocite, chalcopyrite and bornite is presented to put the present work in the right perspective.

SECTION 1

LITERATURE SURVEY

1.1 LEACHING OF COPPER SULPHIDES.

The more important work on the leaching of copper sulphides will be briefly reviewed in the following pages. Leaching studies carried out in acidic ferric salt solutions are discussed first followed by work done with different oxidants in less detail.

1.1.1 Leaching of Covellite.

J.D.Sullivan[1] studied the dissolution of natural covellite in acidic ferric sulphate solutions and proposed reaction (1) for the overall process.

$$CuS + 2Fe^{+3} \longrightarrow Cu^{+2} + 2Fe^{+2} + S^{o} \qquad (1)$$

The leaching rate increased with increasing temperature, but was not affected by ferric ion concentrations greater than 1gm/l Fe^{+3}. Studies with acidic ferric chloride solutions showed that although at 25°C ferric sulphate was a more efficient leaching agent than ferric chloride, at 95°C both were equally effective. Different leaching rates were observed for natural samples of different origin and for the synthetic mineral.

Thomas and Ingraham[2] leached discs of synthetic CuS in acidified ferric sulphate solutions in the temperature range of 25°C to 80°C. Compared to Sullivan's covellite leaching rates, their dissolution rates were high. The rate

curves showed an initial rise and then became linear. Ferric ion concentration directly influenced the rate below about 0.005M Fe^{+3} but had no effect at higher concentrations. Arrhenious plot showed a break indicating two rate controlling steps. Below 60°C a chemical reaction at the surface with an apparent activation energy of 22 kcal/mole and above 60°C mass transport in solution with an associated activation energy of 8 kcal/mole was felt to be rate determining. This duality of mechanism has not been confirmed by other workers. In fact McDonald in a recent review[3] pointed out that this probably reflects an experimental error.

Thomas and Ingraham found only 4 percent of sulphur present in the mineral in the form of sulphate.

King[4] reported a value of 25 kcal/mole for the activation energy for the dissolution of covellite formed in the leaching of synthetic chalcocite in acidic ferric chloride and believed that a chemical reaction is rate controlling.

King found that the rate depended on the Fe^{+3} ion concentration over the entire range studied, 0.212 to 1M. Higher porosity or the non-stoichiometry of his CuS intermediate or both may be responsible for this.

Lowe[5] investigated the leaching of pure natural covellite by the rotating disc technique. He reported an apparent activation energy of 14 kcal/mole. Rate curves were essentially linear. Dissolution rate was a function of ferric ion concentration over the range 0.0064 to 0.212M Fe^{+3}.

Mulak[6] studied the dissolution of dispersed synthetic CuS in acidified ferric sulphate solutions over the temperature range 30 to 90°C. Linear kinetics were observed. The dissolution rate was independent of the agitation speed, the pH when below 3, and the ferric ion concentration if it did not exceed 0.005M. A slow surface reaction was suggested as rate determining in view of the high activation energy (20 kcal/mole) and the independence of rate on the agitation speed.

The most recent work published on the leaching of covellite was done by Dutrizac and MacDonald[7]. They leached pure synthetic CuS discs and high grade natural covellite in acidified ferric sulphate in the temperature range 15 to 95°C. They observed slow, essentially linear kinetics with an activation energy of 18 kcal/mole. Microscopic observations of partially leached samples suggested preferential attack and the resulting pit formation was suspected to cause the initial rise of the observed rate. Rate was insensitive to ferric ion concentration above 0.005M Fe^{+3}. A chemical reaction at the surface was thought to be rate controlling although pitting suggested a galvanic action. Natural covellite leached in the same way and with approximately the same activation energy as the synthetic CuS. In either case the percentage of sulphur recovered as sulphate was low, generally below 10 percent.

Some pressure leaching work is reported in the literature(8,9). Warren[10] leached natural covellite in sulphuric acid with oxygen gas. The extraction rate was

TABLE 1 LEACHING OF COVELLITE

Material	Fe^{+3} Dependence	Activation Energy(kcal/m)	Temp.(°C)	Rate Controlling Process	Ref
Natural ores	No effect for $Fe^{+3} > 1g/l$	High	35 - 95	-	1
Synthetic	No effect for $Fe^{+3} > 0.005M$ Fe^{+3}	22	T 60	Essentially linear kinetics	2
Intermediate product from the leaching of pure synthetic Cu_2S	Increases with Fe^{+3} in the range 0.25M to 1.0M Fe^{+3}	25	20 - 80	Chemically controlled	4
Mounted natural crystals	Increased gradually between 0.0064M and 0.212M	14	40 - 70	Chemisorption process with linear kinetics	5
Synthetic powders	$Fe^{+3} > 0.005M$, no effect. $Fe^{+3} < 0.005M$ rate prop. to ferric strength	20	30 - 90	Slow chemical step with linear kinetics	6
Pure synthetic and natural crystals	No effect for $Fe^{+3} > 0.0054M$ Directly proportional at lower levels	18	15 - 95	Rate increased slightly with time. Lin. kinetics essentially	7

insensitive to oxygen partial pressures above 200p.s.i. The activation energy obtained from leaching rates at two temperatures(!) was 11.7 kcal/mole. The value obtained from the second stage leaching of chalcocite was 6.6 kcal/mole.

Peters and Loewen[11] leached both natural covellite and covellite produced in the second stage leaching of chalcocite in perchloric acid solutions with oxygen. The activation energy calculated for the second stage leaching of chalcocite was 11.4 kcal/mole. They postulated an electrochemical mechanism for the leaching of covellite with associated anodic and cathodic reactions.

$$CuS \longrightarrow Cu^{+2} + S^{o} + 2e \quad \text{(anodic)} \qquad (2)$$

$$2H^{+} + \tfrac{1}{2}O_2 + 2e \longrightarrow 2H_2O \quad \text{(cathodic)} \qquad (3)$$

If the anodic reaction was rate controlling in the leaching of covellite, they argued, the activation energies must be the same irrespective of the oxidant. Since this is not realized in practice, they concluded the cathodic reaction to be rate determining.

Table (1) summarises the results obtained for covellite leaching.

1.1.2 Leaching of Chalcocite.

Sullivan[12,13] found that leaching of natural chalcocite in acidic ferric sulphate solutions occurs in two stages. The first stage was very much faster than the second. He proposed reactions to describe the two stages.

$$Cu_2S + Fe_2(SO_4)_3 \longrightarrow CuS + CuSO_4 + 2FeSO_4 \qquad (4)$$

$$CuS + Fe_2(SO_4)_3 \longrightarrow CuSO_4 + 2FeSO_4 + S^{o} \qquad (5)$$

The rate of the first half of the reaction was markedly dependent on particle size, but the second half was not. Both stages were independent of acid concentration. The first half was insensitive to ferric ion concentration over the range 0.2 gm to 1.0 gm of ferric ion per litre, but the rate of the second half increased with increasing ferric ion concentration over the range 0.2g to 0.6g of ferric ion per litre. Sullivan believed that the solid produced in the first stage of leaching was not the same as natural covellite.

Similar results , especially the CuS intermediate formation during leaching, were reported by several workers. (Colombo and Frommer[14] , Tkachenco and Tseft[15], Kopylov and Orlov[16])

Mulak[17] investigated the kinetics of dissolution of synthetic Cu_2S in acidic ferric sulphate solutions using a rotating disc technique in the temperature interval 30 - 90°C. He too observed a CuS intermediate. At temperatures below 60°C the rate was thought to be controlled by solution mass transport with an activation energy of 1.5 kcal/mole. Above 60°C, the rate of dissolution of CuS became significant, and mixed kinetics with an apparent activation energy of 5.3 kcal/mole were observed. The initial rate depended on the ferric ion concentration in the range 0.005 to 0.05M Fe^{+3}, but was independent of pH.

King[4] studied the dissolution of high purity synthetic Cu_2S in acidified ferric chloride solutions. He showed that copper was selectively leached from Cu_2S to create a continous solid solution phase between Cu_2S and CuS. The phases found in this range were Cu_2S, $Cu_{1.96}S$(djurlite), $Cu_{1.8}S$(digenite)

and CuS. Between $Cu_{1.82}S$ and $Cu_{1.70}$ the displacements of diffraction lines were regular and even continued until the $Cu_{0.8}S$ composition, when the lines of sulphur appeared. This suggested the existence of a metastable nonstoichiometric range between $Cu_{1.5}S$ and $Cu_{1.0}S$, or possibly upto $Cu_{0.8}S$. The apparent activation energy for the first part was 0.8 kcal/mole, a very low value, and King believed the diffusion of copper ions in the lattice was rate controlling. He also showed that the 'artificial covellite' produced during the leaching of chalcocite was the same as natural covellite, but the dissolution rates of 'artificial covellite' were higher because it was very porous.

Dissolution kinetics of synthetic chalcocite discs in acidic ferric sulphate were studied by Thomas et al[18]. Their results closely agreed with those of King, but they found only digenite $Cu_{1.8}S$ and 'blaubleibender covellite' (covellite was not detected). However, they concluded that the transformations are:

chalcocite → djurlite → digenite

blaubleibender covellite → covellite

The apparent activation energy for the first part of the reaction was 5-6 kcal/mole, and the dissolution rate was directly dependent on the ferric ion concentration and on the square root of the disc rotation speed indicating mass transport in solution to be rate controlling.

Lowe[5] studied the dissolution of mounted pieces of high grade natural chalcocite in acidified ferric sulphate solutions in the temperature range 40 to 70°C. The reaction proceeded via a CuS intermediate. The initial rate was first

Table : 2. Leaching of Chalcocite.

Material	Medium	Rate Dependence on Oxidant	E_A (kcal/mole)	Temp. (^oC)	Rate Controlling Process.	Ref.
Natural Cu_2S	$Fe_2(SO_4)_3$	Ind. of Fe^{+3} conc.	low	23-95	Solution controlled	4 & 5
Cu_2S in tailings	"	Bet. 2-10% $Fe_2(SO_4)_3$ independent.	-	25	-	
Pure nat. Cu_2S	$FeCl_3$	-	low	60-105	solution controlled	
Synth. Cu_2S	$Fe_2(SO_4)_3$	Dir. prop. to Fe^{+3}	1.5	30-90	60 " "	17
Nat. Cu_2S	"	Slight effect bet. 5 - 27 Fe^{+3}.	low	20-70	solution controlled	
pure synt Cu_2S	$FeCl_3$	Independent	0.8	20-80	Solid state diffn. of Cu in $Cu_{2-x}S$	4
Synt. Cu_2S and $Cu_{1.8}S$	$Fe_2(SO_4)_3$	Dir. prop. to Fe^{+3}	5-6	5-80	Soln. control. Fe^{+3} diffn. to Cu_2S srfc.	18
Pure nat. Cu_2S	"	" " " "	6-7	28-70	- do -	5
Nat. Cu_2S	O_2/H_2SO_4	Prop. to , (H^+), $(SO_4^{-2})^{-1.18}$, p_{O_2}	6.6	30-67	O_2 adsorption foll. by surfc. reaction	19
Nat. Cu_2S	$O_2/HClO_4$	On p_{O_2} (assumed lin.) Also on H^+	1.8	105-140	Solid state diffn. of copper.	11

order with respect to ferric ion concentration for ferric strengths between 0.007 and 0.299M Fe^{+3}. It was also proportional to the 0.25 power of acid concentration. These together with the activation energy of 6.7 kcal/mole led him to suggest solution mass transport as rate controlling.

Fisher and Roman[19] studied chalcocite dissolution in sulphuric acid-oxygen media in the temperature range 29.6 to 67°C. They found that at these temperatures, covellite was the final product. The overall reaction proposed was:

$$Cu_2S + \tfrac{1}{2}O_2 + 2H^+ \longrightarrow CuS + Cu^{+2} + H_2O \qquad (8)$$

The kinetics were described by the expression:

$$\text{Rate} \propto p_{O_2}[H^+][SO_4^{-2}]^{-1.18}$$

The activation energy found was 6.59 kcal/mole. The reaction mechanism was thought to consist of adsorption of oxygen followed by a series of surface reactions.

Peters and Loewen[11] found that natural chalcocite was transformed to CuS by a very fast reaction, when leached in perchloric acid solutions at 95 p.s.i. oxygen pressure in the range 105-140°C. The activation energy found for this process was 1.8 kcal/mole. The CuS produced decomposed very slowly.

The results of chalcocite leaching are summarised in Table 2.

1.1.3 Leaching of Chalcopyrite.

Literature covering the leaching of chalcopyrite is quite considerable. This is not surprising because it is the most abundant but the most difficult to leach of the copper

sulphide minerals. Chalcopyrite hydrometallurgy has been extensively reviewed recently.[20 - 26]

Sullivan[12] and Brown and Sullivan[27] studied the dissolution of chalcopyrite concentrates in both ferric sulphate and ferric chloride media. The chalcopyrite dissolution reactions suggested were :

$$CuFeS_2 + 4Fe^{+3} \longrightarrow Cu^{+2} + 5Fe^{+2} + 2S^o \qquad (7)$$

$$CuFeS_2 + 4Fe^{+3} + 2H_2O + 3O_2 \longrightarrow Cu^{+2} + 5Fe^{+2} + 2H_2SO_4 \qquad (8)$$

About 75 percent of the chalcopyrite dissolved according to reaction (7) and the remainder according to reaction (8). The minor amount of sulphate produced was attributed to dissolved oxygen and not to the action of ferric ion. They also noted that ferric chloride was a better leaching agent for chalcopyrite than ferric sulphate.

Klets and Lispo[28] believed that chalcopyrite dissolved according to reaction (7) and the elemental sulphur produced was subsequently dissolved according to reaction (9).

$$8S^o + 6H_2O \longrightarrow H_2S_3O_6 + 5H_2S \qquad (9)$$

Ermilov, Tkachenko and Tseft[29] studied the leaching of chalcopyrite in ferric chloride solutions in the temperature range 60 to 106°C. The reaction rate increased moderately with increasing temperature: the apparent activation energy was about 12 kcal/mole. The rate depended directly on the ferric ion concentration for initial ferric chloride concentrations between 50 and 100 g/l. The sulphur formed did not interfere with the kinetics.

Ichikuni[30] found that ferric sulphate attacked chalcopyrite according to reaction (7). Later he postulated that iron was preferentially leached from chalcopyrite lattice. Also he found that mixtures of chalcopyrite and pyrite were attacked with little selectivity suggesting the absence of galvanic effects.

Dutrizac, MacDonald and Ingraham[31] studied the leaching of sintered discs of synthetic chalcopyrite in acid ferric sulphate solutions over the temperature range 50 to 94°C. The chemistry of dissolution was described by reaction (7). The reaction displayed parabolic kinetics with an apparent activation energy of 17 kcal/mole. The rate was independent of the disc rotation speed, acid concentration between 0.001 and 1.0 M H_2SO_4 and ferric ion concentration above 0.01 M. Below about 0.01 M Fe^{+3} concentration the diffusion of ferric sulphate through a constantly thickening sulphur layer and above 0.01 M Fe^{+3} the outward diffusion of ferrous ion were thought to be rate controlling. Natural chalcopyrite dissolved very slowly compared to the synthetic mineral and this was attributed to the high porosity of the synthetic material. Above 50°C chloride ion was found to increase the rate of leaching.

Lowe[5], studying the leaching of natural chalcopyrite reported linear kinetics, his results agreed very closely with those of Dutrizac et al. otherwise. But he believed a surface-controlled chemisorption to be rate determining.

In an attempt to devise a hydrometallurgical route for the extraction of copper from chalcopyrite, Haver and Wong[32] studied the leaching of chalcopyrite concentrates in acidified ferric chloride solutions, in the temperature range 30 to 106°C. Mass transport through a sulphur coating was felt to be responsible for the observed parabolic kinetics. About 70 percent of the sulphur was found in the elemental form. At a ratio of $FeCl_3$ to $CuFeS_2$ of 1 to 2.7 virtually all the copper in solution was found to be in the monovalent form. Therefore reaction (10) was proposed to represent the stoichiometry of chalcopyrite dissolution.

$$CuFeS_2 + 3FeCl_3 \longrightarrow CuCl + 4FeCl_2 + 2S^o \qquad (10)$$

Baur, Gibbs and Wadsworth[33] studied the dissolution of powdered natural chalcopyrite in acidified ferric sulphate solutions using radio chemical techniques. The parabolic rate constant was directly dependent on the ferric ion concentration below 0.01 M Fe^{+3} but was insensitive at higher concentrations. The calculated activation energy was 20 ± 5 kcal/mole in reasonable agreement with that of Dutrizac et al. According to Baur et al. elemental sulphur was produced by the anodic dissolution of chalcopyrite by the reaction :

$$CuFeS_2 \longrightarrow Cu^{+2} + Fe^{+2} + 2S^o + 4e \qquad (11)$$

Ferric ions were consumed by the cathodic reaction (12).

$$4Fe^{+3} + 4e \longrightarrow 4Fe^{+2} \qquad (12)$$

Charge transfer processes associated with reactions (11) and (12) were shown not to be rate controlling by the observation that although the potential of a piece of chalcopyrite measured against a calomel electrode changed markedly during leaching, the actual leaching rate did not change. Therefore ferric ion diffusion through a sulphur coating was suggested as the slow step.

Ferreira[34] recently studied the leaching of synthetic chalcopyrite. He synthesised two forms of the mineral, a cubic β-form of composition $CuFeS_{1.83}$ and an α-form, apparently tetragonal, $Cu_{1.12}Fe_{1.09}S_2$ having about 10.7 percent excess copper and 8.3 percent excess iron over the stoichiometric $CuFeS_2$. Powdered samples of these were leached in acidic ferric sulphate, hydrogen peroxide and hydrochloric acid solutions.

In acid ferric sulphate leaching of β-chalcopyrite, the rate curves displayed three distinct stages. The first stage, in which about 17.5 percent of the copper and some iron were removed, was shown to be controlled by the diffusion of copper in the solid to the solid-liquid interface.

Rate curves were nearly linear in the second stage during which 20 to 30 - 35 percent of the copper was extracted. Arrhenius plots indicated that a homogeneous reaction was favoured above 65°C, (activation energy 20 kcal/mole), whereas at lower temperatures a heterogeneous process was evident with an apparent activation energy of 1.5 kcal/mole.

During first and second stages of leaching the crystal lattice underwent dramatic changes. Initially the d spacings became progressively smaller, they then passed through a minimum, and rose to values close to those of α-chalcopyrite and remained unchanged thereafter. A $\beta \rightarrow \alpha$ transformation took place as was evident from the splitting of some lines of the X-ray powder patterns (Fig 1). This was substantiated by the chemical analysis of the leach residues which yielded a composition $CuFe_{1.2}S_{2.3}$ close to that of α-chalcopyrite.

The third stage was the chemical reaction of $CuFe_{1.2}S_{2.3}$ to produce elemental sulphur.

To explain these observations Ferreira postulated that 34 percent of the iron in β-chalcopyrite exists as ferrous, the rest being in the ferric state. Then the formula could be written :

$$Cu^{+}Fe^{+2}_{0.34}\ Fe^{+3}_{0.66}\ S^{-2}_{1.83}$$

The initial stages of leaching was represented by reaction (13).

$$2.3CuFeS_{1.83} + 0.574Fe_2(SO_4)_3 \longrightarrow 0.47CuSO_4 + 1.252FeSO_4 + 1.83CuFe_{1.2}S_{2.3} \qquad (13)$$

During this process electron transfer occured within the solid to maintain charge neutrality. Ferreira's model predicted a composition $Cu^{+}Fe^{+3}_{1.227}S^{-2}_{2.3405}$ after about 34 percent of the copper removed in reasonable agreement with the observed $CuFe_{1.2}S_{2.3}$. The third stage was the straight dissolution of $CuFe_{1.2}S_{2.3}$ to give elemental

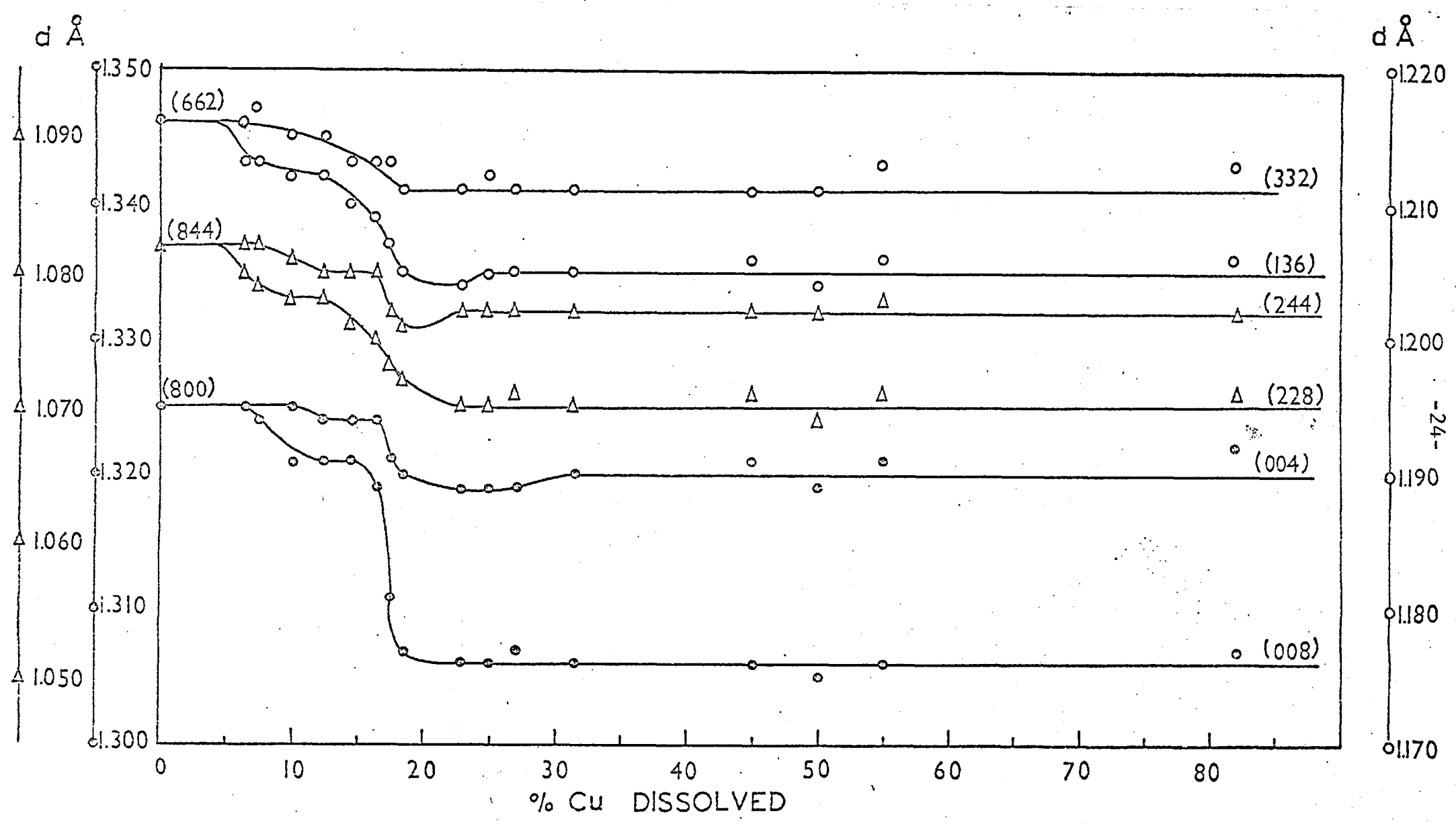

Fig. 1 Cubic → Tetragonal Transformation During the Leaching of β -Chalcopyrite. (Ferreira[34])

sulphur.

$$CuFe_{1.2}S_{2.3} + 2.2Fe_2(SO_4)_3 \longrightarrow CuSO_4 + 5.6FeSO_4 + 2.3S^o \qquad (14)$$

The rate of leaching of α-chalcopyrite in acidic ferric sulphate was slower than that of β-chalcopyrite. Storage time affected the leaching rate possibly due to the diffusion of excess copper to the surface. The leaching behaviour of α-chalcopyrite paralleled that of natural chalcopyrite after an initial rapid removal of the excess copper. Although the leach residues of β-chalcopyrite after 30 - 35 percent copper removal were structurally very similar to α-chalcopyrite, the former leached much faster. This led Ferreira to conclude that the relative proportions of the elements in the lattice were more important than the structure itself in controlling the leaching behaviour.

α-chalcopyrite dissolved much faster in 0.1 M hydrochloric acid at 80°C than in acidic ferric sulphate at 95°C. This was thought to be due to the formation of $CuCl_2^-$ complex. In agreement with the findings of Dutrizac et al. the addition of Cl^- to acidic ferric sulphate improved the leaching immediately.

Some work on the leaching of chalcopyrite has been done under autoclave conditions. Warren[10] studied the kinetics of leaching of chalcopyrite in acid solutions between 120 and 180°C. He found that the rate of leaching was surface controlled and was independent of oxygen pressure at 'moderate' pressures. The activation energy was 23 kcal/mole. Similar work by Dobrakhotov and Mairowa[45]

gave 7 kcal/mole for the activation energy. The linear rate varied directly with acidity and with oxygen pressure to the one-half power. Stanczyk and Rampack[36] found complete dissolution in 30 miniutes at 230°C for oxygen partial pressures over 90 p.s.i.

Peters and Loewen[11] studied the dissolution of chalcopyrite in perchloric acid solutions and proposed the formation of covellite as an intermediate according to reaction (15), which is thermodynamically possible.

$$CuFeS_2 + 2H^+ + \tfrac{1}{2}O_2 \longrightarrow CuS + Fe^{+2} + S^o + H_2O \qquad (15)$$

Covellite was not detected in leach residues because it leached much faster. The activation energy for the chalcopyrite dissolution was 11.4 kcal/mole and 15 kcal/mole for the sulphate formation according to reactions (16) or (17)

$$CuS + 2O_2 \longrightarrow Cu^{+2} + SO_4^{-2} \qquad (16)$$

$$CuFeS_2 + 4O_2 \longrightarrow Cu^{+2} + Fe^{+2} + 2SO_4^{-2} \qquad (17)$$

Yu, Hansen and Wadsworth[37] studied the leaching of chalcopyrite in autoclaves at high temperature and acid concentration (0.5 N H_2SO_4) in order to have all the reaction products in solution. The temperature range was 125 - 175°C; the pressure range was 75 - 400 p.s.i. of oxygen. Partially leached residues did not show any evidence of layer formation and the diffraction lines were identical to those of the original mineral. Overall stoichiometry was represented by the reaction (18).

$$2CuFeS_2 + \frac{17}{2}O_2 + H_2SO_4 \longrightarrow 2CuSO_4 + Fe_2(SO_4)_3 + H_2O \qquad (18)$$

Table : 3. Leaching of Chalcopyrite.

Material	Medium	Rate Dependence on Oxidant.	E_A (kcal/mole)	T (°C)	Rate Controlling Process.	Ref.
$CuFeS_2$ conc.	$FeCl_3$	None between	High	35-100	Not given	12
	$Fe_2(SO_4)$	0.25 & 5% $Fe_2(SO_4)_3$	High	35-100	Not given	27
$CuFeS_2$	$FeCl_3$	Direct. Fe^+bet. 50 - 100 gm/1 $FeCl_3$	12	60-106	Not given	29
Synth. $CuFeS_2$	$Fe_2(SO_4)_3$	Direct. Fe^+ 0.01 M	17	50-94	Parabolic kinetics.	31
		None. Fe^+ 0.01 M			Transport control.	
Nat. $CuFeS_2$	"	None. Fe^+ 0.02 M	18	32-50	Linear kinetics. Chemisorption.	5
$CuFeS_2$ conc.	$FeCl_3$	-	High	30-106	Parabolic kinetics. Transport control.	32
Nat. $CuFeS_2$	$Fe_2(SO_4)_3$	Direct. Fe^{+3} 0.01 M	20	27-85	Parabolic kinetics.	33
		Little. Fe^{+3} 0.01 M			Transport control.	
Synth. β-chalcp.	"	None. Fe^{+3} 0.01 M	20(65°C) 1.5(65°C)	50-95	Stage 1:diffusion Stage 2:chemical	34
Nat. $CuFeS_2$	O_2/H_2SO_4	None on $p(O_2)$ (mod. p)	23	120-180	Surface controlled.	10
Nat. $CuFeS_2$	"	Rate α $(H^+)(p_{O_2})^{\frac{1}{2}}$	7			35
Nat. $CuFeS_2$	$O_2/HClO_4$	-	11.4	105-130		11
$CuFeS_2$ conc.	O_2/H_2SO_4	-	8.4	60-150		66

Mathematical analysis of the data showed that the reaction was not inhibited by any solid product which may have formed. Adsorption of oxygen followed by a surface reaction was thought to explain the observed kinetics. The enthalpy of activation for oxygen adsorption was about 33 kcal/mole and that for the surface reaction was about 9 kcal/mole. Charge transfer process were not rate controlling.

Jackson and Stickland[38] studied the dissolution of chalcopyrite in aqueous chlorine solutions and found the reaction rate to be controlled by mass transport, the ore becoming coated with a layer of sulphur - sulphur monochloride mixture. Groves and Smith[39] used sodium hypochlorite as the source of chlorine and envisaged the reaction to be :

$$CuFeS_2 + 8.5Cl_2 + 8H_2O \rightarrow Cu^{+2} + Fe^{+3} + 2SO_4^{-2} + 16H^+ + 17Cl^- \quad (19)$$

1.1.4 Leaching of Bornite.

Sullivan[12,40] studied the leaching of crushed natural bornite in both ferric sulphate and ferric chloride media. The observed kinetic rate curves showed two distinct parts : a very rapid initial step followed by a slower step. Over the temperature range 23 to 98°C the initial step increased moderately with increasing temperature in either medium. Bornite dissolution rate appeared to be independent of the acid strength and the ferric ion concentration over the range 0.25 to 10 percent Fe^{+3}. Neither elemental sulphur nor soluble ion was

found in the first stage of leaching. Sullivan proposed reaction (20) for the overall process.

$$Cu_5FeS_4 + 12Fe^{+3} \longrightarrow 5Cu^{+2} + 13Fe^{+2} + 4S^o \qquad (20)$$

Uchida et al.[41] obtained similar results and confirmed that ferric ion concentrations higher than 0.5 g/l did not appreciably increase the rate

Kopylov and Orlov[16,42] studied the dissolution of pure natural bornite by a rotating disc technique over the temperature range 30 to 70°C. They found that the rate increased slightly with increasing ferric ion concentration in the range 9 g/l to 35 g/l. The rate was quite sensitive to temperature and the activation energy was found to be 5.5 ± 1.4 kcal/mole. Accordingly a diffusion process was felt to be rate controlling. The most important outcome of their work, however, was the discovery of a new solid phase as an intermediate in the leaching of bornite. They identified this phase as chalcopyrite. The transformation was described by reaction (21)

$$Cu_5FeS_4 + 8Fe^{+3} \longrightarrow CuFeS_2 + 4Cu^{+2} + 8Fe^{+2} + 2S^o \qquad (21)$$

Dutrizac, MacDonald and Ingraham[43] investigated the leaching of synthetic bornite by a rotating disc technique. Rate curves were linear above 40°C and became increasingly parabolic at lower temperatures. Rates were independent of the acid concentration and the ferric ion concentration if it exceeded 0.1 M Fe^{+3}. The apparent activation energy was 5.7 ± 1.3 kcal/mole which led the authors to suggest ferric sulphate diffusion to bornite as rate controlling.

Pellets which had been partially leached at temperatures above 40°C consisted of three layers. Innermost unreacted bornite was sorrounded by a layer of 'non-stoichiometric bornite', which had an X-ray powder pattern very similar to bornite but with slightly different lattice parameters. Lattice parameters decreased with increasing distance from bornite. Outermost was a yellow layer identified as a mixture of chalcopyrite and sulphur. Below 40°C non-stoichiometric bornite was the only phase produced, reaction virtually stopping once that conversion was complete.

Electron microprobe analysis made across the pellets indicated that the S/Fe ratios remained fixed at 4 across both bornite and non-stoichiometric bornite but the Cu/S and Cu/Fe ratios dropped steadily.

Based on these observations they proposed the following reactions for the dissolution of bornite in acidic ferric sulphate solutions.

At temperatures above 40°C :

$$Cu_5FeS_4 + xFe_2(SO_4)_3 \rightarrow Cu_{5-x}FeS_4 + xCuSO_4 + 2xFeSO_4 \qquad (22)$$

$$Cu_{5-x}FeS_4 + (4-x)Fe_2(SO_4)_3 \rightarrow CuFeS_2 + (4-x)CuSO_4 + (8-2x)FeSO_4 + 2S^o \qquad (23)$$

$$CuFeS_2 + 2Fe_2(SO_4)_3 \longrightarrow CuSO_4 + 5FeSO_4 + 2S^o \qquad (24)$$

Below 25°C the process did not proceed beyond reaction (22).

The behaviour of natural bornite towards leaching was similar to the synthetic mineral.

Lowe[5] studied the dissolution of mounted pieces of natural bornite, which contained upto 10 percent chalcopyrite in acidified ferric sulphate solutions. The observed dissolution rates fell rapidly with time and levelled off. This led him to postulate that the reaction occurs in three stages. The first stage was given by reaction (25).

$$Cu_5FeS_4 + 4Fe^{+3} \longrightarrow Cu_3FeS_4 + 2Cu^{+2} + 4Fe^{+2} \qquad (25)$$

Whether this Cu_3FeS_4 intermediate is synthetic idaite (Cu_3FeS_4) or the limiting composition of non-stoichiometric bornite of Dutrizac et al. is not clear.

The apparent activation energy reported for the first stage is 6 kcal/mole. Acid had no effect on the rate. The initial rate varied directly with the ferric ion concentration over the range 0.006 M to 0.28 M $Fe_2(SO_4)_3$.

the second stage of bornite leaching was considered to be the diffusion of cuprous ions through the Cu_3FeS_4 layer formed. The activation energy for this stage of leaching was 10 kcal/mole, and the rate was only slightly dependent on the ferric strength. This stage proceeded according to reaction (26)

$$Cu_3FeS_4 + 2Fe^{+3} \longrightarrow Cu_2FeS_3 + Cu^{+2} + 2Fe^{+2} + S^o \qquad (26)$$

It is not certain if Cu_2FeS_3 represents a new metastable phase since Cabri's[44] recent extensive work does not mention it.

The final stage in the bornite dissolution was felt to be a chemisorption reaction with an apparent activation

energy of 12 kcal/mole.

Ugarte did a comprehensive study on the leaching of synthetic bornite in acidified ferric sulphate solutions.[45]

Below 40°C, the dissolution proceeded in two stages. A rapid one until approximately 27 percent of the copper is dissolved and a slow one, which practically stopped at about 40 percent copper extraction. At higher temperatures a two stage process was still evident, but the slow second stage proceeded to total copper dissolution.

No iron or sulphur was detected in the leach liquor during the first 40 percent of copper dissolution. The apparent activation energy for this stage was approximately 2 kcal/mole.

The proposed mechanism may be represented by the following reactions.

At temperatures above 40°C :

$$Cu_5FeS_4 + 4Fe_2(SO_4)_3 \longrightarrow Cu_3FeS_4 + 2CuSO_4 + 4FeSO_4 \qquad (27)$$

$$Cu_3FeS_4 + 4Fe_2(SO_4)_3 \longrightarrow 3CuSO_4 + 9FeSO_4 + 4S^o \qquad (28)$$

Below 40°C reaction (27) proceeded in two stages. Viz :

$$Cu_5FeS_4 + xFe_2(SO_4)_3 \longrightarrow Cu_{5-x}FeS_4 + xCuSO_4 + 2xFeSO_4 \qquad (29)$$

$$Cu_{5-x}FeS_4 + (2-x)Fe_2(SO_4)_3 \longrightarrow Cu_3FeS_4 + (2-x)CuSO_4 + \\ + (4-2x)FeSO_4 \qquad (30)$$

Reaction (29) is very much faster than reaction (30).

At lower temperatures reaction (28) is extremely slow and the reaction virtually stopped when reaction (27)

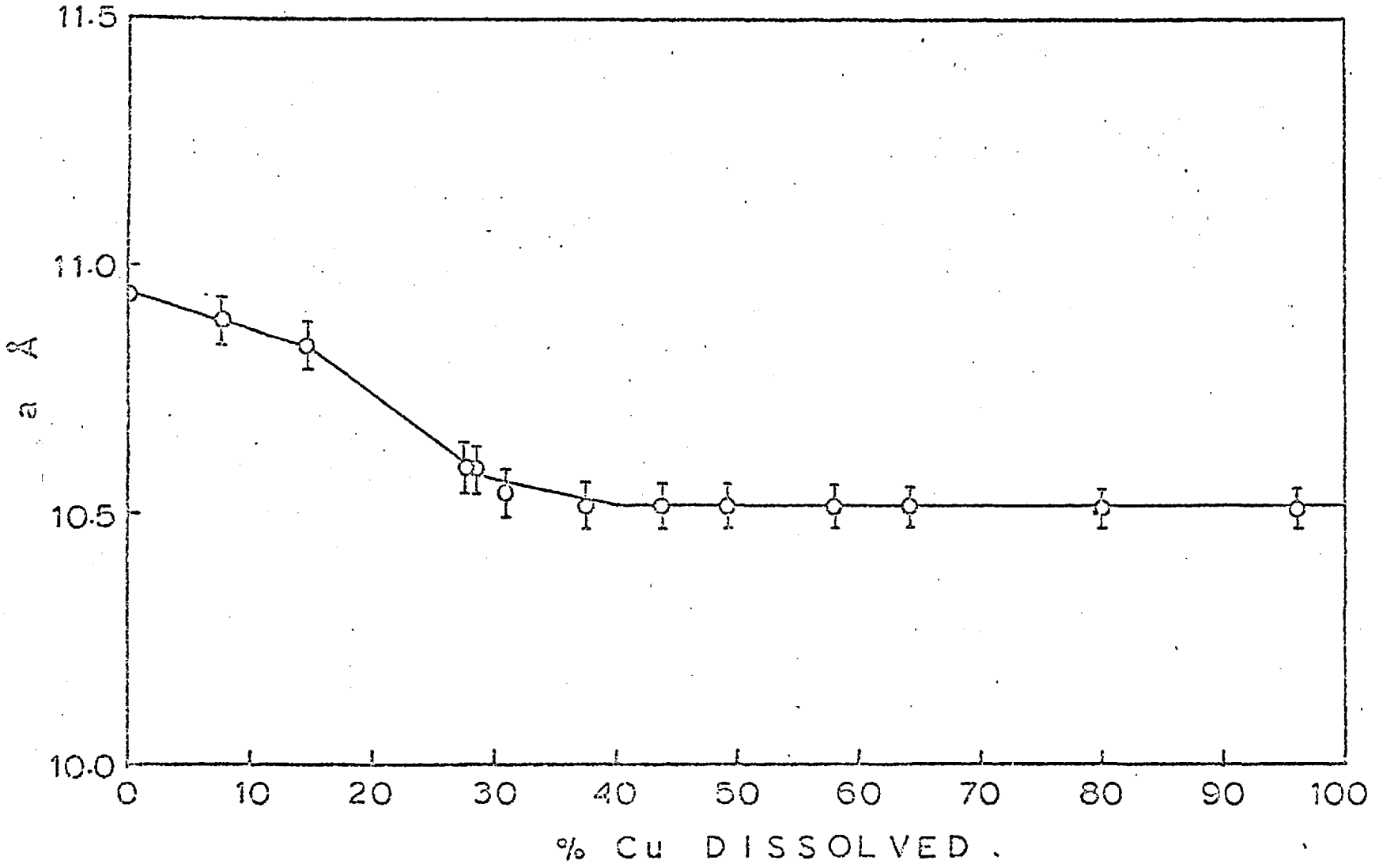

Fig. 2 Variation of Lattice Parameters a of Bornite During Leaching. (Ugarte[45])

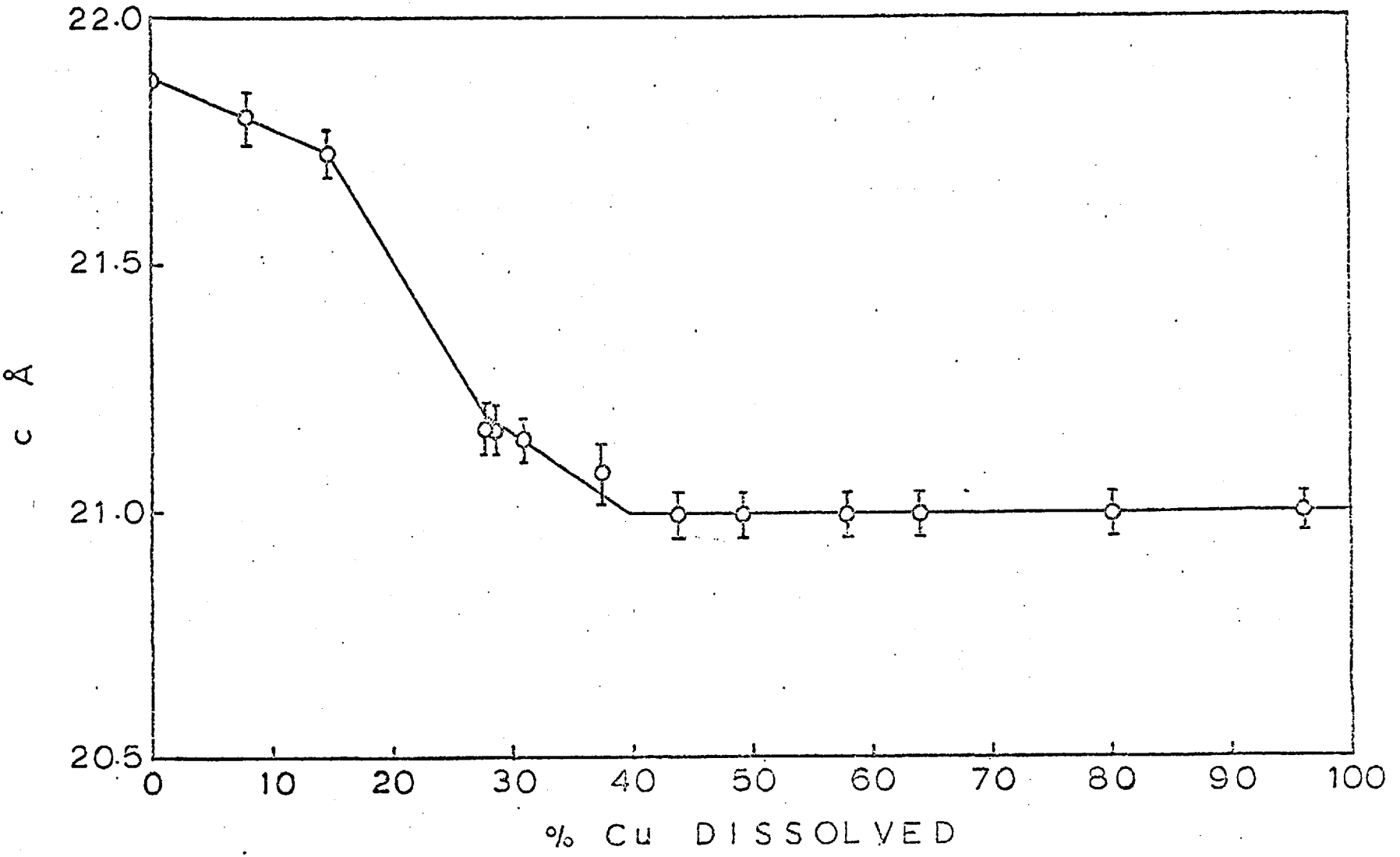

Fig. 3 Variation of Lattice Parameter c of Bornite During Leaching. (Ugarte[45])

was complete. The maximum value of x was 1.35.

the low value of activation energy was interpreted as being due to control of reaction (27) by diffusion of copper through the crystal lattice.

Careful X-ray studies showed that the first stage of leaching was accompanied by a marked contraction of the unit cell. (Figs 2 & 3)

Ugarte proved quite convincingly that the composition of the solid phase was Cu_3FeS_4 which was shown to be idaite and not chalcopyrite as was thought by other investigators He explained the solid state transformations occured during leaching of bornite using the hypothetical structure of bornite proposed by Manning. According to Manning the structure of bornite may be represented by :

$$(Cu_3FeS_4)^{-2}2Cu^{+}$$

In other words, bornite has a structure of the sphalerite type with layers of ionically bound copper. In the initial leaching stage, this ionic copper was removed by diffusion with remarkable ease resulting in a lattice contraction. A crystal structure very similar to chalcopyrite with almost identical cell dimensions with a formula Cu_3FeS_4 emerges when all the ionically bound copper is removed. Further leaching of this phase is extremely difficult because it is highly ordered and compact. In the process a total collapse of the crystal structure occurs producing elemental sulphur and ferrous ions.

Table : 4 . Leaching of Bornite.

Material	Medium	Rate Dependence on Oxidant.	E_A (kcal/mole)	T (°C)	Rate Controlling Process.	Ref.
Nat. Bornite	$Fe_2(SO_4)_3$	None. 0.25-10% Fe^{+3}	low	23-98	Not given	12
	$FeCl_3$	in either medium.	low	23-98	Not given	40
Nat. Bornite	$Fe_2(SO_4)_3$	Rate increased with increasing Fe^{+3} bet. 9-36 gm/l Fe^{+3}	4-6	30-70	Initially diffn. controlled.	16 42
Synth. Bornite	"	-	6	5-40	Parabolic kinetics (Soln. diffusion)	43
		Direct. $Fe^{+3} < 0.1$ M	5	40-94	Linear kinetics	
		None. $Fe^{+3} > 0.1$ M				
Nat. Bornite	"	Initial rate varied directly with Fe^{+3}.	6	28-70	Soln. Diffusion	
			10		Cu^+ solid state diffusion	5
			12		Chemisorption	
Synth. Bornite	"	Stage 1: independ.	2	15-90	Cu diffusion in solid state.	45
		Stage 2: direct for $Fe^{+3} < 0.065$ M none above.				

Dutrizac et al.[46] studying the leaching of synthetic bornite doped with pyrite, chalcopyrite and digenite concluded that although electrochemical reactions are important they are not necessarily rate determining in the leaching of bornite.

1.2 SOLID STATE DIFFUSION IN SULPHIDES.

Correct interpretation of the apparent activation energy is of great importance in understanding the mechanisms of leaching reactions. A low activation energy, generally lower than 4 kcal/mole, is customarily taken to indicate what is rather loosely termed 'a diffusion controlled process'. It is well established that the diffusion processes in the liquid phase are characterised by such low values whereas for processes in the solid phase this may not necessarily be true. On the other hand if a leaching process is controlled by a chemical reaction one expects a high apparent activation energy - 20 kcal/mole or more. Many leaching reactions are known to have values in between which understandably are difficult to interpret. Work of King [4] and Ugarte[45] demonstrate the unquestionable importance of the diffusion processes occuring in the solid state in leaching reactions. As far as is known, no attempt has been made to correlate the solid state diffusion and the apparent activation energy of the leaching reactions. Therefore a brief survey on the solid state diffusion of some selected sulphides was felt to be desirable.

Diffusion data are available for a few sulphides in the temperature range 300 to 800°C, and rarely above 150°C. This is because most diffusion experiments concerning sulphides demand the use of molten sulphur or vapour. This obviously limits the use of such data to interpret the

leaching results, nevertheless they are useful as a guide. Arrhenious plots for the diffusion processes in some metals and ionic solids sometimes show a break indicating different activation energies at high and low temperatures. So far the only sulphide for which a similar effect is observed is high temperature zinc sulphides.(Wurtzite (It is noteworthy that sphalerite-Wurtzite transformation occurs in the same temperature range)

One of the earliest solid materials in which an adequate understanding of transport and growth processes was obtained was silver sulphide, through the work of Tubandt, Jost, Wagner[48] and their co-workers. Self diffusion coefficient D of silver in the cubic, high temperature ($>177^{o}C$) form α-Ag_2S was reported by Allen and Moore[49] to be

$$D = 2.8 \times 10^{-4} e^{\frac{-3450}{RT}} \quad cm^2 sec^{-1}$$

for the temperature range 200 to $400^{o}C$. This is an exceptionally high value. (The self-diffusion coefficients of the ions in crystalline halides range from $10^{-7} cm^2 sec^{-1}$ down to very low values)[50]. The diffusion coefficient was independent of the sulphur pressure. This together with the X-ray measurements, low activation energy and the high D value indicated that the silver ions move freely among the relatively immobile sulphide ions.

Sulphidation experiments carried out with and without markers by Mussner and Birchnall[51] showed that sulphide ion transport is relatively insignificant in the

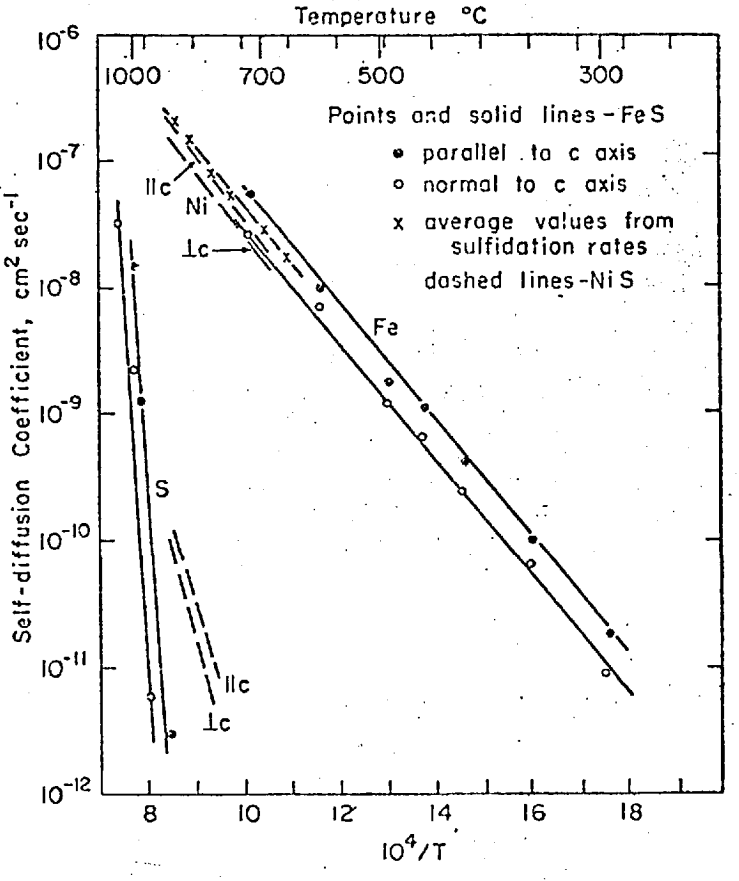

Fig. 4 Self-diffusion coefficients of iron and sulphur in FeS and NiS[49].

monosulphide of iron $Fe_{1-\delta}S$.

Condit and Birchenall[49] and later Hobbins and Birchenall[49] synthesised single crystals of ferrous sulphide and determined self diffusion coefficients of both iron and sulphur parallel and perpendicular to the hexagonal axis for a wide range of compositions. Their results, together with sulphidation growth data are shown in Fig. (4). Clearly the sulphidation rates are completely explained by iron diffusion control. Both iron and sulphur diffusion is faster parallel to the hexagonal or c axis than normal to the c axis. Similar experiments by Klotsman, Timofear and Traktetenberg[49] led to the same results in NiS which has the same crystal structure. Again the cation is several orders more mobile than the sulphide ion. For both iron and sulphur the diffusion coefficients parallel and perpendicular to the c - axis do not differ greatly and have the same activation energy. Also iron diffusivity was quite sensitive to non-stoichiometry. Mrowec[52] showed that unlike α-Ag_2S, the self diffusion of iron in FeS depended on sulphur pressure. Diffusivity varied from 1.2×10^{-6} at $a_s = 1.24 \times 10^{-3}$ to 10.5×10^{-8} cm^2sec^{-1} at $a_s = 1$.

Turkdogan[53] found that in the temperature range 300 to 900°C, the self diffusion coefficient of iron in two non-stoichiometric ferrous sulphides could be expressed by :

$$\log D_{Fe} = -\frac{4140}{T} - 3.71 \quad \text{for } FeS_{1.008}$$

and $$\log D_{Fe} = -\frac{5770}{T} - 1.15 \quad \text{for } FeS_{1.15}$$

From these the activation energies are calculated to be 18.9 kcal/mole for $FeS_{1.008}$ and 26.4 kcal/mole for $FeS_{1.15}$. It follows therefore that the diffusion in the solid state may have high activation energies.

Lambertin[54] et al. published diffusion data for copper sulphides formed in the sulphidation of 99.99% pure copper wires. In the temperature range 150 to 310°C and at a sulphur vapour pressure of 3×10^{-2} torr. CuS was formed. At higher temperatures (335 to 425°C) non-stoichiometric $Cu_{2-x}S$ was formed. Sulphidation rates were determined by the diffusion of copper ions through the protective sulphide layer. Calculated activation energies for the self diffusion of copper ions were :

$$E_A = 19 \pm 1 \text{ kcal/mole} \quad \text{for CuS}$$

and $$E_A = 12 \pm 1 \text{ kcal/mole} \quad \text{for } Cu_{2-x}S.$$

The most recent value for the activation energy for the leaching of covellite in ferric sulphate is 18 kcal/mole.(Dutrizac and MacDonald). Similar values are reported by other workeres also. (Lowe, 14 kcal/mole, Mulak - 20 kcal/mole, Thomas and Ingraham - 22kcal/mole). Therefore it may be that the leaching of covellite is controlled purely by the diffusion of copper ions in the solid state

Pokroovskii[55] et al. studied the diffusion of copper in a copper sulphide scale produced by the sulphudization of a copper bar 25 x 25 x 40 mm in boiling sulphur for 5 hours, using ^{64}Cu. Although the composition of the sulphide is not reported it is probably Cu_2S.

The activation energy was 5 kcal/mole.

Pavlyuchenko[56] et al found that the self diffusion coefficient for copper in $Cu_{2-x}S$ was $(9 \pm 0.7) \times 10^{-6}$ cm^2sec^{-1} using radioisotopes.Later they studied the diffusion of copper in $Cu_{1.99}S$ and $Cu_{1.77}S$ in the temperature range 140 to 450°C. At 134°C $D \sim 6 \times 10^{-7}$ cm^2sec^{-1}, further increase in temperature did not significantly increase D indicating a low activation energy. ($\sim$5 kcal/mole). In the composition range studied Cu/S between 1.77 and 1.99, D did not change with composition.

Parlynchenko[58] et al. studied the self diffusion of copper and sulphur in Cu_2S and $Cu_{1.77}S$ using ^{64}Cu and ^{35}S isotopes. Self diffusion coefficient of copper varied from 2.4×10^{-10} cm^2sec^{-1} to 64×10^{-10} cm^2sec^{-1} in the temperature range 300 to 425°C. (From these two values a crude value for the activation energy may be calculated as 4.6 kcal/mole). Even at 400°C the self diffusion coefficient of sulphur was only about 10^{-12} cm^2sec^{-1}, indicating that the sulphide ions are immobile in cuprous sulphide.

Weiss[59] reported the "effective diffusion coefficient" (although the precise meaning of this expression is not clear) of copper in digenite to be $(7.1 \pm 1 \times 10^{-2}$ cm^2 sec^{-1} at 440°C. The self diffusion of Cu in Cu_2S was studied by Barktkiewicz[60] et al. in the temperature range 350 to 550°C. Self diffusion coefficients of copper vacancies, D_d , was :

$$D_d = 3.3 \times 10^{-2} e^{-7300/RT}$$

The defect concentration N_d obeyed the equation :

$$N_d = 4.3 \times 10^{-1} e^{-760/RT}$$

Although it is difficult to compare the values of self diffusion coefficients of copper in Cu_2S reported by different workers, there is general agreement that the activation energy for the process is low.

Sreedhar[61] and others studied the diffusion of copper from Cu_2S to CdS at different temperatures.

Kato and Oki[62] studied the anodic reaction mechanisms of Cu_2S in H_2SO_4. They measured the electrode potentials, anodic polarisation behaviour of the Cu_2S - CuS system and the copper concentration by X-ray microanalysis. The crystal structure of the electrode surface was studied by X-ray diffraction. The electrode potentials of the Cu_2S - CuS system showed three characteristic values for Cu_2S, $Cu_{1.8}S$ and CuS. The anodic dissolution of Cu_2S in H_2SO_4 solutions was described by reactions :

$$Cu_2S \longrightarrow CuS + Cu^{+2} + 2e$$
$$CuS \longrightarrow Cu^{+2} + S^{o} + 2e$$

The apparent activation energy for the diffusion of copper atoms in Cu_2S was 3.4 kcal/mole.

These results strongly favour the suggestion of King that the first stage of leaching of Cu_2S is controlled by the diffusion of Cu ions in the Cu_2S crystal lattice.

Gurvich Shamanov[63] studied the diffusion of Cu in CdS - ZnS mixtures, in the temperature range 450°C to 750°C. The apparent activation energies were 19 kcal/mole for copper in ZnS and 11 kcal/mole for copper in $Cd_{0.5}Zn_{0.5}S$.

Secco's[47] studies into the diffusion of Zn in high temperature zinc sulphide (wurtzite) are interesting for two reasons. First, it is the only sulphide for which three diffusion processes are supposed to be operative. The experiments were done in temperatures in the range 925 to 1075°C. The suggested expressions are:

$D = 3 \times 10^{-4} e^{-35kcal/RT}$ below 940°C

$D = 1.5 \times 10^{4} e^{-75kcal/RT}$ 940 to 1030°C

$D = 1 \times 10^{16} e^{-150kcal/RT}$ above 1030°C

Second it reports one of the highest self diffusion coefficients ever published, the only exception being that of Ba in BaO (about 10^{30} $cm^2 sec^{-1}$)

From the foregoing discussion it is clear that high activation energy of a leaching reaction does not necessarily mean a chemically controlled process. But still the low values indicate a diffusion controlled process in the liquid phase or in the solid phase. Diffusion control in the liquid phase can be readily eliminated isolating the solid state diffusion control if one existed. When the activation energy is high deciding between a chemically controlled process and

a solid state diffusion process is extremely difficult and calls for very careful design of experiments.

1.3 PREVIOUS WORK ON THE LEACHING OF STANNITE.

The first work related to this topic, though not strictly a leaching study, was published by Gruner and Lin[65] in 1929. They studied the solubility of cassiterite and stannite in different solvent systems at room temperature. The stannite which contained pyrite , chalcopyrite, wolframite and traces of arsenopyrite as impurities came from Cornwall, England while the cassiterite examined was from Ehrenfridersdorf, Saxony and had fluorite and apatite as gangue. Specimens of stannite and cassiterite were pulverised to pass 100 mesh and five gram portions of stannite were put into 250 cc pyrex flasks with the solutions given in Table (5). The same procedure was followed for cassiterite. A few milligrams of fluorite was added to each flask because it was thought that the fluoride ion could influence the solubility of tin minerals. The flasks were corked and shaken once a day. After two months 20 ml samples from each flask were tested for tin. This was done colourimetrically using ammonium molybdate as the colouring agent. They claim that the limit of detection of tin by this method is of the order of 1 ppm.

The results of their investigation are presented in Table (5). Tin was found to be present in all the solutions with stannite except for sodium carbonate. No tin was detected in the solutions containing cassiterite. Their resulte seem to suggest the following :

Table : 5 Solubility of Stannite in Dilute Acid and Carbonate Solutions After Two Months. (Gruner and Lin[65])

Solution	Tin Dissolved (ppm)
50 ml N/20 H_2SO_4	5
25 ml N/20 H_2SO_4 + 25 ml N/20 $Fe_2(SO_4)_3$	8
25 ml N/20 H_2SO_4 + 25 ml N/20 $FeSO_4$	2
50 ml N/20 HCl	20
25 ml N/20 HCl + 25 ml N/20 H_2SO_4	15
25 ml N/20 HCl + 25 ml N/20 $Fe_2(SO_4)_3$	2
25 ml N/20 HCl + 25 ml N/20 $FeSO_4$	Faint trace
50 ml N/20 Na_2CO_3	None

1. Hydrochloric acid is very effective in attacking stannite.
2. Addition of ferric and ferrous sulphates to hydrochloric acid considerably reduces the solubility of stannite.
   This is more pronounced in the case of ferrous sulphate.
3. The ability of sulphuric acid to attack stannite is low compared to hydrochloric acid.
4. Addition of ferric sulphate to sulphuric acid increases the stannite solubility while ferrous sulphate addition decreases it.

However, without a clear knowledge of the separation and analytical techniques used it is difficult to asses the validity of these results. First it is not clear whether the precipitation of tin, which invariably occurs in this type of solution, is accounted for in the analysis. Secondly the accuracy of the colourimetric method adopted by these authors to estimate the reported very low tin concentrations is questionable.

Gerlach and others[66] (1970) studied the pressure leaching of synthetic stannite as part of a research programme to correlate the lattice structure and a newly defined parameter "Leaching property". Three series of sample substances were chosen for this investigation.

They were :

1. FeS_2 (pyrite and marcasite) - FeAsS - NiAsS - - CoAsS - NiSbAs
2. ZnS (sphalerite) - ZnSe - ZnTe
3. $CuFeS_2$ - Cu_2FeSnS_4 - Cu_3SbS_4

All these minerals were synthesised by sinter-annealing of the elements. Pressure leaching experiments were done using oxygen gas in sulphuric acid in the temperature range 60 to 150°C. For the series :

FeS_2 - NiAsS- CoAsS - FeAsS - NiSbS

oxygen partial pressure was 8 atmospheres, sample weight was 20 gms which was leached in 1 litre of 0.2 M sulphuric acid. For the rest, an oxygen partial pressure of 10 atmospheres was used and the sample weight was 50 gms. Samples were withdrawn from the autoclave at suitable time intervals and analysed for the extracted elements using atomic absorption spectrophotometry, complexiметry or X-ray fluorescence analysis. Although kinetic rate curves and postulated rate equations are presented for all the minerals, only those of $CuFeS_2$ and Cu_2FeSnS_4 will be discussed here. Cu_3SbS_4 is excluded because the crystal structure of the studied sample was not known with absolute certainty.

The kinetic rate curves for chalcopyrite and stannite are shown in Fig (5)

It was found that the chalcopyrite leaching rate

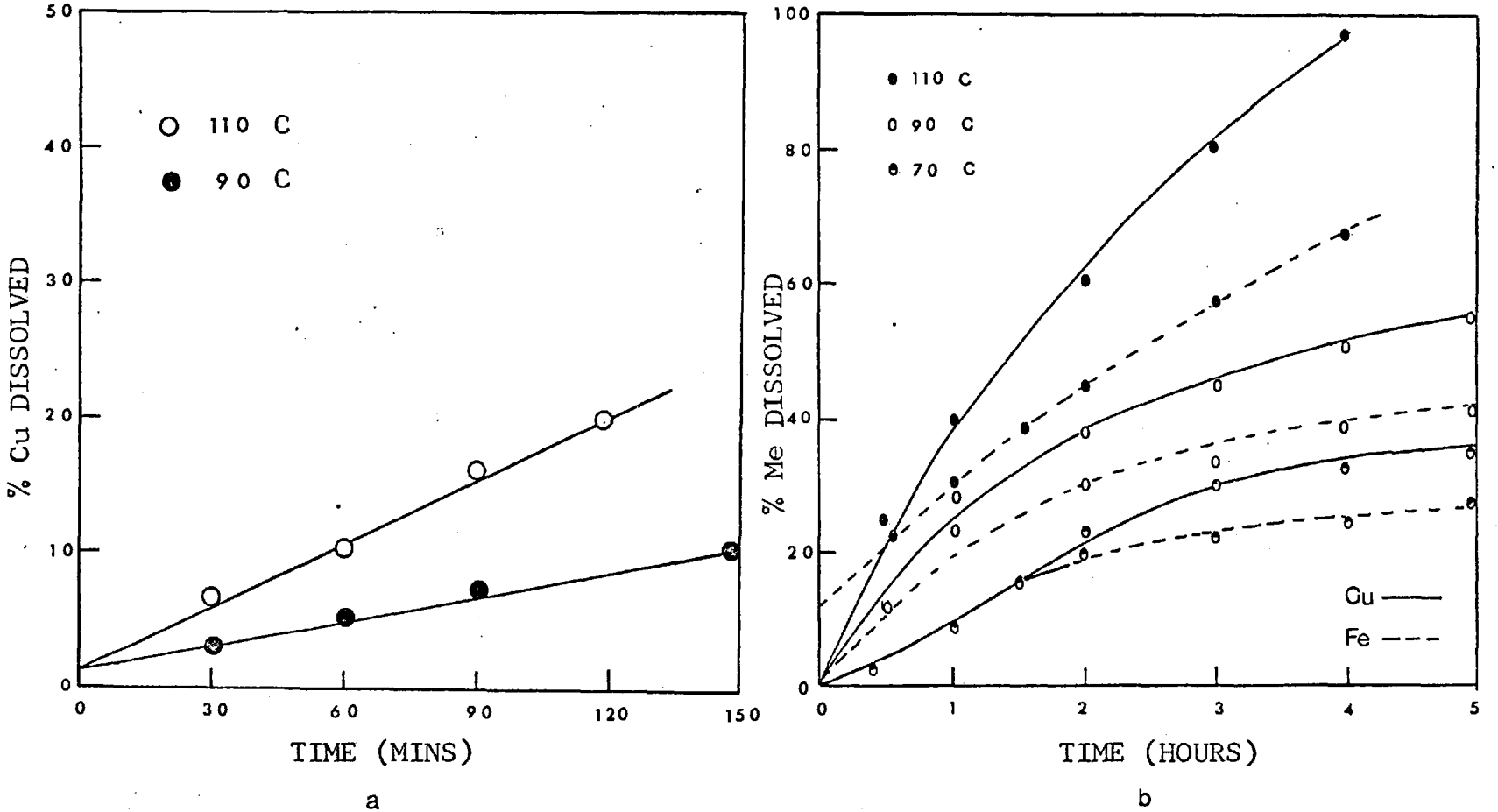

Fig.5 Pressure leaching of (a) chalcopyrite
(b) stannite (Gerlach et al.[66]).

was very slow and that the copper content in the solution followed a linear course. On the contrary, the leaching behaviour of stannite was much more complex. Only during the initial stage - with the exception of the test at 110°C - the copper and iron extraction rates were the same. After some time the copper content in the solution increased more than the iron content which was attributed to the precipitation of iron with tin as (Sn,Fe)(O,OH) The bending of the copper extraction curves and the transition to a linear course after about 90 miniutes was thought to be due to a blocking, especially of the active sites of the leach residue. The leach run at 110°C was extraordinary in that ten percent of the iron was already in the solution even before the addition of oxygen to the autoclave. For the kinetic calculations a reaction of the zeroth order was assumed for the leaching of chalcopyrite and a first order reaction was assumed for the leaching of stannite. Then, the rate equations were :

$$\frac{d(CuFeS_2)}{dt} = -k_1$$

and $$\frac{d(Cu_2FeSnS_4)}{dt} = -k_2 \; Cu_2FeSnS_4$$

where k_1 and k_2 are constants.

Table : 6 Leaching Property and Other Relavent Data for the Minerals Studied. (Gerlach et al.[66])

Substance	Leaching Property (%Me/hr)	E_A (kcal/mole)	Cond. $\Omega^{-1}cm^{-1}$	Lattice Param. A	Max. Atom Sp. A
CoAsS	25	10.3	0.17	a= 5.61	2.39
NiAsS	40	4.1	20.0	a= 5.71	2.41
NiSbS	85	7.1	66.7	a= 5.92	2.57
Pyrite	31	13.1	1.0	a= 5.42	2.26
FeAsS	45	10.4	1.1	a= 6.43	2.41
				b= 9.53	
				c= 5.66	
Marcasite	53	8.9	-	a= 3.39	2.25
				b= 4.45	
				c= 5.42	
ZnS	9	3.7	$5x10^{-11}$	a= 5.41	2.34
ZnSe	17	10.3	$6x10^{-11}$	a= 5.67	2.45
ZnTe	100	22.3	10^{-7}	a= 6.11	2.64
$CuFeS_2$	7	8.4	0.021	a= 5.25	2.32
				c= 10.32	
Cu_2FeSnS_4	36	11.0	0.0071	a= 5.47	2.43
				c=10.73	
Cu_3SbS_4	12	5.6	0.15	a= 5.28 or a=10.74	2.34
CuS	15	-	10.0	a= 3.79	2.35
				c=16.33	
NiS	26	-	5.0	a= 9.59	2.39
				c= 3.15	

The following values were reported for the apparent activation energy :

$CuFeS_2$: 8.4 kcal/mole

Cu_2FeSnS_4 : 11.0 kcal/mole

They introduced a new term called the "leaching property" to compare the leaching rates of the different minerals studied. This was defined as "the metal content in the solutions (in percentage) after one hour of leaching at 110°C with an oxygen partial pressure of 8 or 10 atmospheres". The introduction of this term was necessary, they said, because it was not possible to compare the velocity constants as different reaction orders were found for the minerals studied. Their results are presented in Table (6) together with the specific conductivity measurements and other relavant crystal lattice data.

Ignoring the two iron sulphides the following observations were made for individual sample series :

1. Within a series the leaching property increases with increasing specific conductivity.
2. The leaching property increases with the expansion of the unit cell of the minerals of the same series.

The improvement of leaching behaviour with higher specific conductivities was explained by correlating the leaching reaction with electrochemical corrosion.

On the solid surface "a local element formation" was assumed and to maintain the mass transport between anodic and catodic areas the material should have a certain conductivity. This was supported by the observation that the leaching property of some poorly conducting materials like ZnS could be improved by increasing their conductivity by UV-irradiation. However specific conductivity alone could not account for all the observations as was pointed out by the authors. The results of the series $CuFeS_2$ - Cu_2FeSnS_4-Cu_3SbS_4 show this point very well. The conductivities of these minerals are at least five orders of magnitude higher than those of the series ZnS - ZnSe - ZnTe. Nevertheless, all the minerals of the first series exhibit a poor leaching property. Moreover, sometimes even within the same series there is a marked anomaly. For axample, in the $CuFeS_2$ - Cu_2FeSnS_4 - Cu_3SbS_4 , series stannite, with a conductivity of 0.0071 $\Omega^{-1}cm^{-1}$ is expected to leach slower than chalcopyrite (specific conductivity 0.021 $\Omega^{-1}cm^{-1}$), but the observed leaching property of stannite is nearly five times larger than

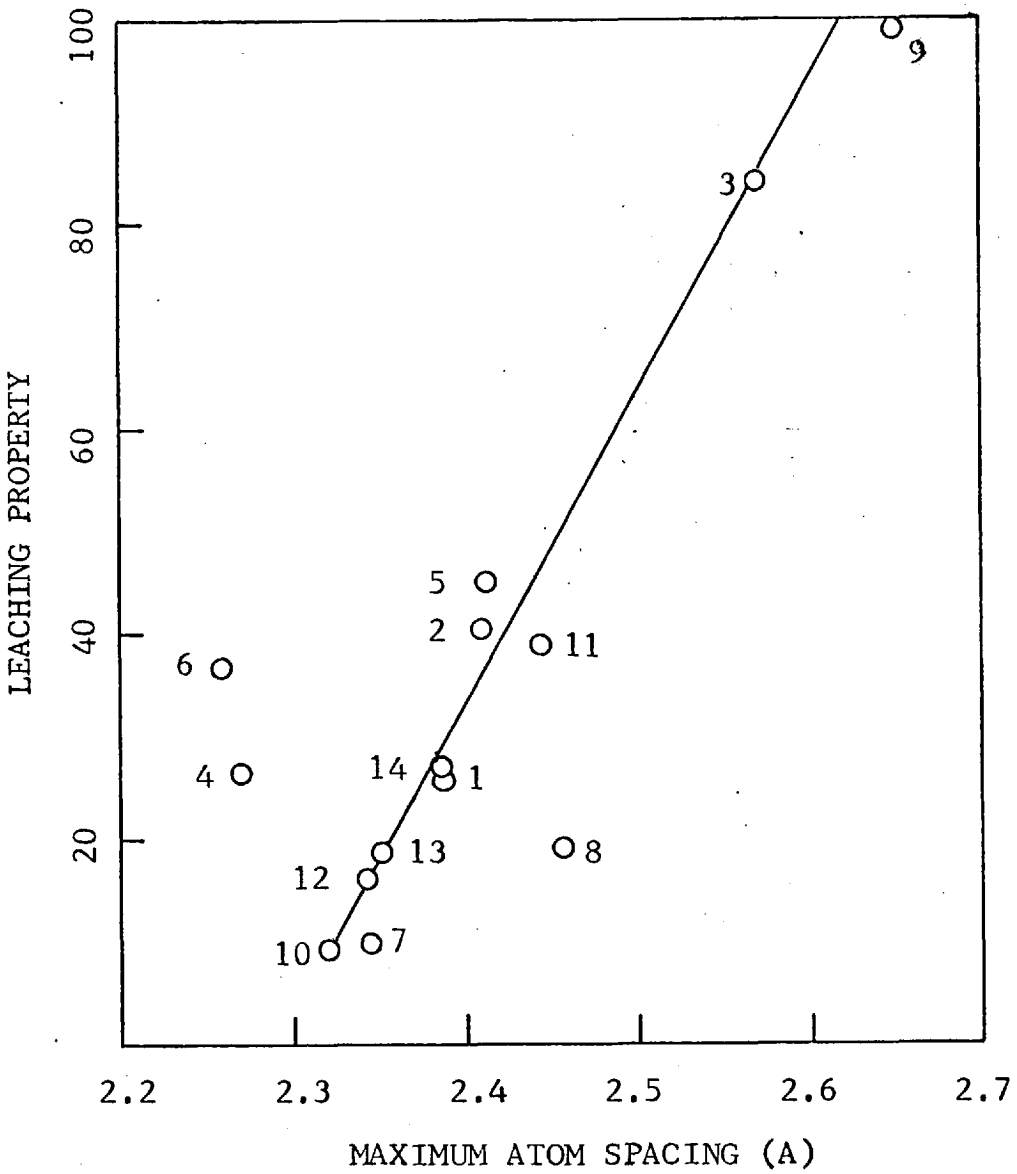

Fig. 6 Relation between leaching property and maximum atom spacing (Gerlach et al.[66])

1- CoAsS. 2- NiAsS. 3.NiSbS. 4- Pyrite

5- FeAsS. 6- Marcasite 7- ZnS 8- ZnSe

9- ZnTe. 10- $CuFeS_2$ 11- Cu_2FeSnS_4

12- Cu_3SbS_4 13- CuS 14- NiS

that of chalcopyrite. Therefore the authors safely concluded that "the conductivity alone is therefore a necessary but by no means a sufficient condition for describing the leaching behaviour of all those metallic compounds investigated."

In the pressure leaching of the test minerals in the sulphuric medium with oxygen as the oxidant, it was shown that for most cases, the adsorption of the dissolved oxygen on the solid matter forming an activated complex was the rate determining step. By analogy with the adsorption of gaseous hydrogen on carbon compounds, they stated that the adsorption process favoured if the atom spacing of the gas molecules to be adsorbed is considerably smaller than that of the adsorbant. Furthermore larger atom spacing in the solid matter favours the ensuing dissociation of the adsorbed gas molecules according to them.

A linear relationship was found between the leaching property and the maximum atom spacing (for stannite this represents the Sn - S distance) for most of the minerals as shown in Fig (6).

1.4 STRUCTURES OF STANNITES.

L.J. Spencer (1901)[67] was the first to publish a detailed study on the crystallography of stannite. His samples came from Bolivia and he reported extensive measurements of interfacial angles made on selected single crystals and deduced the crystalline symmetry of stannite to be Scalenohedral - Tetragonal. Also he reported the chemical composition of stannite as Cu - 31.52 %, Fe - 12.06 %, Sn - 27.83 %, and S - 28.59 % compared to the values Cu - 29.54 %, Fe - 13.01 %, Sn - 27.65 % and S - 29.80 % required by the formula : Cu_2FeSnS_4.

In a paper almost entirely devoted to the structure determination of chalcopyrite, Gross and Gross (1923)[68] suggested a crystal structure for stannite, based on Debye - Schrerrir diagrams. By analogy with a chalcopyrite structure derived by them, they proposed a tetragonal unit cell with $a_o = 5.577$ Å and $c_o = 5.180$ Å. The atom positions were Sn at 100, Fe at ½½0, 2Cu at ½0½, 4S positions were not indicated. (Fig 7). This structure leads to an axial ratio of a : c = 1 : 0.9287 whereas that obtained by the calculations based on Spencer's interfacial angle measurements is a : c = 1 : 0.9827. This discrepancy together with the need for accurate bond length data in sulphide minerals led Brockway[69] (1934) to undertake a detailed examination of the crystal structure of stannite.

Brockway carried out the structure determination by analysing Laue photographs and oscillation photographs obtained from single crystals of stannite of Bolivian origin. Laue photographs revealed the presence of two pairs of perpendicular symmetry planes separated by 45^{o}, which suggested D_{4h} as the X-ray point group symmetry of stannite. This information coupled with Spencer's observation that a four-fold reflection axis is present in stannite suggested the point group symmetry. D_{2d} . This inference was not conclusive, however, for two reasons. First, since copper and iron atoms have nearly equal scattering powers for X-rays, it was difficult to differentiate between the point groups D_{2d} and S_4 . (The two structures based on these point groups would have given very similar photographs. The structure with D_{2d} symmetry is changed to one with S_4 simply by interchanging the iron with half of the copper atom positions). Second, because good single crystals were not available, photographs taken along the c-axis with the available crystal which had only one developed face, could not firmly establish the presence of four vertical symmetry planes required by the point group D_{2d} . "In the absence of any positive discrepancy", he chose the point group symmetry of stannite to be D_{2d} .

Oscillation photographs taken with 45^{o} oscillation of the crystal about the c-axis from (110) using zirconia filtered Mo radiation afforded measurements on the equatorial zone and layer line spacings which lead to the values $a_o = 5.46$ Å and $c_o = 5.36$ Å. However at

least six faint but apparently real reflections occured which would require c_o to be doubled. This was subsequently confirmed by the fact that thirteen reflections were observed at $n\lambda$ values lower than 0.22 Å, compared to the lower limit of the incident radiation, 0.24 Å, assuming a unit cell with c_o = 5.36 Å. Therefore the true unit cell was assumed to have the dimensions :

$$a_o = 5.46 \text{ Å} \quad \text{and} \quad c_o = 10.725 \text{ Å}.$$

which represent the average of several measurements. These values give an axial ratio of a : c = 1 : 0.982 for the pseudo-cubic unit in agreement with Spencer's value of 1. : 0.9827.

The density of stannite calculated assuming the unit cell to contain two Cu_2FeSnS_4 units is 4.44 whereas that determined by Spencer was 4.45 gm cm^{-3}.

Detailed analysis of the photographs eliminated face centred and end centred lattices leaving a body centred lattice for the mineral. The only space groups based on this lattice and isomorphous with the point group D_{2d} are D_2^{11} - $I\bar{4}2$ m and D_2^{12} - $I\bar{4}2d$. Of the two, allowed reflections considerations eliminated D_2^{12}. Therefore the correct space group of stannite was taken to be D_2^{11} - $I\bar{4}2$ m. Based on this Brockway proposed a structure with the atom positions :

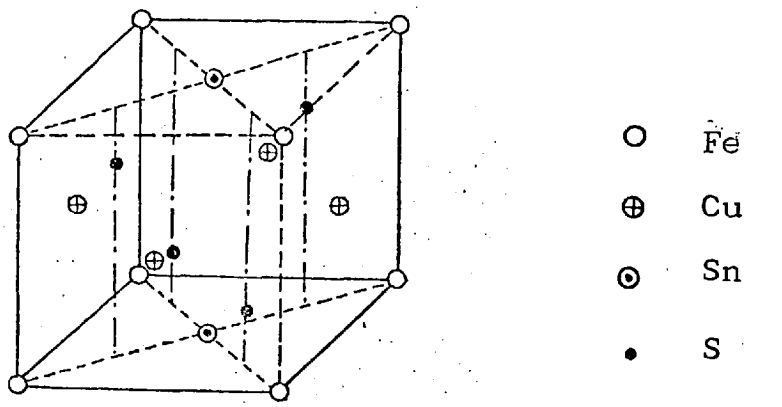

(a)

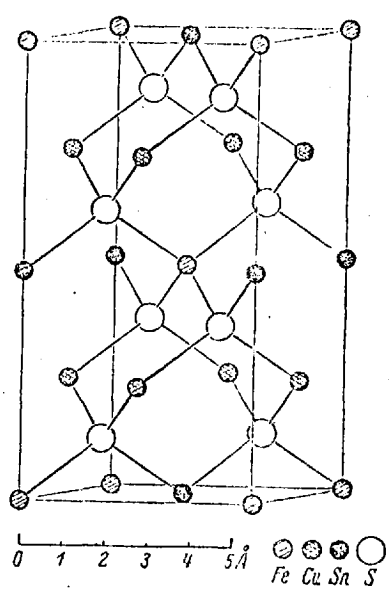

(b)

Fig. 7 Crystal structures of stannite (a) Gross and Gross[68]
(b) Brockway[69]

2Fe in 000 , $\frac{1}{2}\frac{1}{2}\frac{1}{2}$

2Sn in $00\frac{1}{2}$, $\frac{1}{2}\frac{1}{2}0$

4Cu in $\frac{1}{2}0\frac{1}{4}$, $\frac{1}{2}0\frac{3}{4}$, $0\frac{1}{2}\frac{1}{4}$, $0\frac{1}{2}\frac{3}{4}$

8S in UUV , $U\overline{UV}$, $U+\frac{1}{2}$ $U+\frac{1}{2}$ $V+\frac{1}{2}$, $U+\frac{1}{2}$ $\frac{1}{2}-U$ $\frac{1}{2}-V$,

$\overline{UU}V$, $\overline{U}V\overline{U}$, $\frac{1}{2}-U$ $\frac{1}{2}-U$ $V+\frac{1}{2}$, $\frac{1}{2}-U$ $U+\frac{1}{2}$ $\frac{1}{2}-V$

with $U = 0.245 \pm 0.002$ Å

$V = 0.132 \pm 0.002$ Å

The structure found by Brockway is closely related to those of chalcopyrite and sphalerite. Each sulphur atom is sorrounded by four metal atoms, two copper, one iron and one tin located at the corners of a not quite regular tetrahedron. Each metal atom is similarly sorrounded by four sulphur atoms. In contradistinction to chalcopyrite the copper atoms occupy planes by themselves. Smallest interatomic distances are :

Cu - S = 2.31 Å, Fe - S = 2.36 Å and Sn - S = 2.43 Å

The Cu - S and Fe - S interatomic distances were not in good agreement with the tetrahedral covalent radii sums of the individual atoms suggested by Pauling (1967)[69A] or by Van Vechtan and Phillips (1970)[ ]. The covalent radii sums are :

Cu - S = 2.39 Å , Fe - S = 2.23 Å , and Sn - S = 2.44 Å

It is interesting to note that the Fe - S distance of 2.36 Å in the proposed structure is much larger than that in chalcopyrite, 2.257 ± 0.03 Å, or in any other

iron - sulphur compound studied so far. No satisfactory explanation was offered by Brockway for the stability of a structure with such an anomolous bond distance.

The author cautiously pointed out that a structure based on the space group S_4^2, is as plausible in every respect as the one described above. The only difference lies in the interchange of the iron atoms with two of the copper atoms so that the copper atoms would no longer occupy planes by themselves. A complete test involving all possible parameter values for Cu-S, Fe-S and Sn-S distances was not attempted and therefore this second structure cannot be ruled out. However, in the absence of any prospective contender, the crystal structure of stannite is generally accepted to be that proposed by Brockway.

Mineralogists were aware of the occurence of different stannites in addition to the "normal stannites" as early as 1944. (Ramdohr 1944). However the present discussion is confined to stanite structures whose formulae approach that of normal stannite, ie. Cu_2FeSnS_4. Other forms will be treated at some length in a later section.

Claringbull and Hey (1955) succeded in isolating a form of stannite which they called "isostannite", and which was shown to be cubic by X-ray powder photographs. Although they did not publish their results, the present author was previledged to examine the original photographs by courtesey of Dr. M.H. Hey and was able to satisfy himself that isostannite is a cubic mineral.

In 1971 Ernst-Dieter Franz[70] reported two new stannite modifications. Both these were synthetic and they were characterised by X-ray diagrams and microscopic examination.

Stoichiometric amounts of the elements required by the formula Cu_2FeSnS_4 were placed in a silica tube which after sealing was maintained at 420°C for an unspecified time and was then quenched in water. The resulted mass was non-homogeneous and consisted of a cream to light brown isotropic phase, chalcopyrite and an orange substance in noticeable quantities. The isotropic phase was homogeneous and had the formula $Cu_2FeSnS_{3.95}$.. The complete X-ray powder pattern was presented which was indexed assuming a cubic unit cell with $a_o = 5.418$. This required a zinc blende structure with $z = 1$, in which metal atoms should be statistically distributed among the cation sites.(Sect. 3.1) However such a scheme was not consistent with the X-ray powder diagram of $Cu_2FeSnS_{3.95}$. The other indexing alternative was to double the value of a_o to $a_o = 10.837$ Å.. Then, since all the indices were even, which indicated a face centred lattice and since a great similarity with zinc blende was assumed, the space group T_d^3 - $I\bar{4}3$ m with $z = 8$ was assigned for the cubic phase. The density observed was $D_r = 4.438$ gm cm^{-3}.

DTA experiments carried out in a nitrogen atmosphere showed a strong endothermic reaction at 840 ± 5°C .

Franz thought that his synthetic cubic stannite was identical to isostannite of Claringbull and Hey.

Further synthetic experiments carried out at 600°C led to a non-homogeneous mass consisting of cubic $Cu_2FeSnS_{3.95}$, chalcopyrite and a new phase $Cu_2FeSnS_{3.9}$. The X-ray powder diagram, after leaving aside lines due to cubic $Cu_2FeSnS_{3.95}$ and chalcopyrite, could be indexed assuming a tetragonal lattice. The powder diagram differed markedly from natural stannite indicating that the atomic arrangement in the lattice is different. This was thought to have the chalcopyrite structure, which demands a disordered distribution of Fe and Sn atoms in the lattice. The lattice constants suggested by Franz are :

$a_o = 5.42$ Å $\quad c_o = 10.70$ Å $\quad z = 2$ and $D_{2d}^{12} - I\bar{4}2d$

Tetragonal stannite also showed an endothermic reaction at 840 ± 5°C .

Springer (1972)[71] published some interesting obsevations made in the course of a study to establish a phase diagram for the system stannite - kesterite (Cu_2FeSnS_4 - Cu_2ZnSnS_4) . He studied this system mainly by quenching experiments and Differential Thermal Analysis. The different phases were identified by X-ray diffraction reflected optical microscopy and less often by electron micro probe analysis. He noted that at 680°C stannite undergoes a structural transformation from a tetragonal structure to a different tetragonal

Table : 7 Features of Interest of Stannites With Approximate Composition Cu_2FeSnS_4

Stannite Form	Author	Stability Range of Temp. (^oK)	Symmetry	Comments
β-stannite	Springer 1972	Above 680^oC upper limit not reported	D_{2d}^{11} - $I\bar{4}2m$? Tetragonal	Moh reported a high temp. tetragonal form with similar X-ray pattern to r.t. form
α-stannite	Springer 1972 Franz 1971	Below 680^oC lower limit not reported	D_{2d}^{12} - $I\bar{4}2d$? Tetragonal	
Cubic stannite	Franz 1971	Around 420^oC	T_d^3 - $I\bar{4}3m$? F.C.C. ?	Same as isostannite (Claring Bull and Hey , 1955).
Normal stannite	Brockway 1934	?	D_{2d}^{11} - $I\bar{4}2m$ Tetragonal	

form. The phase stable above 680°C was called β-stannite and that which exists below this temperature was designated α . The α-form was different from β in that the lines 011 , 013 , 121 , 123 and 031 which were present in β were not found in the X-ray powder pattern of the α form. If these absences were systematic, he argued that in the α-form the reflections were present only if 1 is even, which would be incompatible with the accepted structure of stannite determined by Brockway. It seems that the α form of Springer is the same as the synthetic tetragonal form of Franz.

It is clear from the foregoing discussion that there exist at least four different forms of stannite with a formula approximately Cu_2FeSnS_4 . They are :

1. The β form of Springer, stable above 680°C.
2. The α form of Springer, probably the same as the tetragonal form prepared by Franz, stable below 680°C.
3. The cubic form synthesised by Franz.
4. The naturally occuring "normal stannite".

Available information on these different forms are summarised in Table (7).

More recent work suggests a higher temperature for the tetragonal-cubic transformation. (Bernhardt (1972)[72], Lee (1972)[73] and Bente (1974)[74]). They report the

inversion temprature as 706°C whereas Franz's work indicates that this should be below 420°C. The present work argrees well with his observation and does not confirm the existence of a cubic phase above 540°C. X-ray powder diagrams of the two phases, as reported by Bente, are reproduced in Tables (16 and 18).

The problem of ascertaining the valency states of copper, iron and tin in stannite was not attempted until at least 1966.

Smith and Zuckermann (1966)[75] published ^{119m}Sn Mossbauer spectra of eleven tin containing minerals, including a natural stannite sample from Cornwall. This was assumed to contain cassiterite as an impurity. The spectrum consisted of two singlets both at room temperature and at liquid nitrogen temperatures. However, judging from their published spectrum, the existence of a resonance peak at $\delta \sim 0$ is doubtful. This hardly visible peak may very well be due to the presence of cassiterite. On cooling the sample they observed that the ratio of areas under the two peaks changed from 5 : 1 to 3 : 1 and that the value of the higher isomer shift changed by about 3 percent. Comparison of the observed isomer shifts with those of the tin compounds of known valence enabled them to conclude that there are two types of tin nuclei in stannite, both in the Sn (iv) state. The predominant amount of tin is present in an environment which resembles that in SnS_2, the remainder is in a symmetrical environment to that of

SnO_2 . It must be stressed, however, that their inference regarding the SnO_2 type tin is valid only if the minor peak at $\delta \sim 0$ is real.

Mossbauer effect studies with ^{57}Fe and ^{119}Sn nuclei supplemented by magnetic susceptibility measurements were used by Eibschutz et al.[76] (1967) to determine the cation valencies of synthetic stannite. The mineral was synthesised from elements and was shown to belong to the space group $I\bar{4}2\,m$ with unit cell constants $a_o = 5.466 \pm 0.005$ Å and $c_o = 10.76 \pm 0.01$ A by X-ray powder photographs.

The Mossbauer spectrum of ^{119}Sn consisted of only a single resonance peak indicating the presence of only one type of tin. The isomer shift value, δ found was 1.48 mm sec^{-1} with respect to a $BaSnO_3$ source, which fall within the isomer shift range reported for the most covalent tin halides SnI_4 and $SnBr_4$.

(SnI_4 - $\delta = 1.55$ Ionicity 15%
$SnBr_4$ - $\delta = 1.15$ Ionicity 23%
Greenwood[77], Hill and Day[78])

They concluded that tin is present as Sn (iv) (ie. $4d^{10}$ configuration).

^{57}Fe Mossbauer spectra were obtained covering the temperature range 80 to 600°K. The isomer shifts observed were in the lower regions of isomer shift values reported for divalent iron (ie. $3d^6$ configuration). Further studies carried out with a series of synthetic

sulphides showed that the isomer shifts of sulphides were generally lower than those of the corresponding oxides indicating a high degree of covalency in sulphides. The quadrupole splitting observed, 2.87 mm sec^{-1} was rather large which suggested non-cubic symmetry of the electron cloud aroun the iron nucleus. Following crystal field arguments, they said that the ground orbital doublet E_g of the Fe^{+2} in the tetrahedral environment splits into two orbital singlets.

Magnetic susceptibility measurements showed that the mineral obeyed the Curie - Weiss law and the paramagnetic Curie temperature Θ , and the Curie constant C were determined. Derived value of C agreed well with the computed spin-only C value assuming monovalent copper and divalent iron as shown in Table (8).

Θ (^{o}K)	C_{obs} (emu.grad/mol.oe)	C_{calc}	
		$Cu_2^{+}Fe^{2+}Sn^{4+}S_4$	$Cu_2^{2+}Fe^{2+}Sn^{2+}S_4$
-82±3	3.09 ± 0.03	3.00	3.75

Table : 8 Curie Constants (Eibschutz et al.)

Therefore they concluded that the cation valencies in stannite are Cu^{+} , Fe^{+2} , and Sn^{+4} .

Greenwood and Whitfield (1967)[79] studied the ^{57}Fe Mossbauer effect on natural stannite and they concluded that "in stannite , Cu_2FeSnS_4 the chemical isomer shift and quadrupole splitting parameters are consistent with ferrous ions in tetrahedral co-ordination and non-cubic point symmetry.".

The existence of divalent iron in stannite was demonstrated by Russian workers Marfunin and Mkrtchyan[80] (1966) and was later confirmed by Marfunin and others[81] (1967) by ^{57}Fe Mossbauer studies. The relatively large values of isomer shifts and quadrupole splitting of stannite compared to other sulphides were attributed to the presence of an 'ionic' radical $(SnS_4)^{4-}$ in stannite. They studied the complex sulphides, wurtzite (ZnS : Fe), sphalerite (ZnS : Fe), pentlandite (Fe(Ni)S), cubanite ($CuFe_2S_3$), stannite (Cu_2FeSnS_4), berthierite ($FeSb_2S_4$), bornite (Cu_5FeS_4) and the tetragonal and cubic forms of chalcopyrite ($CuFeS_2$). Bornite and chalcopyrite had very low isomer shifts ie. 0.51 , 0.63 and 0.60 mm sec^{-1} , and therefore they were thought to contain Fe^{+3}, on the assumption that isomer shifts lower than 0.7 mm sec^{-1} indicate the presence of Fe^{+3} . Pentlandite and cubanite which are known to contain Fe^{+2} had very low isomer shift values (0.64 and 0.71 mm sec^{-1}) closer to Fe^{+3} . The explanation given was as follows : The Fe - S bonds are strongly covalent and there is a formation of π - bonds with empty d-orbitals of sulphur effectively

creating a Fe^{+3} environment about the iron nuclei, which produces low isomer shifts. Stannite and berthierite had exceptionally large isomer shift values in comparison to typical values characteristic of sulphides (0.3 to 0.4 mm/sec rel.to Fe), which were in the vicinity of 'ionic' iron salts. In these minerals, the sulphur atoms bonded to the iron atom formed bonds with "highly charged" Sb^{+3} and Sn^{+4} ions, according to them. These ions draw the electron cloud of sulphur in their direction polarising the Fe - S bond leading to an increase in the ionic character of the σ bond with susequent weakening of the π bonds. As a result complex ions $(SnS_4)^{-4}$, $(SbS_2)^{-4}$ and Fe^{+2} are isolated in these compounds. In sphalerite, wurtzite, berthierite and stannite the nuclear quadrupole splitting at $80^{o}K$ is large. Consequently the ground state of the Fe^{+2} ion in these compounds is an orbital singlet. The strong temperature dependence of quadrupole splitting observed for these compounds indicated that either the axial component of the crystal field is not large, or there is a substantial rhombic component of the crystal field.

The same authors, Marfunin and Mkrtchyan(1968)[82] studied the ^{119}Sn Mossbauer effect of stannite mineral samples from Etyka (Siberia) and Czechslovakia. The spectrum consisted of a single line, the isomer shift relative to - β -tin being -0.5 mm sec^{-1} . No quadrupole splitting was observed. The chemical isomer shifts of sulphides and oxides of tin reported in the literature

Table : 10 ^{57}Fe Mossbauer Spectroscopy Data for Stannite.

Author	Sample	Source	Temp. (^{o}K)	Isomer Shift(mm/sec)	Quad. pole splt(mm/sec)	Isomer shift rel. to Fe metal
Eibschutz et al. 1967	Synthetic	^{57}Co in Pd	r.t. ?	0.26 ± 0.02	2.87 ± 0.03	0.445
Greenwood and Whitfield 1967	Natural	Sodium nitro-prusside	295	0.83	2.90	0.573
Marfunin and Mkrtchyan 1967	Natural	Stainless steel	300 80	0.87 0.93	2.76 3.20	0.78 0.84
Borshagovski 1968	Natural	Sodium nitro-prusside	300 80	1.00 1.06	2.76 3.20	0.743 0.803
Goncharov et al 1970	Natural	Stainless steel	r.t. ?	0.78 ± 0.01	3.00 ± 0.02	0.69
Vaughan and Burns 1972	Synthetic. ann at 592^{o}C	Fe metal	300 300	0.62 0.37	2.78 0.00	0.62 0.37
	Synthetic ann at 700^{o}C	Fe metal	300 300	0.57 0.34	2.90 0.00	0.57 0.34

are presented in Figure 8 .

Since the isomer shift is negative relative to β-tin, this element must be present as Sn(iv) and since the numerical value of isomer shift is low compared to SnO_2 and SnS_2, the Sn - S bond in stannite should be covalent, they suggested. According to them the valency states of cations in stannite are represented by $Cu_2^{+}Fe^{+2}Sn^{+4}S_4$. Also the Fe - S bond in this are less covalent than in most sulphides while the Sn - S bonds are highly covalent.

Another Russian work appeared in 1970 (Goncharov, Ostanevich and Tomilov)[83] dealing with the ^{57}Mossbauer spectra of a number of complex sulphides including stannite. After a detailed discussion of the theoretical aspects of the subject, they suggested a scheme whereby the oxidation state of iron in these sulphides could be easily identified. They plotted the chemical isomer shift δ , against the Fe - S bond distance and found that they are linearly related. From their diagram (Figure 9) it is seen that sulphides with a common oxidation state of iron fall in a separate straight line and the lines representing ionic and covalent bonds have opposite slopes.

Stannite lay in the 'Fe^{+2} ionic' line on this diagram.

Also they calculated, theoretically, the quadrupole splitting for some minerals assuming the presence of Fe^{+2}. (Table 9)

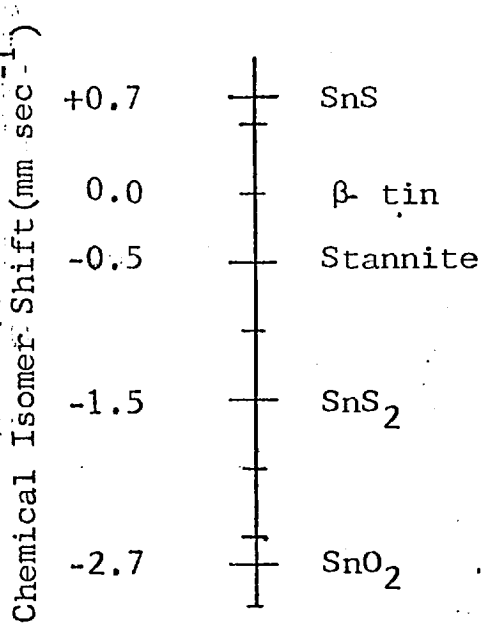

Fig. 8 Mossbauer data for tin compounds.

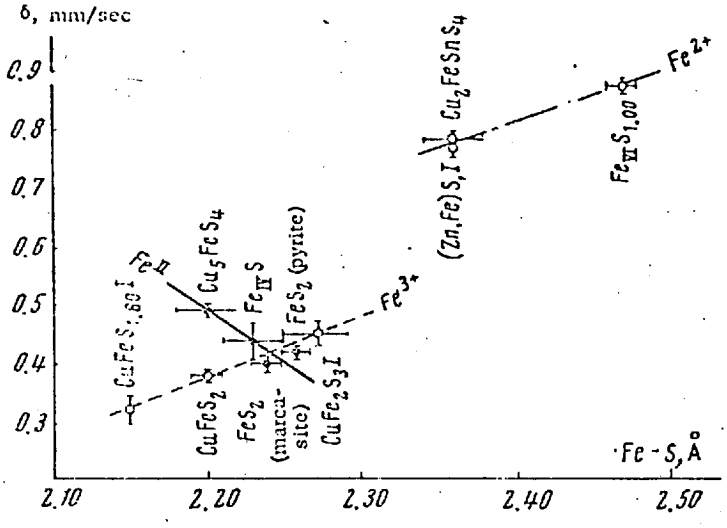

Fig. 9 Correlation of the chemical shift value (δ) of Fe^{57} in sulphides with the length of the Fe-S bond. (Goncharov et al.[83])

Stannite Valency States	E_{calc}(mm sec^{-1})	E_{obs}(mm sec^{-1})
$Cu_2^{+2}Fe^{+2}Sn^{+2}S_4^{-2}$	0.29	3.00
$Cu_2^{+1}Fe^{+2}Sn^{+4}S_4^{-2}$	1.00	

Table : 9 Mossbauer Data (Goncharov et al.[83])

Although their arguments are not very clear, they concluded that these results indicate the iron to be in a $3d^6$ configuration.

In a paper entitled "Mossbauer Spectroscopy and Bonding in Sulphide Minerals Containing Four-Coordinated Iron" Vaughan and Burns (1972)[84] reported the results of two synthetic stannite samples. The samples were annealed at 592°C and 700°C and quenched. Isomer shifts they obtained were comparable to those reported by Eibshutz et al. and Greenwood but were remarkably lower than those published by the Russion workers. Their conclusion was that iron is present as high spin Fe (ii) in stannite.

The results of the various authors are summarised in Tables (10) and (11). To facilitate comparison ^{57}Fe isomer shifts are readjusted relative to an iron metal standard and ^{119}Sn isomer shifts are adjusted relative to a SnO_2 source.

From these tables it is evident that the results of different authors are not in good agreement. If the discrepancy between the isomer shifts reported for natural stannite samples and synthetic specimens is

Table : 11 ^{119}Sn Mossbauer Spectroscopy Data For Stannite.

Author	Sample	Source	Isomer Shift (mm/sec)	Quadrupole Splitting	Isomer Shift Relative to SnO_2
Smith and Zuckermann (1966)	Natural	SnO_2	0.00 ± 0.06	-	0.00
			1.34		1.34
Eibschutz et al. (1967)	Synthetic	$BaSnO_3$	1.48 ± 0.06	-	1.48
Marfunin and Mkrtchyan (1968)	Natural	β-Sn	-0.5	-	2.06
Goncharov et al. (1970)	Natural	SnO_2	1.5 ± 0.1	-	1.50

real, it follows that the bonding in the two forms is significantly different. It must be mentioned however that no satisfactory bonding scheme is available for stannite as yet. In the light of this observation the following remarks can be made regarding the 'nature of the chemical bond' in stannite.

1. The valency states of the cations are : Cu = i , Fe = ii , Sn = iv . All workers agree on this.

2. The anomalously high Fe - S interatomic distance suggests a unique electronic environment about the iron nuclei in stannite, although the exact nature of this is obscure. The quadrupole splitting observed in ^{57}Fe Mossbauer spectroscopy indicates a non-symmetrical electronic environment and therefore it may be that the iron atom is in the centre of a not quite regular tetrahedron of four sulphur atoms.

3. The Fe - S bond and Sn - S bond cannot be described as purely 'covalent' or 'ionic'. The latter exhibits a very high degree of covalency while the former is marginally ionic - ie. has more than 50% ionic character.

4. The nature of the electronic environment about the tin nuclei remains bizarre. Although a quadrupole splitting is not observed in the ^{119}Sn Mossbauer spectrum, which generally implies a symmetrical electronic environment it may not necessarily be so, in view of the fact that no quadrupole splitting is obtained for any of the tetravalent tin compounds studied.

1.5 PHASE RELATIONS.

1.5.1 Stannite Series of Minerals.

Paul Ramdohr (1944)[85] was the first to bring to light the complexity of this group of minerals. He described at least four different stannite-like minerals in addition to the normal stannite. He designated them as Mineral - I , Mineral - II , Mineral - III and Mineral - IV and his descriptions of these are briefly discussed here.

Mineral - I .

A hexagonal phase with a structure very similar to wurtzite, with a_o = 3.84 A and c_o = 12.6 A. It is brown rose (Braun rosa) in colour, strongly anisotropic and vividly pleochroic. Now this mineral is known as "hexastannite".

Mineral - II

This is isotropic, superficially very similar to normal stannite. He predicted that this could be a high temperature transformation product of stannite. Claringbull and Hey (1955) succeeded in isolating a form of stannite which they called "isostannite" and was shown to be cubic by X-ray powder photographs. Their terminology is the one that is generally accepted for this mineral today.

Mineral - III

This is relatively rare and is anisotropic. It is similar to stannite but has a faint tint towards pink grey. The structure resembles that of Mineral - I viz. hexagonal, with a_o = 3.85 A and c_o = 12.65 A .

Mineral - IV

This is isotropic, has a fahlore structure with a_o = 10.35 A .

In his book Ramdohr (1960)[86] gives the X-ray powder diagrams of these four minerals.

Moh (1960)[87] and later Moh ant Ottemann (1962)[88] adopted a synthetic approach to the problem. They compared the different stannites collected from hundreds of localities throughout the world with synthetic specimens . They showed that hexastannite, (Mineral - I) has the formula Cu_6FeSnS_8 and not $Cu_3Fe_2SnS_6$ as suggested by Ramdohr. Their description of isostannite (Mineral - II , cubic) is less straightforward. They were not able to prepare this form synthetically in a pure state. One synthetic sample was found to have a chemical composition identical with normal stannite. The other cubic forms, they report three of these, are substances either with foreign elements or whose chemical composition is not definitely established. They suggested without experimental justification that isostannite could be a thermal transformation product of stannite. They

report one cubic form $Cu_2(Cu , Fe , Sn) SnS_{3-4}$ which is said to result from cooling a normal stannite sample from about 900°C to room temperature. Finally there is Cu_2FeSnS_3 which was synthesised at 500°C in Li - K - Cl melts. Minerals - III and IV were suspected to contain considerable proportions of foreign elements, notably silver. They suggested that mineral - III is $CuAgSnFeS_4$ with a tetrahedral structure and not hexagonal.

Claude Levy (1967)[89] published the results of a detailed study concerning a number of naturally occuring copper - iron - tin sulphides from different localities. Chemical analysis, X-ray powder patterns, and curves of reflecting power are presented for the following minerals.

1. Normal Stannite

All but one of his samples contained zinc upto a maximum of 5.2%.

2. Yellow Stannite

So named because of its orange colour. Exhibited much stronger anisotropy than normal stannite. All samples contained Zn upto 4.6%.

3. Orange Bornite

Not related to bornite as the name suggests. The mineral is usually found between grains of bornite.

4. Mawsonite

A relatively new mineral. First described by Markham and Lawrence (1965)[90] , who assigned the formula $Cu_7Fe_2SnS_{10}$.

Table : 12 Comparison of X-ray Powder Diagrams of Mineral 1, Yellow Stannite and Stannoidite

Mineral 1 (Ramdohr)		Yellow Stannite (Levy)		Stannoidite(Kato)	
d (A)	I/I_o	d (A)	I/I_o	d (A)	I/I_o
		11	10		
		5.4	10	5.4	5
		5.1	10	5.14	1
		4.8	20	4.83	10
		4.1	10	4.13	3
		3.7	10	3.72	2
3.08	90	3.1	100	3.11	100
3.00	10	3.0	10	3.00	3
		2.80	10		
2.67	40	2.69	20	2.70	15
				2.46	2
2.38	10	2.39	10	2.39	4
				2.20	2
2.08	50			2.12	1
				2.00	2
1.892	100	1.901	90	1.906	70
1.785	30	1.79	10	1.795	2
		1.69	10		
1.618	80	1.621	50	1.621	20b
1.553	20	1.554	20	1.556	3
1.482	20				
		1.344	20	1.346	1

5. Kesterite : Cu_2ZnSnS_4

6. Idaite

Traditionally Cu_5FeS_6 . But Levy showed that the true formula is Cu_3FeS_4 .

He concluded that mawsonite and orange bornite are in fact the same mineral. Normal stannite, yellow stannite, orange bornite (mawsonite) and idaite could be regarded as being members of a continous series whose general formula is $Cu_{2+x}FeSn_{1-x}S_4$, x varying from 0 to 1. According to this scheme ;

$x = 0$	for normal stannite
$0 < x < 0.5$	for yellow stannite
$0.5 < x < 1$	for orange bornite
$x = 1$	for idaite .

In 1968 Kato[91] described a new Cu - Fe - Sn - S mineral which he named stannoidite from Konjo mine,Japan. A single crystal X-ray study showed that the mineral is orthorhombic with unit cell constants $a_o = 10.76 \pm 0.02$ A , $b_o = 5.40 \pm 0.01$ A and $c_o = 16.09 \pm 0.04$ A . Electron microprobe analysis led to a formula $Cu_5(FeZn)_2SnS_8$ or $Cu_5Fe_2SnS_8$. The X-ray powder diagrams, optical properties and other physical properties when compared to those of mineral - I of Ramdohr (hexastannite) and the yellow stannite of Levy showed striking similarity. The X-ray powder diagrams are presented in Table (12) to bring out

this point (d values of Mineral - I in Table (12) are the ones recalculated from 2θ values of Ramdohr assuming he used unfiltered Fe radiation). Kato concluded that stannoidite is the same as the yellow stannite of Levy. He further suggested that stannoidite may also represent Mineral - I of Ramdohr, which seems very plausible.

In the same year Springer (1968)[92] published the results of analyses of stannite, mawsonite, hexastannite and a new mineral he called rhodostannite. Most of the stannite samples had compositions close to Cu_2FeSnS_4 though deviations from this were not uncommon. All samples contained zinc, the atomic ratio Cu : (Fe + Zn) : Sn was not always 2 : 1 : 1 but the total metal to sulphur ratio remained 1: 1 .

The three mawsonite samples he analysed had almost identical formulae, close to $Cu_6Fe_2SnS_8$. Although this was slightly different from that of Markham and Lawrence $Cu_7Fe_2SnS_{10}$, it agreed with that given by Levy : $Cu_{5.94}Fe_{1.89}Sn_{0.98}S_{8.20}$.

Hexastannite from two different localities had different formulae : $Cu_8(Fe,Zn)_3Sn_2S_{12}$ for Bolivian samples and $(Cu,Fe,Zn)_{11}(Sn,Sb,As)_2S_{12}$ for samples from Peru. These are very close, though not identical, to that suggested by Kato for stannoidite. Springer also described a new mineral from Vila Apacheata, Bolivia which he called "rhodostannite" because of its red colour. It had a formula $Cu_2FeSn_3S_8$. The X-ray powder pattern is presented in Table (14). Kato suggested that the X-ray

Table : 13 Members of the Stannite Series.

Mineral	Other Names	Formula	Crystallography	Comments
Stannite	Zinkies (Ger)	Cu_2FeSnS_4	Tetragonal	Undergoes thermal transformations cubic $\xrightarrow{500}$ tetragonal $\xrightarrow{700}$ tetragonal
Isostannite	Zinkies II Cubic stannite	Cu_2FeSnS_4 (?)	Cubic	Possibly a high temp. idiomorph of norm. stannite
Hexastannite	Zinkies I Stannite jaune Stannoidite	$Cu_3Fe_2SnS_6$ (Ram) $Cu_8Fe_3Sn_2S_{12}$ (Spr.) Levy, M&L, Moh $Cu_5Fe_2SnS_8$ (Kato)	Hexagonal Tetragonal Orthorhombic	Kato's crystallography generally preferred.
Mawsonite	Bornite orange	$Cu_7Fe_2SnS_{10}$ (M & L) Levy $Cu_6Fe_2SnS_8$ (Spr.)	Pseudocubic	
Rhodostannite	-	$Cu_2FeSn_3S_8$ (Spr.)	Hexagonal (?)	

Table : 14 X-ray Powder Patterns of Stannites.

Stannite (Cu/Ni) ASTM (B & T)		Isostannite (Fe/Mn) Franz		Mawsonite (Co) Markham		Stannoidite (Cu/Ni) Kato		Rhodo-St. (Cu/Ni) Springer	
d (A)	I/I_o	d (A)	I/I_o	d (A)	I/I_o	d (A)	I/I_o	d (A)	I/I_o
								6.09	40
								5.93	60
		5.42	1			5.40	5		
5.37	5			5.37	20				
						5.14	1		
4.85	5					4.83	10		
				4.37	20				
						4.13	3		
		3.82	10	3.80	10				
						3.72	2		
								3.64	16
				3.34	10				
3.12	100	3.12	100			3.11	100	3.12	100
				3.09	100				
						3.00	2	2.99	6
				2.875	20				
2.71	30	2.70	30			2.70			
				2.68	50				
								2.58	50
2.46	5					2.46	2		
		2.42	20						
				2.395	10	2.39			
2.38	5								
								2.37	4
								2.31	2
				2.287	10				
2.21		2.21				2.20			

Table : 14 contd...

				2.185	5				
						2.12	1	2.12	4
				2.098	5				
						2.00	2		
								1.993	10
				1.959	5				
1.922	70								
		1.917	80					1.917	4
						1.906	70		
				1.895	80				
								1.837	20
								1.819	30
		1.802	10						
						1.795	2		
				1.788	5				
								1.755	2
				1.739	5				
		1.715	5						
1.642	40							1.637	2
		1.633	50						
1.626	30					1.621	20b		
				1.618					
								1.583	2
1.570	10								
		1.562	10						
						1.556	3		
				1.547	10				
		1.504	3						
								1.498	2
				1.460	5				
		1.447	5						
1.368	20								
		1.355	2						
1.347	20					1.346			

Table : 14 contd.....

				1.343	20				
		1.312	5						
		1.277	5						
1.245	30	1.243	30						
				1.232	30				
		1.211	10						
				1.201	5				
		1.183	5						
		1.160	3						
1.114	30								
1.105	10	1.106	40						
		1.083	5						
		1.063		1.065					
1.048									
		1.043							
1.037									
				1.034					
		1.007	5						
		0.991	5						
0.967	5								
0.958	10								
				0.950	20				
				0.908					

powder pattern may be satisfactorily indexed assuming a hexagonal unit cell with a_o = 7.27 A and c_o = 18.07 A .

It is clear from the foregoing discussion that the stannite series of minerals constitute a very complex mineral group. Our knowledge of the chemistry and crystallography of its members is far from complete. Table (13) summarises some information of the minerals of this group whose identity is well established. The formulae are only representative, noticeable deviations being quite common. Also extensive substitution by 'foreign' elements especially zinc, and many others like antimony and arsenic, is the rule rather than the exception.

1.5.2 The System Fe - Sn - S

Moh found that around 400°C only three ternary phases are stable.

1. Sn_5FeS_6 : A grey, darker phase than SnS. Strongly anisotropic and pleochroic. Softer than SnS, and has rhombic symmetry.

2. Fe_3SnS_4 : Pseudocubic, probably tetragonal. Darker than Sn_5FeS_6 . Colour - brown to grey.

3. Fe_5SnS_6 : Similar to pyrrhotite in colour. Distinctly anisotropic.

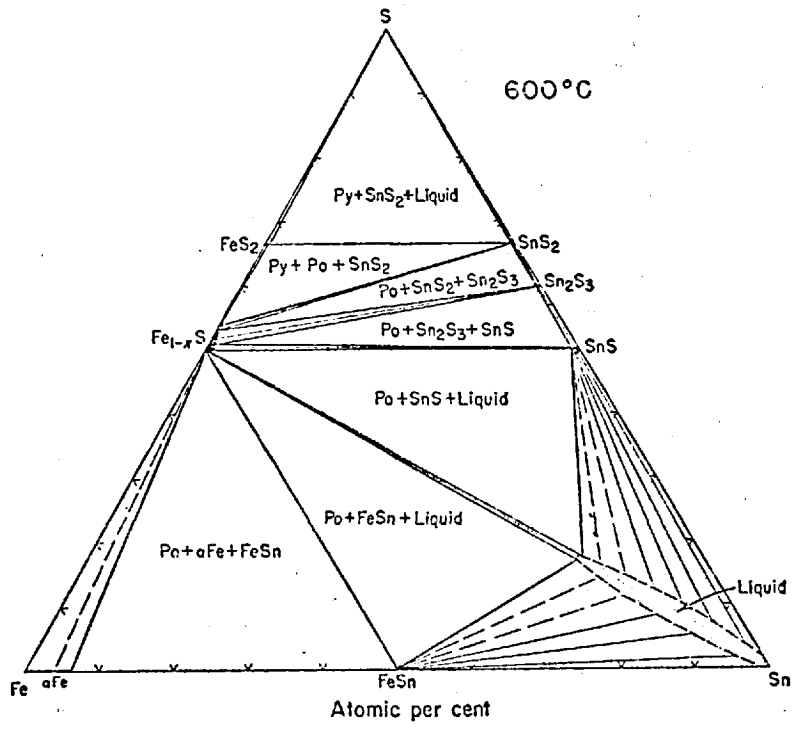

Fig. 10 Phase relations for the system Fe-Sn-S at 600°C. (Moh[93])

No ternary phases were found at 600°C[93] . The stable phases were pyrrhotite - $Fe_{1-x}S$, and pyrite - FeS_2 on the Fe - S join ; herzenbergite - SnS, Sn_2S_3 and SnS_2 on the Sn - S join; and α - Fe solid solution with upto 6 atomic percent tin, hexagonal FeSn and liquid on the Fe - Sn join. Solid solution between different phases were generally of the order of 1 percent or lower.

Phase relations at 600°C are given in Fig. (10).

1.5.3 The System Cu - Sn - S.

Moh claimed to have observed several ternary phases around 400°C in this system.

1. Cu_3SnS_4 : This is the most stable phase. Strongly anisotropic and pleochroic.
2. Cu_5SnS_6 : Dissociated above 550°C. Hexagonal.
3. $CuSnS_2$: Similar to stannite. Dissociated above 400°C.
4. Sn_5CuS_6 : It was not possible to obtain in pure form. Completely dissociated above 400°C.

At 600°C, the binary phases are digenite - chalcocite Cu_9S_5 - Cu_2S on the Cu - S join; and herzenbergite SnS, Sn_2S_3 and SnS_2 on the Sn - S join. In addition, a number of phases exist on the Cu - Sn join; α -copper containing 0 to 8.9 atomic percent Sn ; a cubic β phase

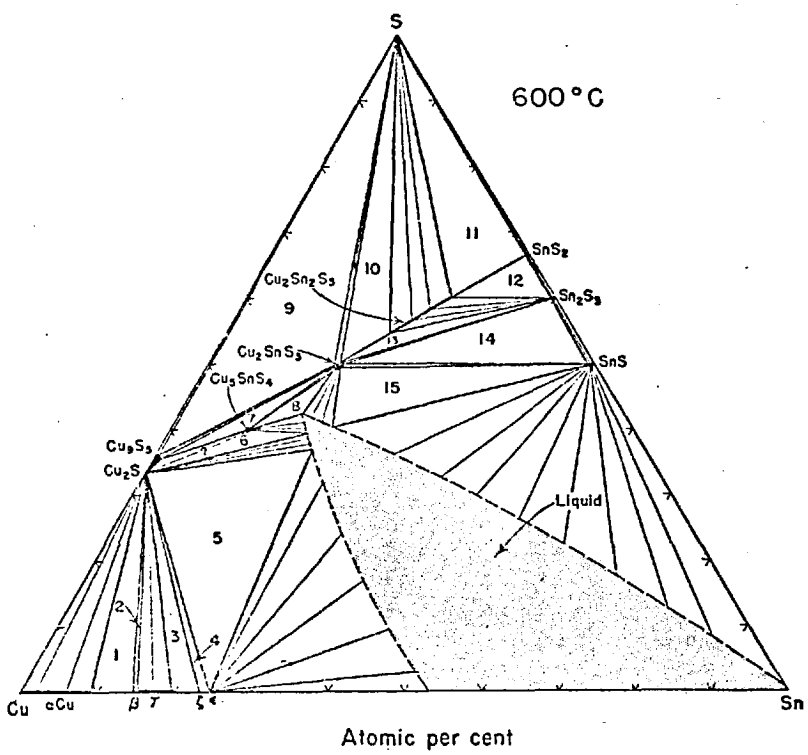

At 600°C a large liquid field exists in the Cu-Sn-S system. Two ternary phases, Cu_2SnS_3 and $Cu_2Sn_2S_5$, are stable at this temperature. The univariant assemblages, all including vapor in addition to the phases listed below, are: 1, αCu + β phase + Cu_2S. 2, β phase + γ phase + Cu_2S. 3, γ phase + ζ phase ($Cu_{20}Sn_6$) + Cu_2S. 4, ζ phase ($Cu_{20}Sn_6$) + ϵ phase (Cu_2Sn) + Cu_2S ss. 5, ϵ phase (Cu_3Sn) + Cu_2S ss + L. 6, Cu_2S ss + Cu_3SnS_4 + L (experiments indicate that the relations in this field are more complicated than indicated here). 7, Cu_9S_5-Cu_2S ss + Cu_3SnS_4 (tin bornite) + Cu_2SnS_3 ss. 8, Cu_3SnS_4 (tin bornite) + Cu_2SnS_3 ss + L. 9, Cu_2S_5 ss + L + Cu_2SnS_3 ss. 10, Cu_2SnS_3 ss + L + $Cu_2Sn_2S_5$ ss. 11, $Cu_2Sn_2S_5$ ss + L + SnS_2. 12, $Cu_2Sn_2S_5$ ss + SnS_2 + Sn_2S_3. 13, Cu_2SnS_3 ss + $Cu_2Sn_2S_5$ ss + Sn_2S_3. 14, Cu_2SnS_3 ss + Sn_2S_3 + SnS. 15, L + Cu_2SnS_3 ss + SnS.

Fig. 11 Phase relations for the system Cu-Sn-S at 600°C. (Moh[93])

with 14.9 percent tin; a cubic γ-phase with about 15.5 to 20.0 percent tin; a hexagonal ε-phase $Cu_{20}Sn_6$; and orthorhombic ζ-phase Cu_3Sn and liquid. At this temperature two stable ternary phases exist.

1. Cu_2SnS_3 : Has the tetragonal lattice. This at $780 \pm 3^{o}C$ inverts to a cubic form that melts incongruently at $842 \pm 3^{o}C$.

2. $Cu_2Sn_2S_5$: This is non-cubic and anisotropic, forms a large field of solid solution which has not been studied in detail.

Phase relations are presented in Fig. (11).

1.5.4 Some Binary Systems.

Naturally occuring intergrowths of chalcopyrite and stannite are well known, but experiments carried out at $700^{o}C$ in KCl - NaCl melts showed that stannite dissolved only a little chalcopyrite. On the other hand chalcopyrite formed a continous mixture series with stannite upto a composition $Cu_4Fe_3SnS_8$ with 66.66 mole percent of chalcopyrite.

Phase diagrams for the binary systems stannite - kesterite, stannite - briarite and stannite - sphalerite are presented in Figs. 12 - 15.

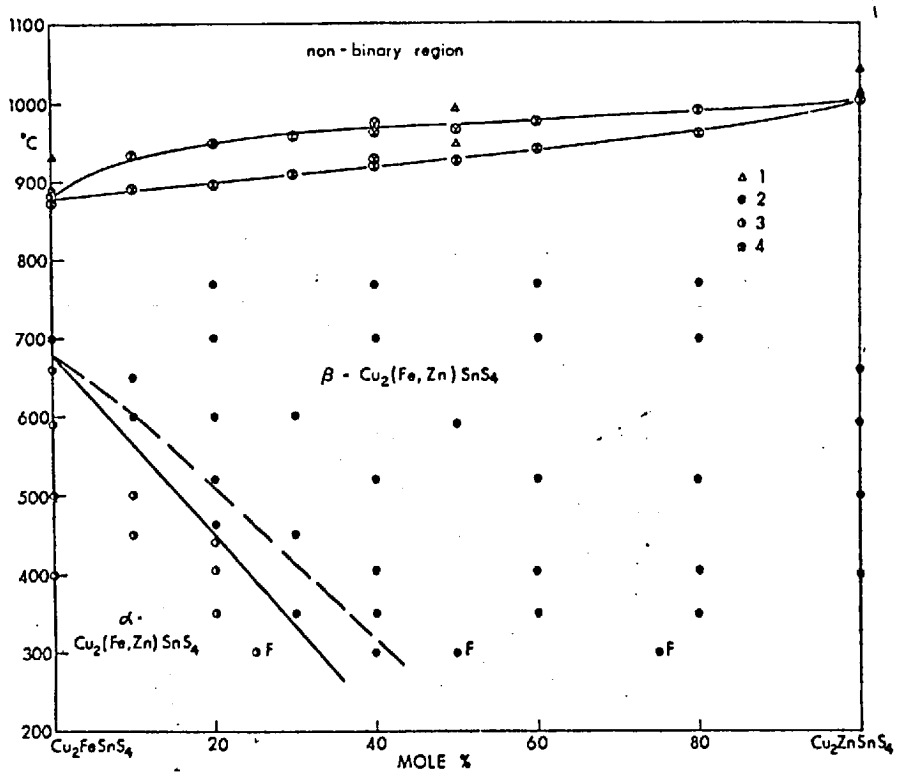

Fig. 12 Phase diagram stannite-kesterite.
(Springer[71])

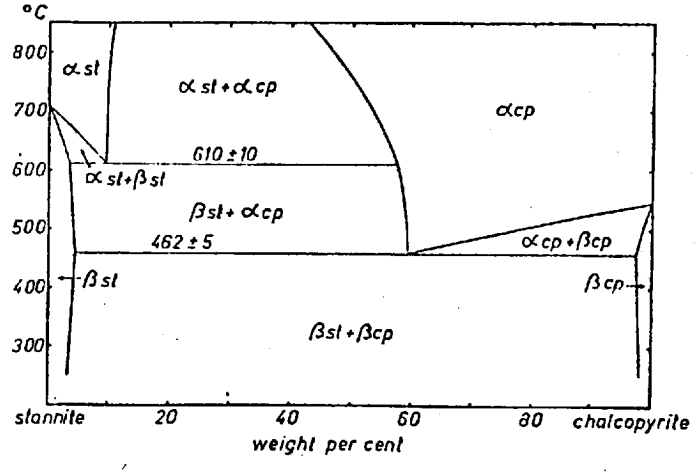

Fig. 13 Phase diagram stannite-chalcopyrite.
(Bernhardt[72])

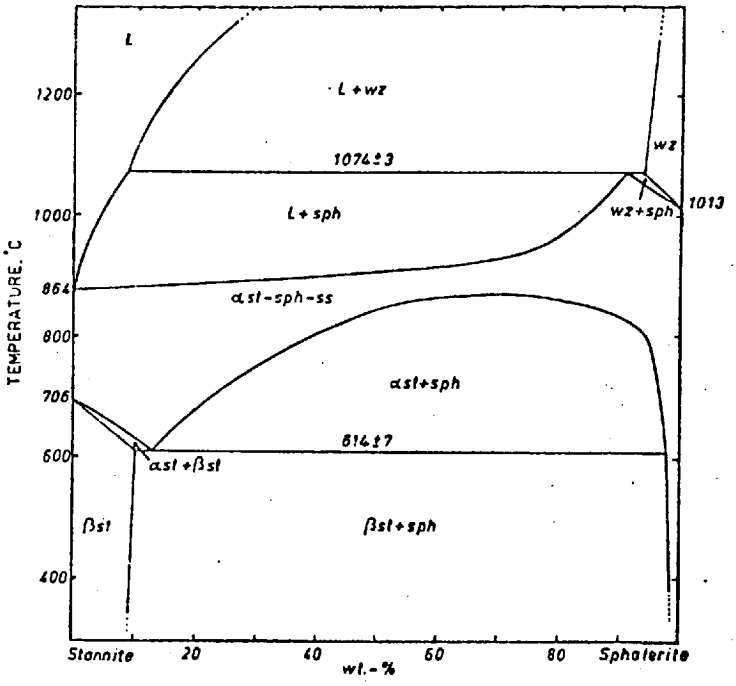

Fig. 14 Phase diagram stannite-sphalerite.
(Lee[73])

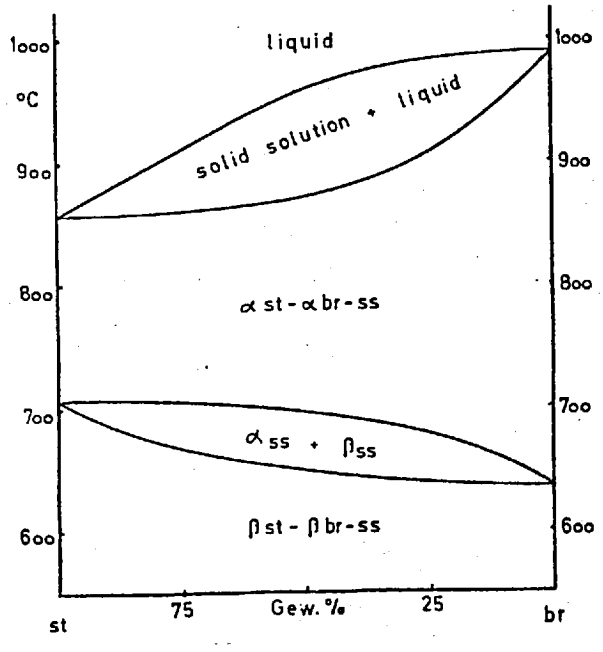

Fig. 15 Phase diagram stannite-briarite.
(Bente[74])

1.6 PREVIOUS WORK ON THE SYNTHESIS OF STANNITE.

The first reported synthesis of stannite was carried out by Moh who sintered the elements at 500 - 600°C for 10 to 14 days.

A rather unorthodox procedure was adopted by Nekrasov[94] for stannite synthesis. This was done in an autoclave, with the pH regulated by HCl, NH_4Cl and NaOH ; from $SnCl_2.2H_2O$, $FeCl_2.4H_2O$, $Na_2S.9H_2O$ and CuO. Mixtures of these four components were reacted at temperatures ranging from 200 to 550°C for 140 to 1460 hours. Some stannites he obtained had compositions considerably different from the stoichiometric formula. Some of his analyses are presented in Table (15).

Samples 1 and 2 (in Table 15) have compositions close to normal stannite Cu_2FeSnS_4 ; sample 3 has it near mawsonite $Cu_7Fe_2Sn_3S_8$; sample 4 is rhodostannite $Cu_2FeSn_3S_8$ and sample 5 is hexastannite $Cu_8Fe_3Sn_2S_{12}$. There is no known mineral which has a composition found for either 6 or 7. Therefore he stated that stannite is a member of a continous solid solution series.

Nitsche et al.[95] prepared stannite crystals by a novel method, involving crystal growth from the vapour phase by chemical transport with iodine. Stoichiometric amounts of the elements were reacted in sealed quartz tubes at 1100°C in the presence of 5mg of iodine per cc., the metals being transported via the gaseous iodides in

a temperature gradient of 800 to 750°C. The crystals were obtained as black plates (5 x 5 x 0.1 mm). The same workers extended this method for the crystal preparation of a number of chalcogenides of general formula :

$$A_2^{I}\,B^{II}\,C^{IV}\,X_4^{VI}$$ where A = Cu , B= Zn , Cd... , Fe , Mn , Ni; C = Si , Ge , Sn and X = S and Se

Element	1	2	3	4	5	6	7
%Cu	30.0	28.2	44.0	14.7	38.9	22.4	36.3
%Fe	18.1	16.3	11.2	8.8	11.3	38.0	8.8
%Sn	22.5	26.7	13.3	41.5	18.6	10.8	17.8
%S	30.0	29.1	31.2	32.3	29.3	29.0	36.8

Table : 15 Synthetic Stannite Analyses (Nekrasov[94])

SECTION 2

EXPERIMENTAL PROCEDURES

2.1 SYNTHESIS OF NORMAL STANNITE.

The standard method in use in the Hydrometallurgy Group, Royal School of Mines, for the synthesis of copper iron sulphides, by holding mixtures of pure elements in two compartment silica tubes at high temperatures, was not successful for stannite synthesis.

A horizontal tube electric furnace designed to reach 1100°C was used for the attempted synthesis, with a central zone of constant temperature. Power supply to the furnace was controlled by a eurotherm temperature controller which enabled temperature control within ± 2°C.

Spectrographically pure copper and tin rods, sulphur powder and iron sponge were used as starting materials. Iron sponge was reduced in a stream of hydrogen for three hours at 550 - 600°C prior to synthesis. After cleaning a copper rod mechanically and chemically, using emery papers and dilute hydrochloric acid to remove surface corrosion products, it was weighed and placed in acetone. From the weight of the copper rod, the stoichiometric amounts of other elements needed to prepare Cu_2FeSnS_4 were calculated. Only mechanical cleaning was employed to clean the tin rods.

The calculated weight of sulphur was accurately weighed and was transferred to the small compartment of the silica tube. Then it was positioned horizontal and the iron powder plus a small quantity of tin powder (less than 5mg) needed to make-up the exact weight of tin were introduced by means of a special funnel and a powerful magnet. It was necessary to keep apart the sulphur and iron powders initially to avoid a possible explosion which may result from the extremely vigorous reaction between iron powder and molten sulphur. Copper and tin rods were placed last in the large compartment and the tube was immediately connected to an oil diffusion pump. When the lowest pressure was attained, about 0.00004 mm of mercury, the tube was sealed off with an oxygen torch while the pump was still working.

The sealed silica tube was placed in the furnance. The temperature of the silica tube was measured with a Pt - 13%Rh/Pt thermocouple placed inside the furnance and in contact with the tube. The potentiometer used was a Croydon Type 4 connected to the thermocouple with compensating wires. The furnance temperature was increased stepwise to 600°C in four days. Past experience has been that in the synthesis of copper iron sulphides in similar systems the initial reaction between sulphur vapour and the other elements was complete in three days at temperatures around 600°C.

Even after six days of heating at 600°C, sulphur vapour was still visible.

The furnace was switched off and the tube was allowed to cool. Examination of the contents by X-ray diffraction revealed the presence of the following phases : FeS_2 , $Fe_{0.99}S$, SnS_2 , CuS , Cu_5FeS_6 (idaite) , SnS , metallic tin and several unidentified ones. However the important observation was that practically all the tin remained unreacted whereas no free iron or copper was detected.

On thermodynamic grounds tin was expected to react with sulphur to form sulphides at these temperatures although only traces of them were found. Therefore it was evident that a layer of sulphides of copper and iron covered the surface of molten tin preventing it from reacting with sulphur. Data concerning the diffusion of tin in copper or iron sulphides are not available in the literature. Diffusion coefficients for copper and iron in Cu_2S and FeS are of the order of 10^{-7} to 10^{-9} cm^2/sec. It is not known if the self diffusion coefficients of metals bear any correlation to the diffusion of the corresponding cations in ionic compounds. The self diffusion coefficients of copper and iron quoted by Jost[96] are :

$$D_{Cu} = 11 \exp\left(\frac{-57,200 \text{ cal}}{RT}\right) \text{ cm}^2 \text{ sec}^{-1} \qquad (750 - 950^{\circ}C)$$

$$D_{Fe} = 3.4 \times 10^4 \exp\left(\frac{-77,200 \text{ cal}}{RT}\right) \text{ cm}^2\text{sec}^{-1} \qquad (715 - 887^{\circ}C)$$

Fron these the self diffusion of copper and iron at 700°C are calculated as 6.4×10^{-12} cm^2sec^{-1} and 6.4×10^{-13} cm^2sec^{-1} .

Richardson quotes the expression :[50]

$$D_{Sn} = 3.0 \times 10^{-4} \exp\left(\frac{-2,580 \text{ cal}}{RT}\right) \text{ cm}^2\text{sec}^{-1}$$

for the self diffusion coefficient in molten tin in the temperature range 267 to 683°C. At 700°C, self diffusion coefficient is 7.9×10^{-5} $\text{cm}^2\text{sec}^{-1}$.

This means that diffusion of tin in sulphides is the controlling factor for which no data exists.

It would have been possible to bring about a reaction between sulphur and tin by raising the temperature. Ugarte showed that at 750°C the pressure inside the tube could be as high as 25 atm. This approach was therefore abandoned. An independent test was done to check the feasibility of the preparation of stannous sulphide. Stoichiometric amounts of tin and sulphur were placed in a small silica tube and was vacuum sealed. The sulphur was slowly melted and the contents were thoroughly mixed by slowly rotating the tube. Then it was heated in a muffle furnace at 600°C for 12 hours. X-ray diffraction of the products showed 100% conversion to SnS. This clearly demonstrated that as long as tin and sulphur were in contact during heating, stannite synthesis is possible. At the same time contact between sulphur and iron had to be avoided for safety reasons.

Based on these prerequisites two procedures were developed for stannite synthesis.

1. Stoichiometric amounts of copper, iron, tin and sulphur were placed in the two-compartment

silica tube in the usual way, already described, and heated at 600°C for three days so that all the iron and copper were converted to their sulphides. The tube was then removed from the furnace and the unreacted sulphur was cautiously melted down to the large compartment with a Bunsen burner. The constriction between the two compartments was then sealed and the smaller one was removed. The tube was placed in the furnace after thoroughly mixing the contents. The temperature was raised to 600°C and after about 12 hours no more sulphur vapour was visible indicating the initial reaction was complete. Finally the temperature was brought to 1025°C after leaving at 800°C for two days. At this stage stannite was molten.

The system was left at around 1000°C for two days.

Then the temperature of the furnace was gradually reduced to room temperature in four days.

2. Stoichiometric amounts of tin and sulphur corresponding to SnS, calculated from the weight of a copper rod, were placed in the large compartment of a silica tube and this was vacuum sealed. It was then heated at 600°C for three days until no more sulphur vapour was visible. The tube was then removed from the

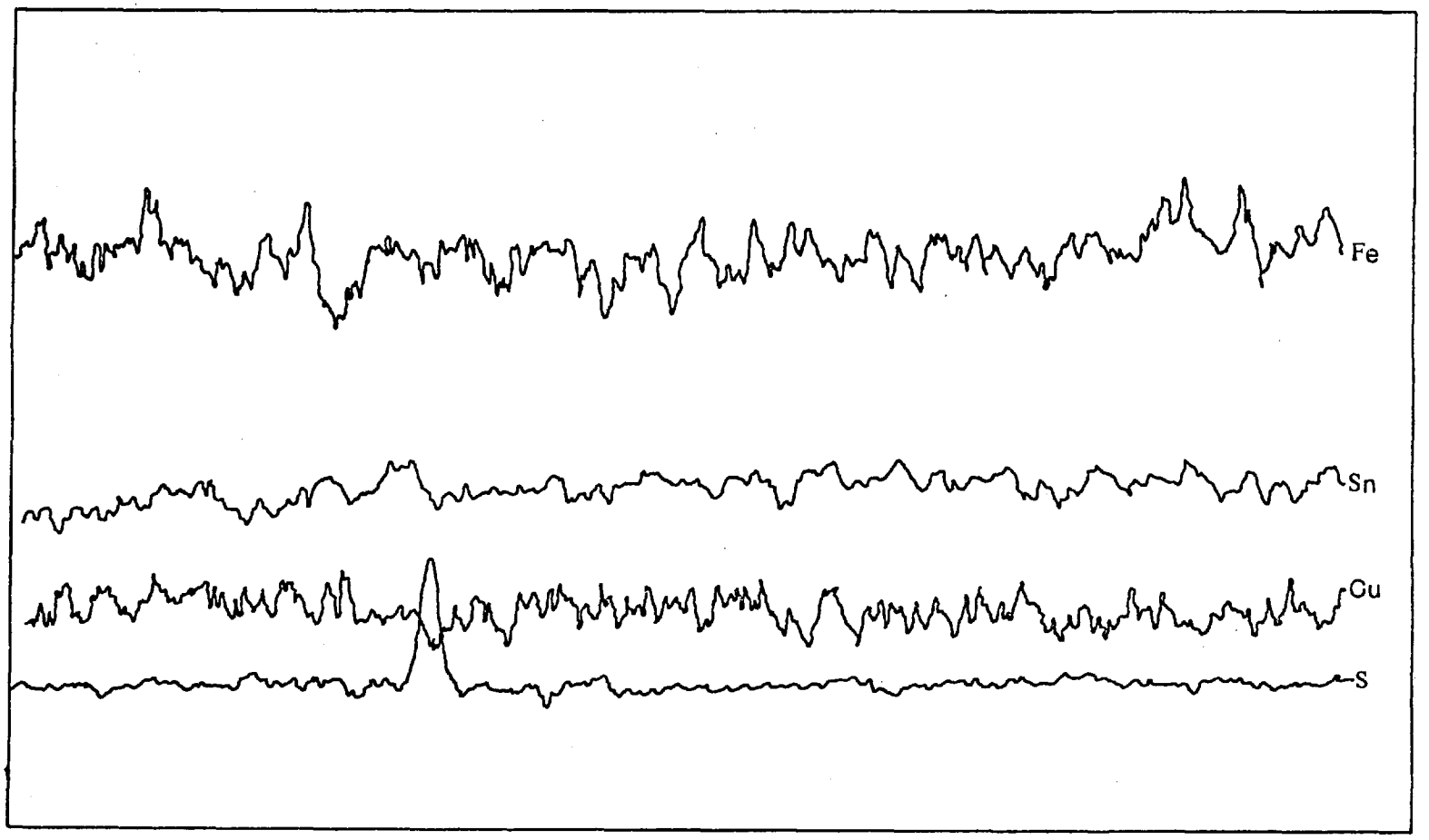

Fig. 16 Electron probe scan across the grain of normal stannite examined.

furnace and the rest of the sulphur required by the formula Cu_2FeSnS_4 was introduced to the small compartment while iron and copper were placed in the large one. (Special devices were designed for this). After vacuum sealing, the tube was subjected to the same heat treatment as in the first procedure.

All the experiments described in this thesis were done with stannite synthesised by procedure 1 .

The synthetic material was black and had a striking metallic lustre. It was very brittle and showed weak anisotropy. Under crossed nicols it was distinctly pleochroic, the colour change being from pink to blue. However the pleochroism was weaker than in the naturally occuring mineral.

Microscopic observation of polished sections taken at random from the bulk showed no evidence for the presence of a second phase, and the mineral appeared to be very homogeneous. This was checked by electron microprobe analysis. Traces made across polished sections for Cu , Fe , Sn and S showed exceptional homogeneity. Fig. 16.

2.2 LEACHING APPARATUS AND EXPERIMENTAL PROCEDURE.

The leaching apparatus used is illustrated in Fig. (17). It consisted of a Quickfit wide neck reaction vessel of capacity 250 ml., joined to a five-necks lid by a metallic clip. The central neck held a mercury (or silicone oil) seal and the shaft of a glass stirrer, which was a simple two blade propeller mixer.

In the other four necks of the lid were an efficient water condenser to minimise evaporation losses, a glass baffle to produce a turbulent regime and to maintain the mineral particles in suspension, a thermometer to check the temperature of the medium, and in the fourth neck, a tube for sample removal. The thermometer was placed exactly opposite to the baffle, in order to have a symmetric baffling of the solution.

The whole system was immersed in an oil bath to the level of the vessel-lid joint.

The oil bath used was a 27 cm wide, 52 cm long Tecam (CTB 2) constant temperature bath. Some specifications of this bath are as follws :

Heater size	2000 watts
Temperature range	60 to 130°C
Temperature sensitivity	± 0.05°C

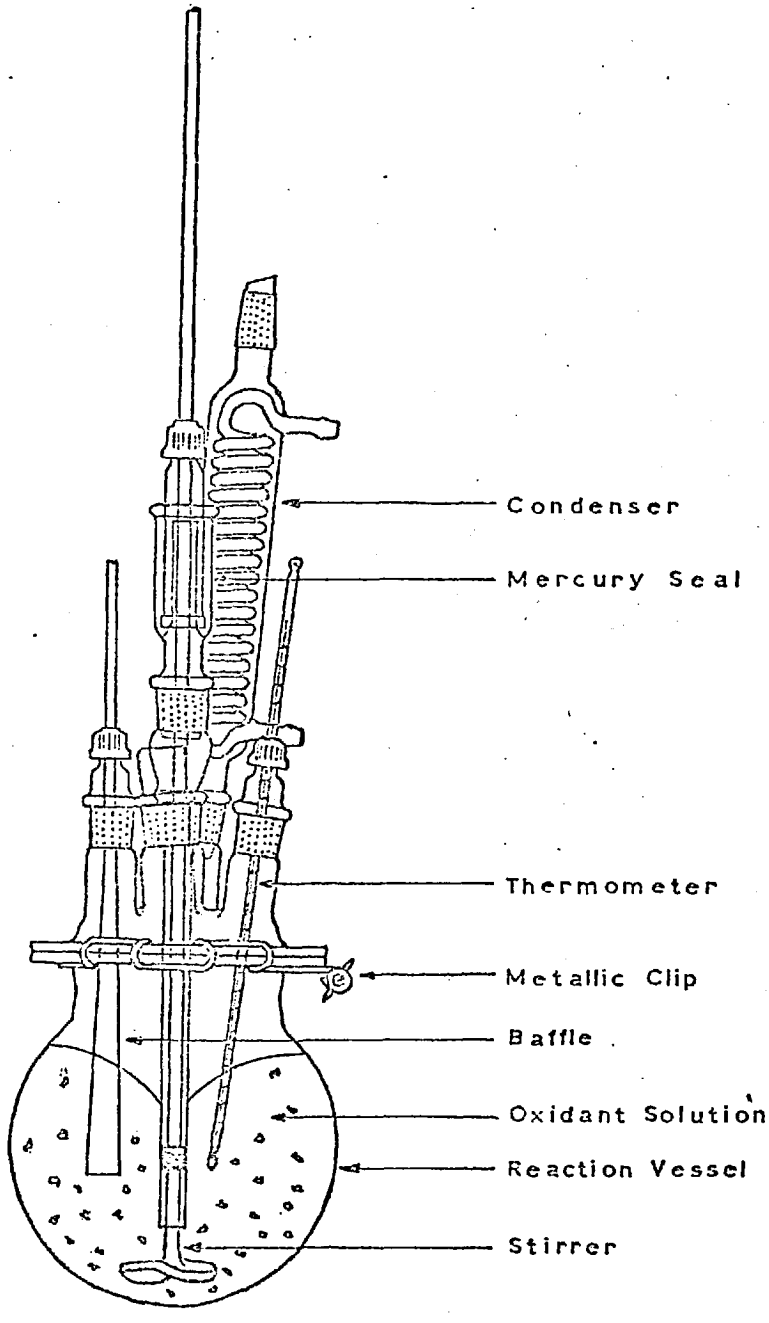

Fig. 17 Leaching apparatus.

For some runs at high temperatures, especially at 95°C, the oil bath had to be avoided for pollution reasons. In such cases the solution temperature was maintained using an electric heating mantle, with the power supply manually controlled. Then the temperature control attainable was only ±0.5°C.

The stirrer was connected by a strong rubber tube to a RTZ motor of variable speed between 170 to 1700 rpm.

The leaching procedure was as follows :

Once the apparatus was assembled, 200 ml of the leaching solution was introduced to the reaction vessel and was allowed, usually by leaving overnight, to reach thermal equilibrium. Miniutes before starting a run, the mineral was crushed in an agate motar and screened using 100 mm diameter stainless steel sieves to the required particle size ranges. With the leaching solution at the required temperature, an accurately weighed amount of the sieved mineral was introduced to the reaction vessel. After about a miniute the stirrer motor, whose rotation speed had been checked stroboscopically, was switched on.

Aliquots of leach liquor were extracted periodically, more frequently at first. The samples, extracted with a 2 ml pipette, were diluted with 0.5 M hydrochloric acid and analysed for Cu and Sn using the atomic absorption spectrophotometer.

Every time a sample was removed, an equal volume of oxidant was added to maintain a constant volume and oxidant amount during a run.

At the end of the leaching run the reaction vessel was dismantled and the contents filtered through Whatman filter paper no: 542 . The volume of the final leach liquor was noted and the Cu and Sn contents corrected accordingly. The solid residue was washed several times with 0.5 M hydrochloric acid and stored in a desiccator after drying at room temperature.

2.3 ANALYSIS OF SOLUTIONS.

The samples removed during the leaching runs and the final leach liquours were analysed for copper, tin and sometimes iron using atomic absorption spectrophotometry. Copper and iron were analysed with a single beam Perkin Elmer Model 290 B instrument. For tin, a Perkin Elmer Model 306, a double beam instrument was used.

The wave lengths used were 324.7 nm for copper, 248.3 nm for iron and 224.6 nm for tin. Mostly copper, iron and tin, single element hollow cathode lamps were used for analyses. Copper and iron analyses in the same solution were carried out with a Au - Cu - Fe - Ni - Cr multi-element hollow cathode lamp.

Manufacturer's instructions were strictly adhered to in all analyses. An air - acetylene mixture was adjusted to obtain a lean blue (oxidising) flame for copper and iron analyses and a slightly yellow flame was used for tin analyses.

Calibration curves of deflection against concentration were drawn using standards prepared from 1000 ppm stock solutions. Tin standards were prepared in 10% v/v hydrochloric acid. Calibration curves showed that linear working range was up to about 5 ppm for copper and iron while for tin it extended up to 100 ppm.

Sample solutions were diluted to within this range using a Hook and Tucker variable diluter, and for accurate work more conventional means, pipettes, volumetric flasks etc. were used.

Some solutions were analysed for the sulphate ion. Nephelometric technique gave erroneous results because of the interference from the amorphous tin containing precipitate. Therefore an indirect method involving atomic absorption spectrophotometry was used. The sulphate was precipitated as barium sulphate by a known excess of $BaCl_2$, and the unreacted barium was subsequently determined by atom absorption.

Two stock solutions were prepared, one containing 1 mg/ml of sulphate ion by dissolving K_2SO_4 in distilled water. The other containing 1 mg/ml of barium by dissolving the required amount of $BaCL_2$ in a high-chloride aqueous medium. The solvent consisted of 50 ml of concentrated HCl , and 20 gm of KCl dissolved in 1 litre of distilled water. A high chloride concentration is necessary to ensure barium chloride dissolution. For barium determination a nitrous oxide - acetylene flame must be used, and at the high flame temperature , barium tends to ionise. Potassium prevents this by preferential ionisation.

Sulphate standards were prepared by mixing 0.1 , 0.2 , 0.3 , 0.4 and 0.5 ml of standard sulphate solution (1000 ppm) with 0.5 ml. of standard barium solution (1000 ppm) and diluting to 25 ml. in volumetric flasks.A typical calibration curve is given in Fig. (18)

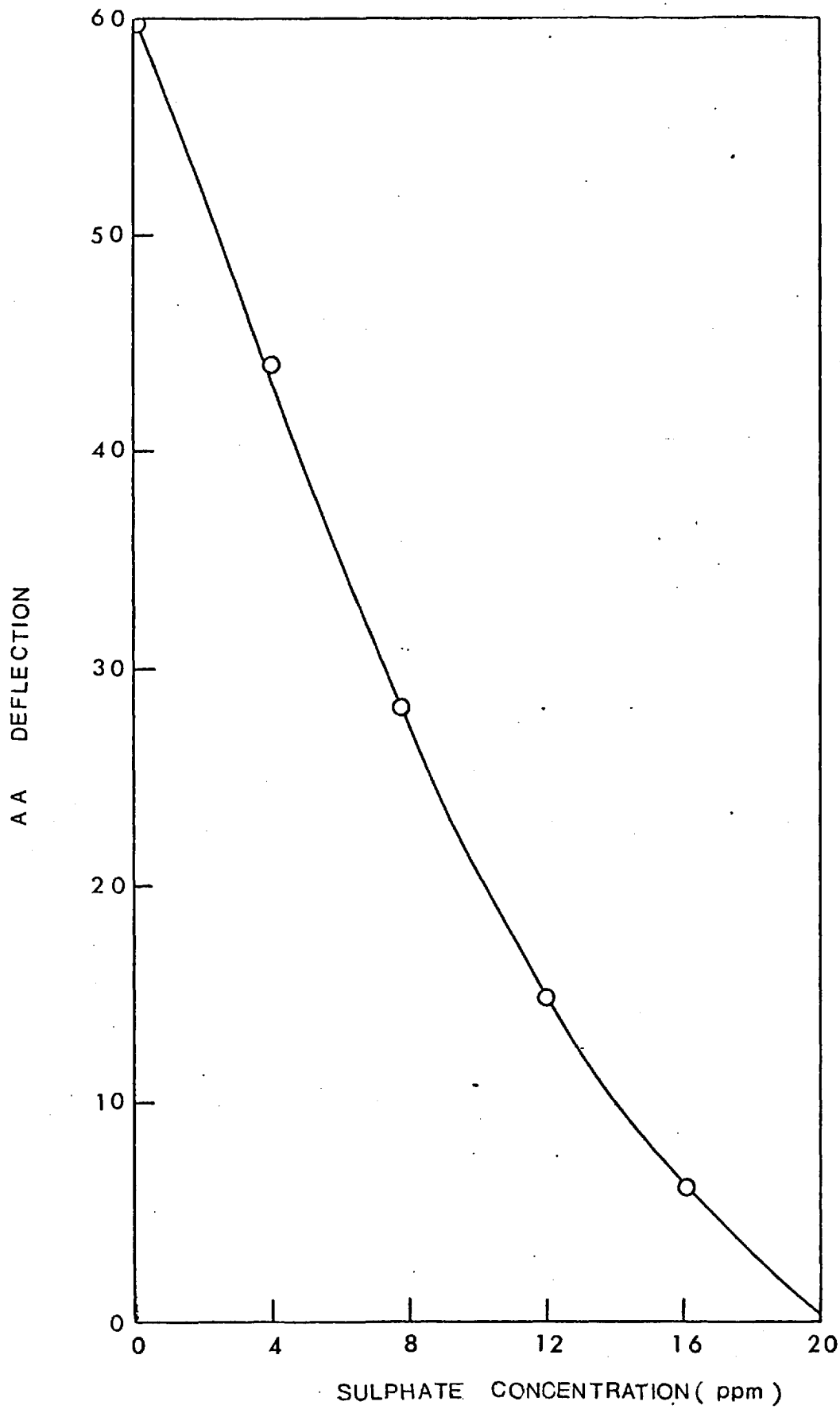

Fig. 18 Typical calibration curve for SO_4^{-2} analysis by atomic absorption spectrophotometry.

2.4 ANALYSIS OF SOLIDS.

2.4.1 Atomic Absorption Spectroscopy.

The chemical composition of the synthetic mineral and the leach residues were checked by atomic absorption spectrophotometry. (Sec. 4.3.1). Presence of tin in sample gave rise to difficulties and a peroxide extraction was done to bring the elements into solution.

About 0.5 to 1.0 gm. of the solid was weighed into a nickel crucible and 4 gm of sodium carbonate was added. After thorough mixing, the mixture was covered with 8 gm of sodium peroxide. The crucible was heated over a small burner to expel any water in the flux until the charge started to melt. The fusion was continued carefully by revolving the crucible around the edge of the flame until the mixture melted quietly. It was heated at the full temperature of the burner for a further two miniutes.

The melt was allowed to cool, the crucible was placed in a 400 ml beaker and 60 ml of water was added to the crucible. After the melt had completely disintegrated the crucible was removed from the beaker and was thoroughly rinsed. 50 ml of hydrochloric acid was added to the beaker which was then heated. The crucible was rinsed with 50 ml of hydrochloric acid which was added to the main solution. The final volume

of the solution was made up to 250 ml with distilled water in a volumetric flask.

A blank was prepared following exactly the same procedure without the material under investigation.

Solutions were analysed almost immediately for tin, because it tends to precipitate on standing.

2.4.2 Microscopic Analysis.

Samples of synthetic minerals and leach residues were mounted in araldyte epoxy resin MY 753 using the araldyte hardener HY 951 . The mounts were first ground on a Struers Lunn Minor grinding machine through a series of papers of standardised grits 220 , 320 ,400 and 600 and then polished on a Struers DP4 automatic polishing machine. Final polishing was done on 6 micron and 1 micron DP clothes using Marcon diamond abrasive compound spray with DP lubricant-red (oil base) for the 6 micron cloth and DP lubricant-blue (water soluble) for the 1 micron cloth.

Preliminary microscopic observations were made with a conventional reflected light microscope prior to photomicrography using a Reichert Universal camera microscope MeF.

Photomicrographs were taken on standard 5" x 4" plates and then printed.

2.4.3 Electron Probe Analysis.

In the present work electron probe micro analysis was employed to (a) check the homogeneity of the synthetic minerals and (b) to investigate the solid leach residues for compositional variations resulting from possible phase changes which may occur during leaching.

The instrument used was a Jeol model JXA - 3A made in 1967, fitted with scanning facilities. The probe diameter was approximately 1 micron and magnifications from 3000X to 2400X could be obtained. The machine was capable of 1 micron resolution for the electron image and between 4 and 5 micron resolution for the X-ray images. It can handle elements of atomic numbers greater than 11 upto 92 and under optimum conditions gave an accuracy of $\pm$ 1% for quantitative analysis of elements if they were present in excess of 10% by weight.

Specimens for microprobe examination were prepared in exactly the same way as for microscopic examination. In addition the samples were vacuum sputtered with carbon to make the surface conducting.

Quantitative analysis of Cu , Fe , Sn and S were done at a number of fixed points on the surface of samples. This was done by comparing the number of counts made by a selected element in the sample in a given time (generally 1 miniute) with the number of counts made by a pure standard during that time. (Standards were pure copper, tin, iron and CdS). After adjusting for the background radiation the raw count data were processed by a computer programme which calculated

the atomic and weight percentages after correcting for the following effects :

1. Absorption effect
2. Atomic number effect
3. Characteristic fluorescence factor.

Electron beam scans were made for all four elements across preselected areas of the samples while X-ray and back-scattered electron images were monitored on an ascilloscope. Recorded scans reflected any variation in composition along specimens.

2.4.4 X-ray Diffraction.

X-ray diffraction was extensively used throught the present work for three different purposes.

1. To identify various solid phases. A multiple Guinier-De Wolf focusing camera (Enraf - Nonius) was used for this.
2. To study the thermal transformations of synthetic stannite. This was done using the same camera modified for high temperature work.
3. To obtain accurate unit cell parameters of leach residues. A Phillips vertical diffractometer was used for this.

2.4.4.1. Guinier-De Wolf Camera : This is of the focusing type that uses X-rays from a curved quartz crystal monochromator. A converging X-ray beam produced by

reflecting the X-rays from a target, is transmitted through a specimen and a semicylindrical film records the reflections. The present model recorded only low angle reflections (0 to 40° Bragg angles). This type of camera had several advantages over the conventional Debye - Scherrer camera. First, since the monochromator almost completely eliminated the white radiation, the powder patterns have practically no background intensity. This allows very weak lines to be observed. Second, since a monochromating crystal with large vertical dimensions permits several cameras to be stacked one above the other several specimens can be observed simultaneously. Last, the exposure times are relatively short, often about 1½ to 2 hours.

A strip of sellotape was attached to a cassette which was divided into four sections in a row. A few milligrams of the material was ground to a particle size of less than 45μ , and was dusted directly on to the sellotape. One compartment was always dusted with powdered sodium chloride which served as a standard.

The position of the undeflected beam was recorded by opening the beam traps for 4 to 5 seconds at a low voltage and a low current.

The radiation used was CoK_α (λ = 1.790 A). At X-ray generator settings of 30 KV and 20 mA, the exposure time was generally about 2½ hours. 174 mm x 76 mm strips of film were used and processed using conventional commercial reagents.

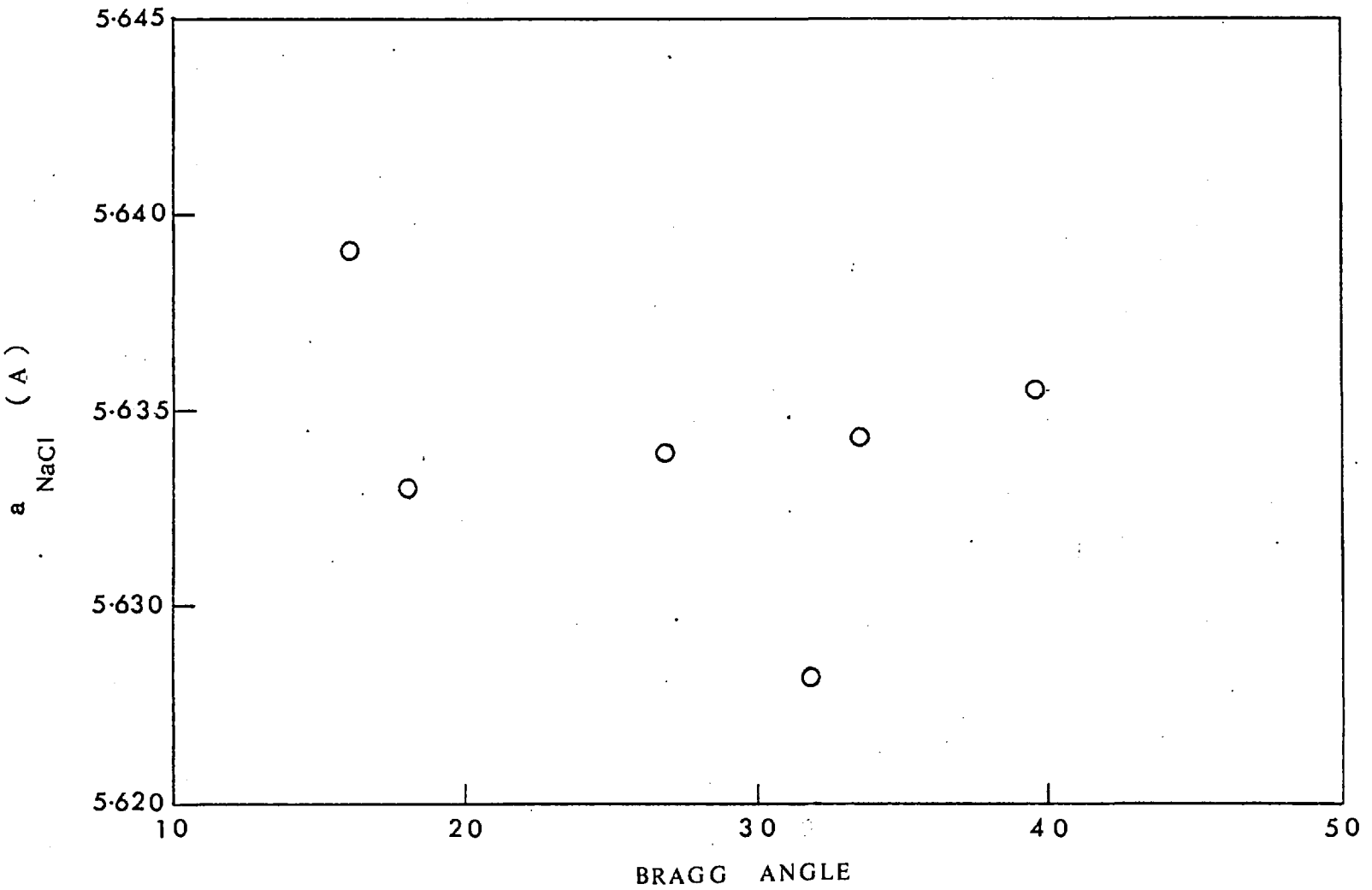

Fig. 19 Investigation of Guinier film for accurate lattice parameter determinations.

After drying the film the line positions were measured with a Hilger--Watts film measuring rule. (1 vernier scale = 0.05 mm). A camera constant (line position/Bragg angle) was computed from the known Bragg angles of the sodium chloride pattern. From the camera constant d values were calculated using Bragg's relation $\lambda = 2d \sin \theta$.

The solid phases were identified by comparing the obtained powder pattern with those in the ASTM file.

Preliminary investigations revealed that the Guinier camera was not satisfactory for the determination of unit cell dimensions. This was established by analysing powder photographs of two primary standards on the same film.

Primary standards chosen were sodium chloride and silicon. From the unit cell length of pure silicon , the Bragg angle for each line was calculated which were used to to obtain the camera constant. The d values of each line of the NaCl pattern were obtained, and knowing the Miller indices a length for the unit cell was calculated from each line. By plotting these against the Bragg angle one expects to obtain an error function, ideally a straight line.

Fig. (19) shows such a plot, which reflects the painful scatter of points.

2.4.4.2 <u>High Temperature Camera:</u> This is an ordinary De Wolf camera modified for use at high temperatures. Sample holder is a platinum wire gauze. After sticking

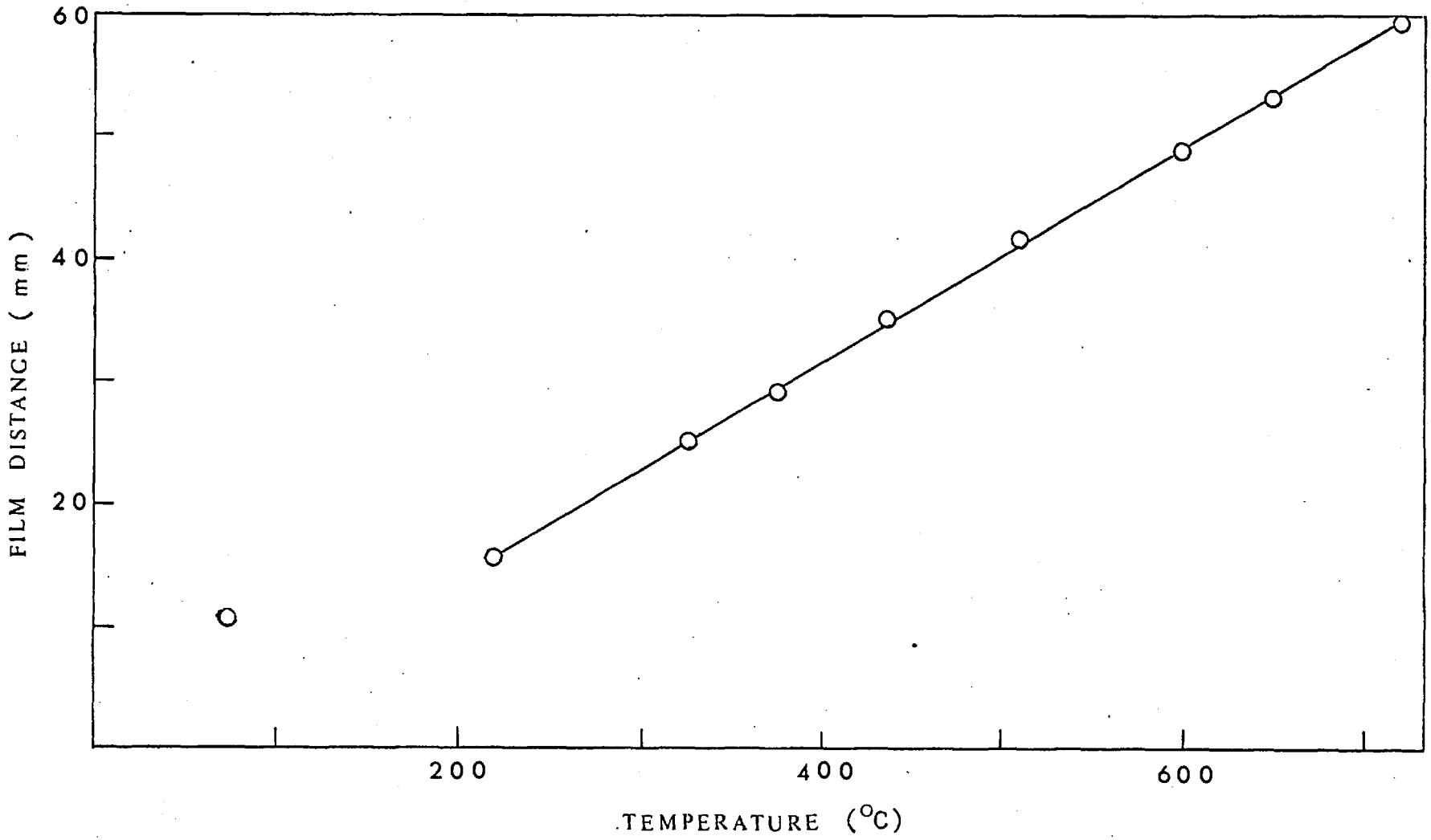

Fig. 20 High temperature Guinier film calibration curve.

the powdered stannite to the sample holder it is placed in an air-tight chamber which is heated electrically. Sample temperature is measured with a Pt - 13%Rh/Pt thermocouple connected to a millivoltmeter. Once the machine is started, the film starts travelling vertically while the temperature in the chamber rises, both at predetermined constant rates. During a run, the distance by which the film has travelled, and the millivolt reading are recorded at regular intervals. From a graph of film distance versus temperature, Fig. 20 phase transformation temperatures may be obtained by examining the processed film.

Preliminary investigations done in an argon atmosphere, showed that most of the lines were absent. However, satisfactory patterns were obtained when helium was used instead. The only possible explanation is the absorption of X-rays by argon (atomic number 18).

2.4.4.3 Diffractometer Techniques. The X-ray diffractometer used was a commercial model manufactured by the North American Phillips Company. Its major units are :

1. A 2 kw X-ray generator, type PW 1310 which operates in the range of 10 - 60 KV upto a tube current of 40 mA. Both the high voltage and the tube current were satbilised to within $\pm$ 0.03%.
2. Vertical goniometer (PW 1050) with a wide range of high and low angles. The scanning

range was from 0 to 165° (2θ) which could be directly read off on the goniometer to an accuracy of ± 0.01° (2θ).

3. Recorder (PW 2400). The intensity of the diffracted beam was measured by a proportional counter aligned both in the axis of the receiving slit and on the focusing circle. This was connected to a pulse averaging circuit; the signal of which was produced as a continuous trace on the strip chart recorder PW 2400. The accuracy obtainable was 0.005° (2θ) at full scale.

A sample of powder was dispersed in an acetone colloidon mixture. This was spread evenly over an area of about 1 cm^2 on a glass slide and allowed to dry. Special care was exercised to ensure sufficient thickness of the sample.

Unfiltered copper radiation was used for all the runs. For diffraction profiles between 2θ values of 0 to 90° , a 1° divergence slit and a 1° scatter slit were used. Wider slits had to be used for higher angles.

Slow scanning speeds were necessary for better sensitivity. Initial runs were done at a scanning speed of 2°/min. Although this was satisfactory for low angle peaks, most of the high angle peaks went unrecorded. Therefore the scanning speed was lowered to ½°/min which was found to be as good as ¼°/min.

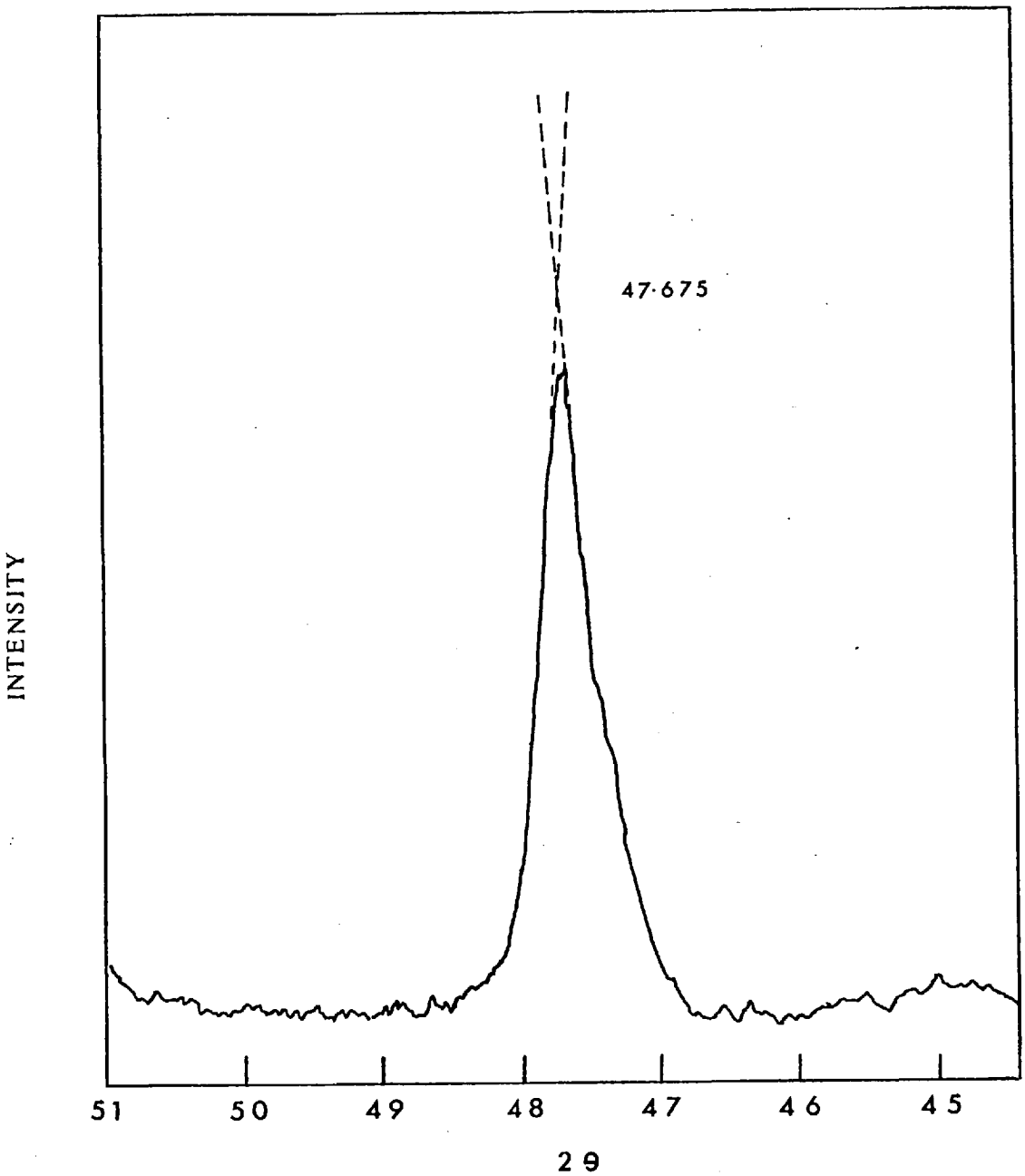

Fig. 21 Determination of peak position in a diffractometer trace.

The basic problem was to obtain precise peak positions. The most accurate method is step scanning followed by a complex mathematical operation to obtain 'centroid' positions. A less tedious but reasonably accurate (1/20000) method recommended by Klug and Alexander[97] was adopted.

To obtain accurate unit cell dimensions, peaks appearing at $80 < 2\theta < 150^{o}$ were chosen. At these high angles doublet resolution of α_1 and α_2 was observable, and only the strong α_1 reflection peak positions were taken into account. The common method of determining the peak position is illustrated in Fig. 21 . The point of intersection of two straight lines projected from the most nearly linear positions of the sloping sides of the profile was taken as the peak position. It could be measured to an accuracy of $\pm\ 0.005^{o}$ (2θ).

Klug and Alexander report that systematic errors arising from the instrument and the sample could be eliminated by a least square fit of the calculated cell parameters from each peak against $\cos\theta.\cot\theta$.

2.5 PURITY OF MATERIALS

a) Copper Rod- Spectrographically Pure

(Johnson Matthey)

Spectrographic Examination:

Element	Estimate of quantity present (ppm)
Silver	5
Lead	3
Nickel	1
Silicon	1
Bismuth, Cadmium, Iron, Magnesium	each less than 1

b) Iron Sponge - Spectrographically Pure

(Johnson Matthey)

Spectrographic examination:

Element	Estimate of quantity present (ppm)
Silicon	3
Magnesium	2
Manganese	2
Nickel	2
Copper, Silver	each less than 1

c) Sulphur Powder - Spectrographically Pure

(Johnson Matthey)

Spectrographic examination:

Element	Estimate of quantity present (ppm)
Aluminium	0.5
Sodium	0.2
Zinc	0.2
Barium	0.1
Nickel	0.1
Copper	0.05
Titanium	0.05
Magnesium	0.03
Manganese	0.03
Silver	0.03
Boron	0.01
Calcium)	
Iron) each less than	1
Silicon)	

d) Tin Rod - Spectrographically Pure

(Johnson Matthey)

Spectrographic examination:

Element	Estimate of quantity present (ppm)
Bismuth	2
Calcium	2

Iron	2
Magnesium	2
Sodium less than	1

e) Ferric Chloride - General Purpose Reagent

(Hopkin & Williams)

Specification

Free chlorine	virtually absent
Ferrous salts	0.03%
$FeCl_3.6H_2O$	97% minimum

f) Hydrochloric Acid - General Purpose Reagent

(Hopkin & Williams)

Specification

Non-volatile matter	0.005% max.
Sulphate(SO_4)	0.01 % max.
Heavy metals and iron	0.001% max.

g) Hydrogen Peroxide - General Purpose Reagent (20 volumes)

(Hopkin & Williams)

Specification

Chloride	0.001% max.
Non-volatile matter	o.2 % max.

6% w/v H_2O_2 minimum

SECTION 3

THERMAL TRANSFORMATIONS OF STANNITES

3.1 NORMAL STANNITE

The identity of normal stannite was established by X-ray powder diffraction. The pattern is presented in Table (16) together with all published diagrams.

All the lines of the pattern could be indexed assuming a tetragonal unit cell. The indexing is consistent with the space group $I\bar{4}2m$ suggested by Brockway. The extra lines present in the synthetic sample of this study are genuine since they fit extremely well to the indexing. It must be noted that Berry and Thompson[98] and Levy[89] report only one strong line around d= 1.92 - 1.91 A for natural stannites whreras two very strong lines were found in this work and by Bente. (However when copper radiation was used only one line was obtained in this study .)

The natural stannite pattern of Berry and Thompson shows two lines at d = 4.85 and 2.38 A, which were not found in any other pattern. On the other hand β-stannite prepared by quenching normal stannite from temperatures above about 700°C also has lines at d = 4.85 and 2 .38 A. Therefore it may be inferred that natural stannite examined by these authors is not normal stannite but high temperature β-stannite.

Table : 16 X-ray Powder Data For Normal Stannite.

This Work Co K_α			ASTM(Berry & Thompson)[a] CuK_α / Ni			Levy[b] Rad.Not Reported		Bente[c] Rad.Not Reported	
d (A)	I/I_o	h k l	d (A)	I/I_o	h k l	d (A)	I/I_o	d (A)	h k l
5.397	8	0 0 2	5.37	5	0 0 2				
			4.85	5	0 1 1				
3.853	8	1 1 0							
						3.5	20		
						3.2	20		
3.134	100	1 1 2	3.12	100	1 1 2 ?	3.10	100	3.122	1 1 2
2.723	28	0 2 0	2.71	30	0 2 0	2.71	10	2.724	2 0 0
					0 0 4				
2.689	9	0 0 4						2.680	0 0 4
2.429	13	0 2 2	2.46	5	0 2 2 ?				
			2.38	5	1 2 1				

.....contd/

Table : 16 contd.....

2.206	5	1 1 4	2.21	5	1 1 4						
						2.116	10				
1.925	94	2 2 0	1.922	70	0 2 4	1.918	50	1.927	2 2 0		
1.913	100	0 2 4						1.909	0 2 4		
1.812	3	0 0 6									
1.639	97	1 3 2	1.642	40	1 3 2	1.644	40	1.640	1 3 2		
1.624	39	0 3 3	1.626	30	0 3 3	1.627	40	1.621	1 1 6		
		1 1 6			1 1 6						
1.564	17	2 2 4	1.570	10	2 2 4	1.568					
1.449	14	1 3 4									
1.356	30	4 0 0	1.368	20	0 4 0			1.363	4 0 0		
a_o = 5.441 A			a_o = 5.469 A					a_o = 5.454 $\pm$ 0.002 A			
c_o = 10.726 A			c_o = 10.769 A					c_o = 10.720 $\pm$ 0.004 A			

a : Sample from Oruro, Bolivia.

b : Sample from Cornwall, England.

c : Synthetic.

Some workers[70,71] doubt the crystal structure proposed by Brockway and suggest an alternative chalcopyrite-like crystal structure based on the space group $I\bar{4}2d$. However the X-ray powder pattern of synyhetic stannite shows that the space group is $I\bar{4}2m$ and not $I\bar{4}2d$ for the following reasons.

1. If the space group was $I\bar{4}2d$ a line at d = 2.206 A (114) is not possible, because hhl lines are allowed only if $2h + 1 = 4n$.
2. Similarly a line at d = 3.85 A (110) is forbidden since hh0 are allowed only if $h = 2n$.
3. The phase transformation from normal stannite to cubic stannite must accompany extraordinary atomic movements if the normal stannite had a chalcopyrite-like structure. But if Brockway's structure is correct this change involves practically no change in atom positions.(Sec. 3.2)

Eibschutz[76] also found no extra lines except those allowed by $I\bar{4}2m$.

Therefore it is concluded that Brockway's crystal structure represents the correct structure of normal stannite..

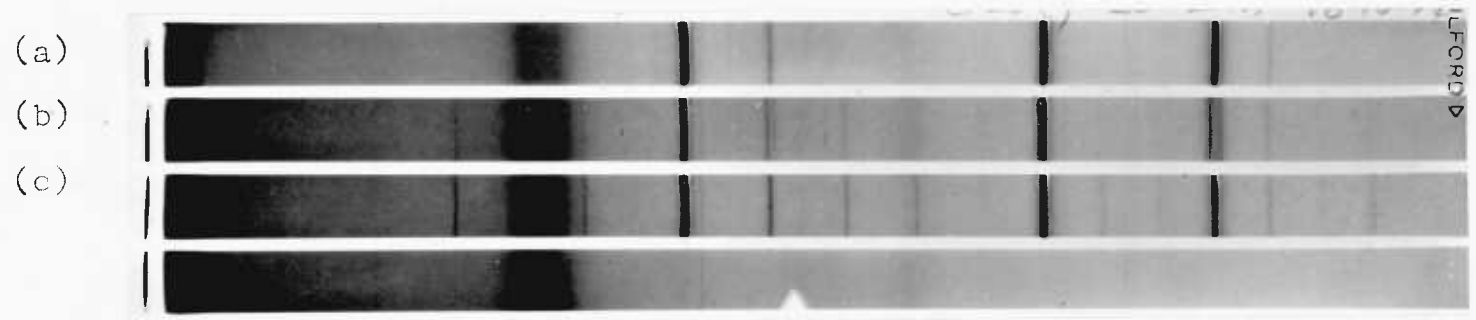

Fig. 22 Guinier photographs of (a) sphalerite
(b) normal stannite
(c) cubic stannite.

In Fig. 22, Guinier photographs of normal stannite and sphalerite are reproduced to highlight the similarity between the two structures.

Atomic absorption analysis yielded the following composition for synthetic stannite:

Cu : 30.2 ± 0.6 %

Fe : 13.1 ± 0.7 %

Sn : 27.3 ± 1.0 %

S : 29.4 % by difference.

These values correspond to the approximate formula: $Cu_{2.07}Fe_{1.02}SnS_{3.99}$ which agrees reasonably well with the stoichiometric formula : Cu_2FeSnS_4 .

Although the mineral is slightly metal rich, throughout the present work it is assumed to be stoichiometric.

3.2 Cubic Stannite

The thermal behaviour of stannite has been the subject of many publications[70-74], yet it remains far from settled. Therefore a complete study was undertaken on the effect of temperature on normal stannite.

Phase transformations were studied with a modified Gunier camera designed for use at high temperatures. (Sec.2.4.4.2)

A typical photograph is reproduced in Fig.23. It is possible to see that a phase change is taking place around 285°C. This is not a sharp change. At this temperature all the doublets present in the low temperature stannite pattern (d= 2.273 & 2.689, 1.925 & 1.913, 1.639 & 1.624 A) merge to singlets indicating a tetragonal $\longrightarrow$ cubic transformation. Another phase change is evident around 500°C in which these singlets again deviate. Also, the line at d = 1.45 A , which belongs to the cubic phase, vanishes. This is the cubic stannite $\longrightarrow$ tetragonal stannite transformation.

Above this temperature the photograph is of no value to study the phase transformations of stannite, because the sample oxidised for unknown reasons. Furthermore, the transformation temperatures are only approximate (the error could be as high as $\pm$ 25°C). Nevertheless the photograph beautifully shows the occurence of these phase changes.

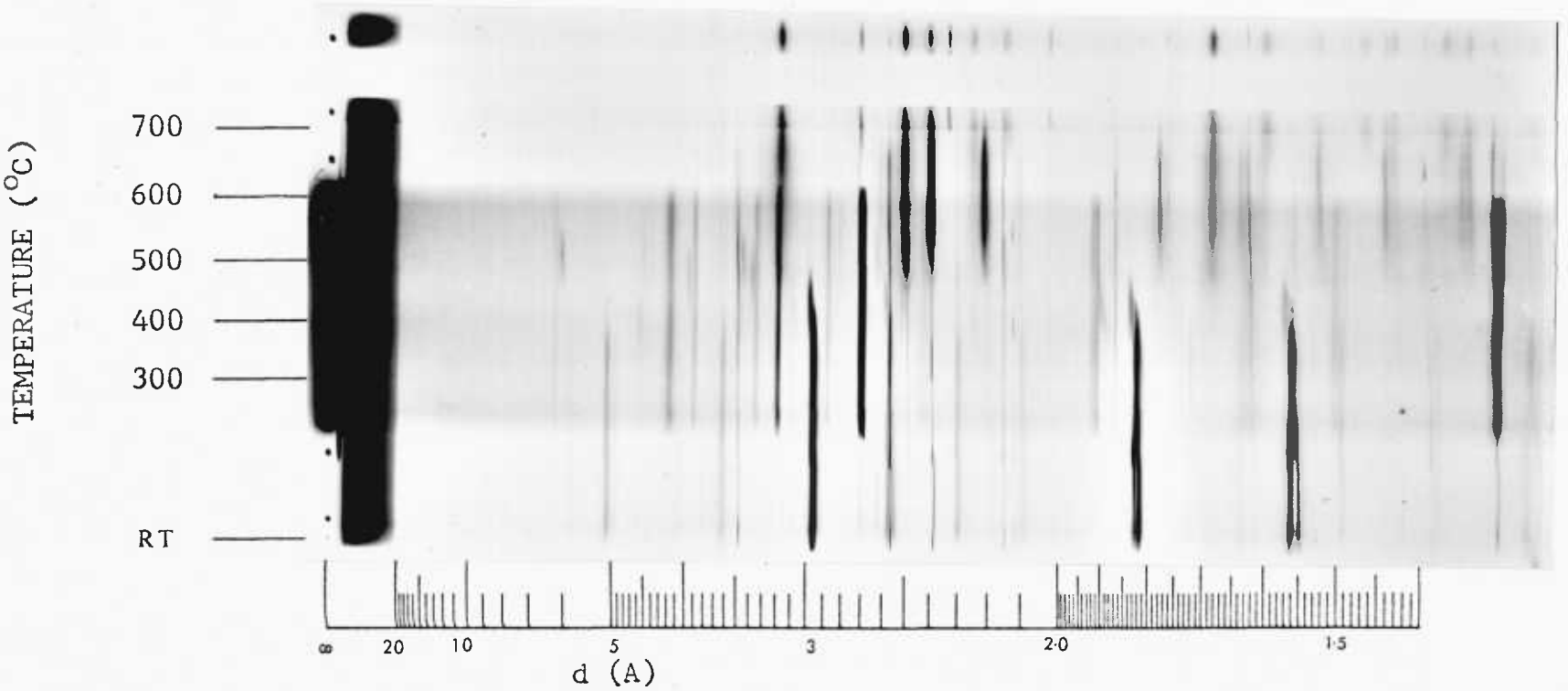

Fig. 23 High temperature Guinier photograph showing the thermal transformations of stannite.

A set of quenching experiments was done to substantiate these findings. About 1 gm of powdered stannite was placed in a small silica tube, sealed under vacuum and was annealed in a muffle furnace at a predetermined temperature. Annealing times were different for each experiment, the lower the temperature the the longer was the annealing time as given in Table 17. After annaeling the tubes were quenched in cold water. After visual and microscopic examination the contents were studied by X-ray powder diffraction.(Fig.24 and Table20)

Microscopic observation of polished sections under polarised light revealed that samples quenched from 300 to 500°C were completely isotropic. The X-ray powder pattern of the isotropic phase is presented in Table 18 together with those of Franz and Bente.

Clearly the cubic phase obtained in this study is the same as that reported by Franz.

On indexing the powder pattern all allowed reflections were found to be present. (All possible values of $h^2 + k^2 + l^2$). This indicates a primitive cubic unit cell. Routine measurements led to the value 5.42 A for the length of the unit cell.

However, Franz rejected a primitive unit cell and chose a unit cell twice as long. This obviously required doubling of the Miller indices. The probable space group was suggested as $I\bar{4}3d$.

There is no justification for doubling the indices

and the present author believes that the correct unit cell for the cubic phase is primitive. If this is true, and if the relative atomic positions were only slightly alterd then there exists only one crystal structure for this phase. This assumption is reasonable since the transformation temperature is too low ($\sim 300^{o}C$) for a radical change of atom positions.

A model of the proposed structure is presented in Fig.25 (This is arrived at assuming the density reported by Franz). This structure is easily derived from the crystal structure proposed by Brockway for normal stannite.

The relation between normal stannite and cubic stannite may be recognised in Fig.26 in which a ball model of four adjacent tetragonal unit cells of normal stannite is shown. (Copper : purple, iron : orange, tin : black and sulphur : yellow.)

If the iron atoms and tin atoms in the 001 planes were interchanged, the cube resulting from the four central iron atoms (ie, the body centred ones) and any four face centred iron atoms , is identical to the cubic unit cell shown in Fig.25.

Table : 17 Quenching Experiments.

Expt.	Temperature (^{o}C)	Annealing Time (Days)
Q1	850	3
Q2	800	4
Q3	740	5
Q4	600	10
Q5	480	30
Q6	400	28
Q7	300	21

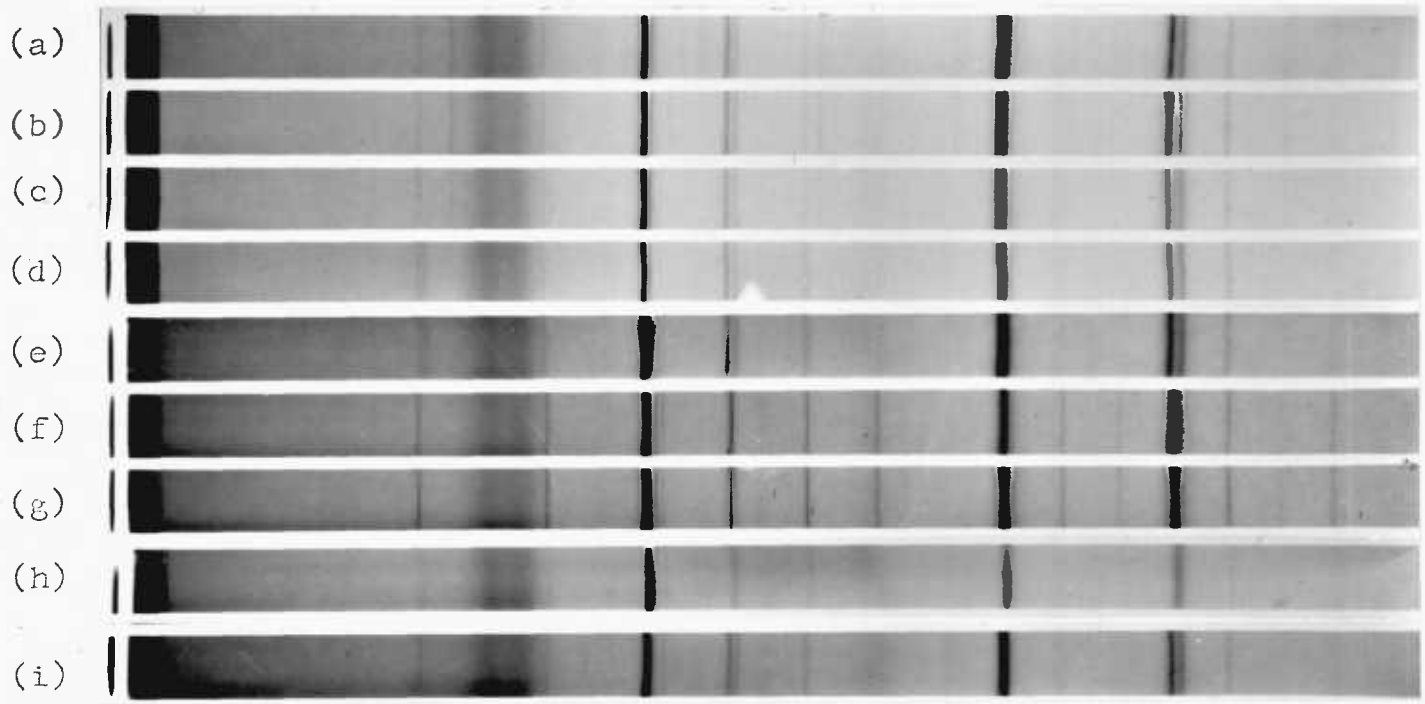

Fig. 24 Guinier photographs of stannites quenched from the temperatures:

(a) 850°C β -phase (d) 600°C α -phase (g) 420°C cubic

(b) 800°C β -phase (e) 540°C α -phase (h) 300°C cubic

(c) 740°C β -phase (f) 480°C cubic (i) R. temp. normal.

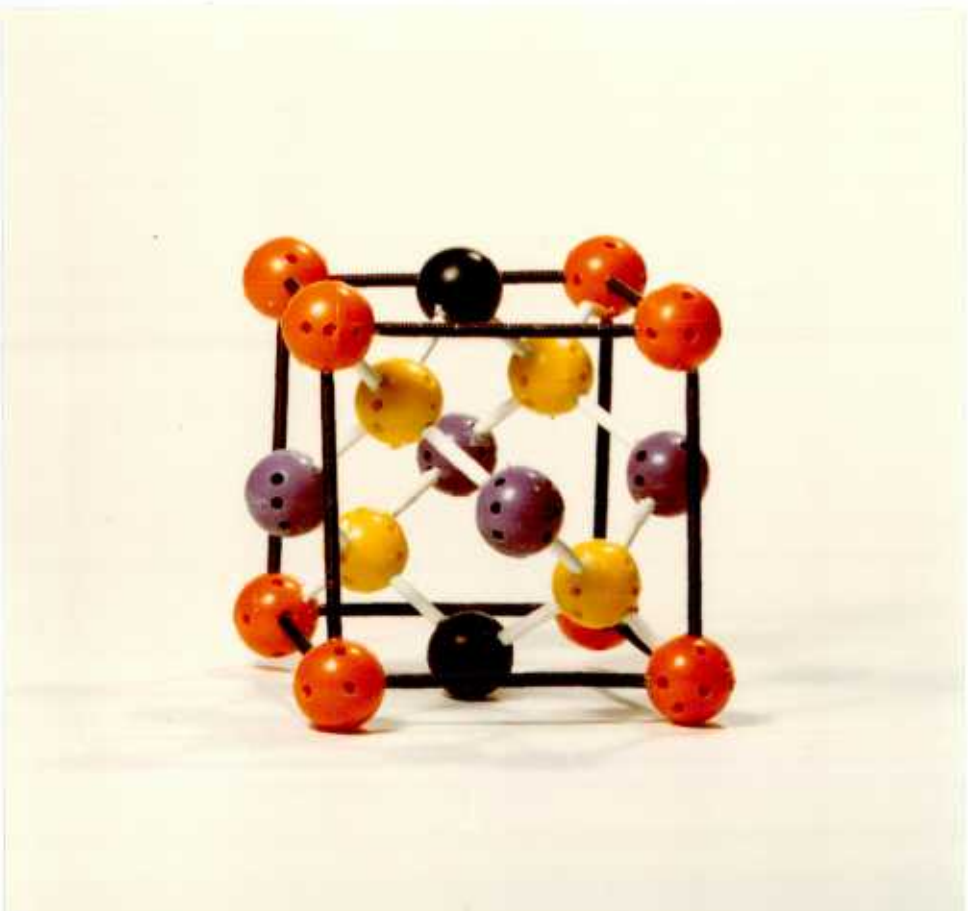

Fig. 25 Ball model of the proposed structure for cubic stannite.

Copper	: purple	Tin	: black
Iron	: orange	Sulphur	: yellow

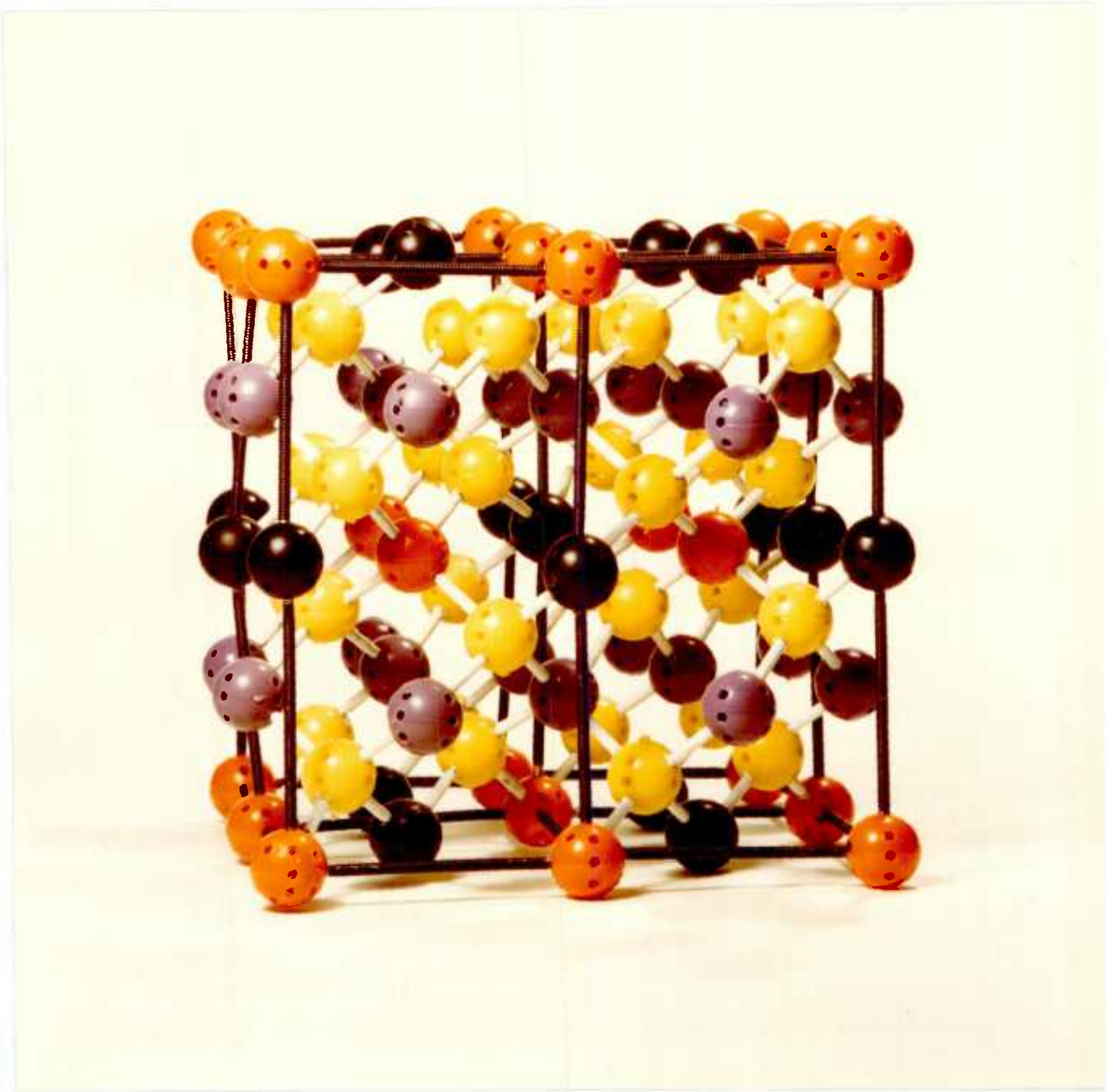

Fig. 26 Ball model showing four adjacent tetragonal unit cells of normal stannite.

Copper	: purple	Tin	: black
Iron	: orange	Sulphur	: yellow

Table : 18 X-ray Data For Cubic Stannite.

Present Work Synth. Fr. 480°C Co K_α			Franz. Synth. Fr. 420°C FeK_α /Mn			Bente. Synth. Fr. 800°C (Rad. not Reported)	
d (A)	I/I_o	h k l	d (A)	I/I_o	h k l	d (A)	h k l
5.413	22	1 0 0	5.42	10	0 0 2		
3.84	19	1 1 0	3.82	10	0 2 2		
3.134	100	1 1 1	3.12	100	2 2 2	3.133	1 1 1
2.716	60	2 0 0	2.70	30	0 0 4		
2.432	24	2 1 0	2.42	20	0 2 4		
2.215	13	2 1 1	2.21	10	2 2 4		
1.920	100	2 2 0	1.917	80	0 4 4	1.936	2 2 0
1.810	10	2 2 1	1.802	10	0 0 6 2 4 4		
1.718	12	3 1 0	1.715	5	0 2 6		
1.636	80	3 1 1	1.633	50	2 2 6	1.650	3 1 1
1.566	15	2 2 2	1.562	10	4 4 4		
1.506	5	3 2 0	1.504	2.5	0 4 6		
1.450	10	3 2 1	1.447	5	2 4 6		
						1.254	3 3 1
						1.116	4 2 2
a_o = 5.42 A			a_o = 10.837 A			a_o = 5.47 ± 0.005 A	

3.3 α and β Stannites.

Springer reported a phase change around 680°C , where a tetragonal form transformed to another tetragonal form. The tetragonal phase stable above 680°C , called β -stannite, had the lines 011 (4.85 A) , 013 (2.99 A), 121 (2.3718 A) , 123 (2.010 A) and 301 (1.787 A) , whereas the low temperature phase, α -stannite, did not show these. In the present work also the same lines were present in samples quenched from temperatures above 700°C but not in low temperature forms. Following Springer's nomenclature the name α -stannite is retained for the tetragonal phase stable between 525 - 700°C found in this work, while the tetragonal phase stable above 700°C will be referred to as β -stannite.

Visually and microscopically β -stannite (its stability range is only approximate) is very similar to normal stannite. Even the X-ray powder patterns are very similar. Table (19) compares the X-ray powder pattern of α -stannite with the published diagram for tetragonal stannite prepared at 600°C by Franz.

The apparent lack of agreement between α -stannite and that of Franz is because Franz's pattern is a 'processed' one. Although he observed lines at d = 4.28 , 3.35 , 2.78 , 2.29 and 1.15 A he discarded them since they were 'sehr schwach'. Also he rejected some lines (probably 5.33 , 3.84) as originating from the cubic phase. This is incorrect since there is no reason why

the line at d = 2.21 A should be absent in α -stannite if the cubic phase was present in any appreciable quantity.

Franz suggested $I\bar{4}2d$ as the space group of α -stannite, which of course is meaningless. Similar arguments advanced in sec. 2.2.1. suggests $I\bar{4}2m$ is the more probable space group for α -stannite. This means that the crystal structures of normal stannite and α -stannite are very similar if not identical.

Stannite samples quenched from 700°C , 800°C and 850°C appeared somewhat different from normal stannite. Pink, blue, and brass yellow crystals were visible but under crossed nicols all were indistinguishable from normal stannite. Moreover the X-ray powder patterns were the same having the 'extra' lines 011 , 013 , 121 , 123 , 301 and several others. Therefore this phase is termed β -stannite following Springer. The cobic phase reported to be stable in this range of temperatures by Bente and others were not found in the present study.

Summarising, the thermal transformations established in the present work can be schematically represented as follows :

$$\text{NORMAL STANNITE} \xrightarrow{300^{\circ}C} \text{CUBIC STANNITE} \xrightarrow{500^{\circ}C} \alpha\text{-STANNITE}$$

$$\alpha\text{-STANNITE} \xrightarrow{700^{\circ}C} \beta\text{-STANNITE} \longrightarrow \text{MELT} \ (\ > 850^{\circ}C)$$

Table : 19 X-ray Data For α - Stannite.

Present Work Synth. fr. 600°C		Franz Synth. fr. 600°C	
d (A)	I/I_o	d (A)	I/I_o
5.33	20		
4.33	17		
3.842	19		
3.357	15		
3.111	100	3.10	100
2.714	100	2.70	20
2.679	69	2.67	10
2.411	37	2.41	5
2.298	15		
2.196	17		
2.176	15		
1.996	7		
1.928*	100	1.918	40
1.905	100	1.905	70
1.804	15		
1.714	14		
1.698	16		
1.633	100	1.633	50
1.618	100	1.617	30
1.560	43	1.562	10
1.445	13	1.443	2.5
1.418	8		

Table : contd/...

Table : 19 contd.....

1.356	69	1.356	20
1.342	26	1.340	10
1.245		1.248	20
1.240		1.240	30
1.213		1.211	10
1.204			
1.185			
1.154		1.108	40
		1.099	20
1.045		1.047	20
		1.042	10
1.034		1.033	10

* with Co K_{α} radiation.

X-ray powder patterns of the four stannites are presented in Table (20) for comparison.

Table : 20 X-ray Powder Diagrams of Normal Stannite, Cubic Stannite, α - and β -Stannite

N-Stannite (Co)		Cubic Stannite Qched.fr.500°C (Co)		α-Stannite Qched.fr.600°C (Cu)		β-Stannite Qched.fr.760°C (Cu)	
d (A)	I/I_o	d (A)	I/I_o	d (A)	I/I_o	d (A)	I/I_o
5.397	22	5.413	22	5.325	20	5.389	23
				4.33	17	4.385	57
3.853	18	3.840	19	3.842	19	3.826	28
				3.3573	15		
(3.243)	7			(3.243)	6	(3.243)	7
3.113	100	3.134	100	3.111	100	3.118	100
						2.984	28
2.723	69	2.716	60	2.714	100	2.714	100
2.689	58			2.679	69	2.683	78
2.429	27	2.432	24	2.411	37	2.423	32
						2.365	40
				2.298	15		
		2.215	13				
2.205	14			2.196	17	2.195	27
				2.176	15		
						2.006	25
				1.996	7		
						1.994	22
1.925	100						
		1.920	100	1.905*	100	1.908*	100
1.913	100						
1.812	14	1.810	10	1.804	15	1.807	11

.....contd/

Table : 20 contd.....

						1.786	15
		1.718	12	1.714	14	1.713	8
				1.698	16		
1.639	100			1.633	100	1.633	100
		1.636	80				
1.624	100			1.618	100	1.620	100
1.564	27	1.566	15	1.556	43	1.562	40
		1.506	5			1.493	12
						1.472	9
1.449	11	1.450	10	1.445	13	1.447	12
				1.418	8		
						1.387	13
1.356	35			1.358	69	1.358	38
1.342	33			1.342	26	1.342	33

* When cobalt radiation is used this line splits to two lines at d = 1.928 and 1.915.

SECTION 3

LEACHING OF NORMAL STANNITE-RESULTS AND DISCUSSION

4.1 FERRIC CHLORIDE LEACHING - GENERAL.

The leaching of normal stannite was investigated mostly in solutions of 0.5 M $FeCl_3.6H_2O$ in 0.5 M hydrochloric acid as described in secction 2.2 . High acid conditions were employed to prevent iron hydrolysis.

The leaching process was generally slow and most runs went on for several days or sometimes for weeks as a result. This made evaporation losses considerable and volume changes had to be taken into account when calculating the percentage dissolutions. Appropriate corrections were made assuming that the volume of the leach liquor varied linearly with time. Naturally the volume changes due to evaporation were more pronounced at higher temperatures. Therefore greater emphasis is laid on the initial part of the process (first 50 hours for example) when interpreting kinetic rate curves. Evaporation losses are minimised in this region.

Fig. 27 shows the extraction curves for copper and tin, of two experiments done under identical conditions. Percent extractions of these elements are calculated from the concentration of copper and tin in solution found by atomic absorption spectrophotometry.

The sort of reproducibility obtainable in the leaching experiments may be judged from Fig. 26 . From the two copper dissolution curves, it is evident that the curves coincide upto about 125 hours, and

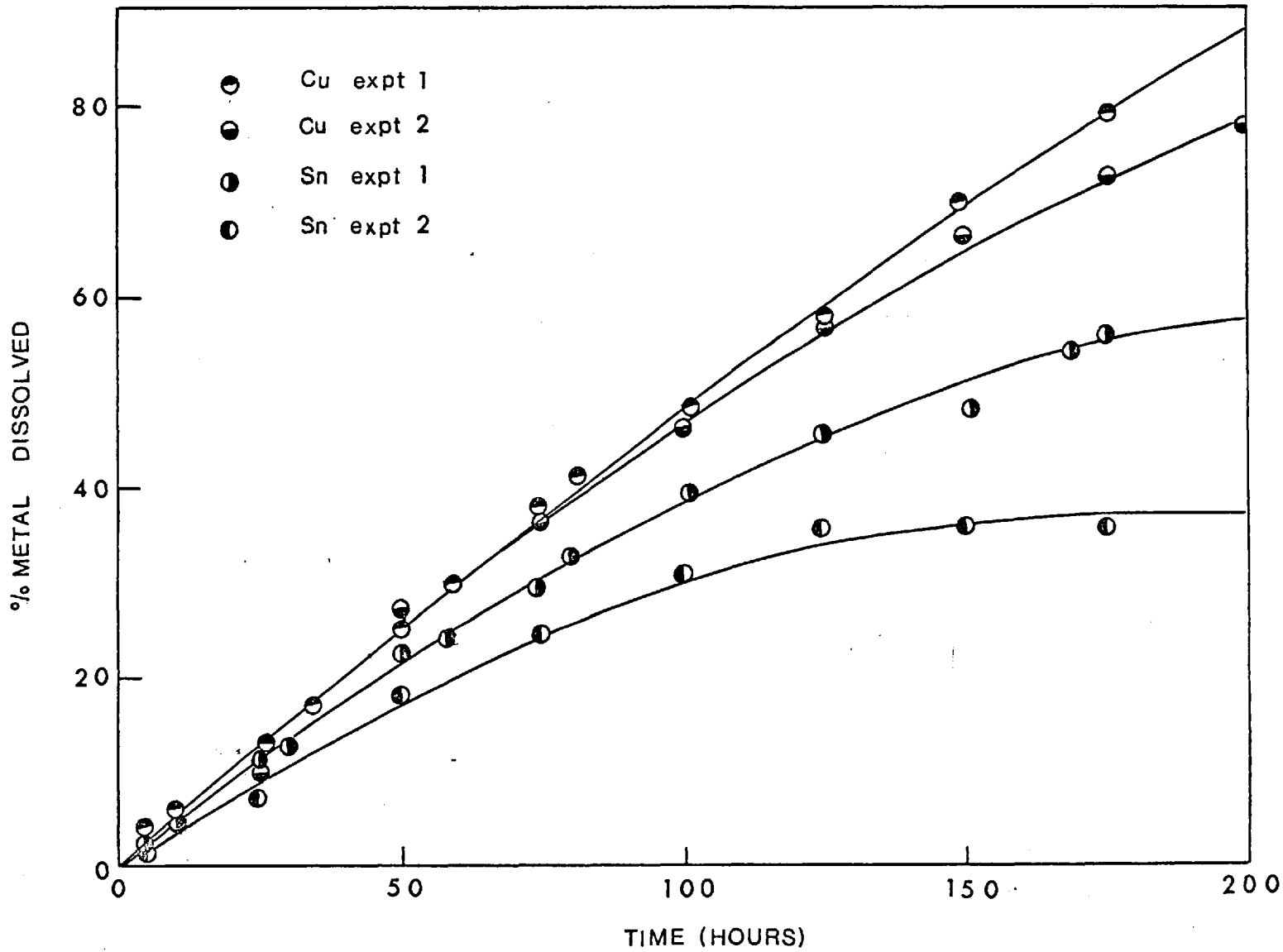

Fig. 27 Reproducibility of the kinetic rate curves.

even at 150 hours the reproducibility is reasonable. After that they begin to deviate.

Tin dissolution curves are less predictable. From the start they follow different curves. Therefore they were not representative of the true kinetics of the process. This will be explained in a later section.

Copper extraction curves are essentially linear. Only at high retention times they tend to bend. This does not reflect any internal process as is shown by the constancy of the lattice parameters and the virtually identical photomicrographs of the unleached and leached mineral specimens. Therefore the apparent parabolic nature of the curves must be due to external factors. Two such mechanisms are concievable :

1. Sticking of the mineral particles along the stirrer shaft and the baffle. Effectively they remain unreacted and this results in apparent non-linear kinetics. But its contribution to overall kinetics is relatively small.

2. Covering of mineral particles by solid products. In fact this is the major factor and therefore deserves a detailed description.

Three secondary solid systems were identified in the leaching vessel. Elemental sulphur, iron precipitates and tin precipitates.

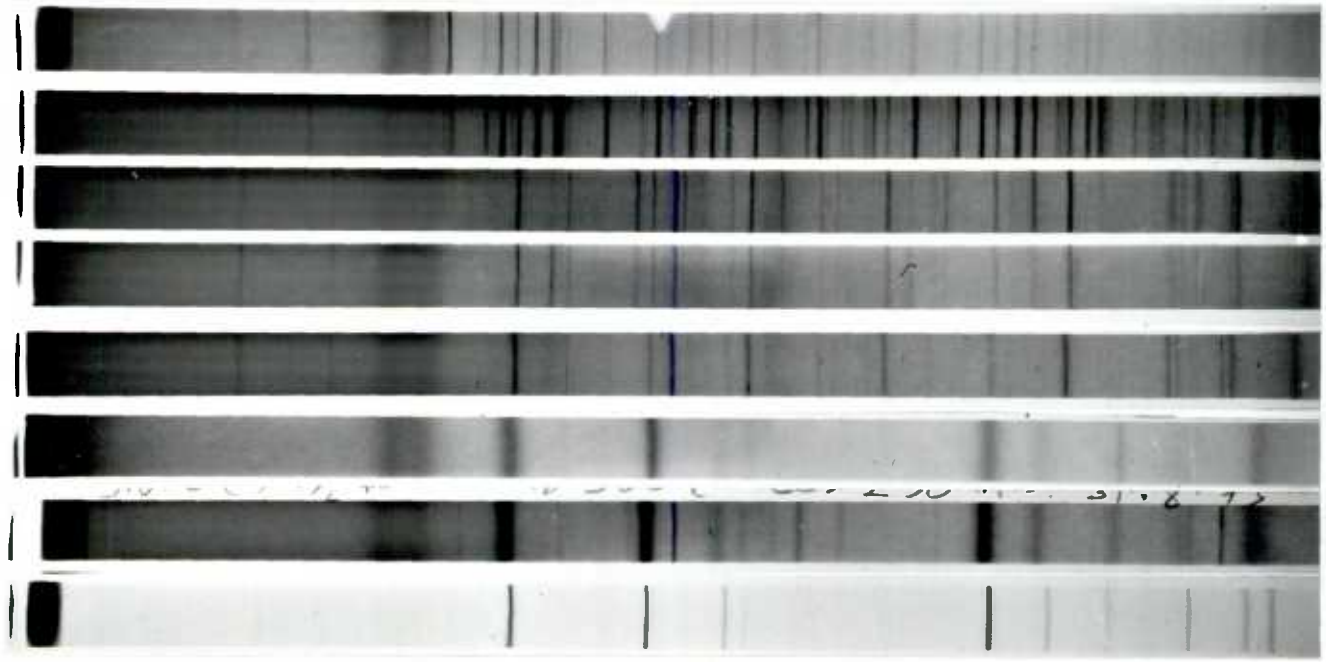

Fig. 28 Identification of leach products by X-ray diffraction.

A. Sulphur.

B. Leach products.

C. Iron precipitates.

D. Iron precipitates.

E. Iron precipitate (prepared)

F. Tin precipitate (prepared)

G. (F) heated to 500°C.

H. Stannic oxide (SnO_2)

A. Elemental sulphur :

This was produced as a direct result of stannite leaching. It was possible to detect elemental sulphur at the early stages of reaction, at 4 % copper dissolution for example, by its characteristic odour. As the reaction proceeded yellow crystals of sulphur condensed on the walls of the vessel, noticeably on the necks. It was identified by X-ray powder diffraction (Fig. 28). But it was never found with the leach residue, covering the mineral particles, so to speak. Although descrete sulphur particles were observable with the residue, sulphur lines did not appear in the powder pattern of hand sorted mineral particles of the leach residue. Contrary to observations of the previous workers (Ugarte[45] , Ferreira[34] , Scheridan[26]), it was never necessary to wash the particles with CS_2 or CCl_4 prior to X-ray powder diffraction in order to eliminate sulphur lines from the powder pattern. The non-existence of sulphur lines may be explained in one of several ways. Either the sulphur produced is amorphous or, the particles are too fine to produce a powder pattern. It could also be that the sulphur produced is 'carried away' by the solution so that sufficient sulphur is not accumulated to produce a pattern in the presence of excess stannite. This last possibility is the most likely case.

B. Iron precipitates :

Although no iron precipitation was expected under the high acid conditions employed , often the hydrlysis was appreciable. Precipitation initiated at the walls of the vessel where the pH would have been considerably higher than in the solution. A brown red precipitate was the result which sometimes changed the nominal ferric concentration by about 4% . This change in concentration also contributes to non-linear kinetics. X-ray powder diffraction revealed the presence of α -Fe_2O_3 and β -FeOOH in the precipitate, among others unidentified.

C. Tin precipitates :

At first the tin dissolution curves suggest that after about 35 to 40 percent tin dissolution it stops. But, analysis of the leach residues showed that they had the same composition as the original mineral, within experimental error. Therefore all the constituents would have come into the solution at the same rate.

Although the X-ray powder pattern of the red brown precipitate did not have lines attributable to any tin compound, it was shown to contain 8 percent tin by atomic absorption analysis. Therefore part of the tin which came inro solution during leaching was precipitated.

Since it was not possible to isolate the tin compound from the iron precipitate, an independent experiment was carried out to establish the nature of the tin precipitate.

Two series of solutions, each containing approximately the same amount of Cu^{+2} and Sn^{+2} ions were prepared by dissolving $CuCO_3.Cu(OH)_2.H_2O$ and $SnCl_2.2H_2O$ in 0.5 M hydrochloric acid. Copper and tin were in the same concentration range as was found in the leach solutions. Ferric chloride was added to the solutions so that the first series was 0.5 M in Fe^{+3} whereas the second series was 0.05 M in Fe^{+3} .

Samples of these were placed in boiling tubes and were maintained at 80°C in an oil bath. The closed tubes were shaken occasionally. After about two days they were removed and examined.

Solutions with 0.5 M Fe^{+3} produced a red brown precipitate similar to that found in the leaching system, in fact with the same X-ray powder pattern. (Fig 28

Other solutions with 0.05 M Fe^{+3} produced a different precipitate. It was yellowish white and passed through filter paper. Its X-ray powder pattern had six very broad lines. The d-values agreed well with the published values for SnO_2 in the ASTM File (Fig 28

The material was vacuum sealed and annealed at 500°C for 17 hours to improve the quality of the X-ray powder pattern. It certainly did improve, but several new lines appeared which could be attributed to Fe_2O_3 (Fig 28

A similar precipitate formed in the leaching with hydrogen peroxide contained about 5 percent iron. (This precipitate did not give a X-ray pattern)

Therefore it is inferred, although the evidence is not conclusive, that the tin precipitate is SnO_2 with adsorbed iron compounds.

Precipitation of tin explains the non-reproducibility of the tin dissolution curves.

It is reasonable to assume that one or all of these solid phases may influence the overall kinetics by covering the mineral particles, forming a barrier between the active sites in the solid and the solution.

A careful analysis of the leach solution for sulphate ion, by atomic absorption spectrophotometry, showed that sulphate ion was not present in the solutions in ferric chloride leaching.

Therefore stannite leaching in this medium involves the direct conversion of sulphide sulphur to elemental sulphur.

The influence of the following variables on leaching was studied to understand the stannite dissolution mechanism.

1. Temperature
2. Particle size
3. Ferric ion concentration
4. Sample weight
5. Stirring speed

4.1.1 Temperature.

Figure 29 shows the effect of temperature on the rate of dissolution of normal stannite.

At low temperatures the rate of leaching was extremely low. Therefore $65^{o}C$ was the lower limit of temperature studied. The general conditions, which were kept constant were :

Particle size	-180 + 125 micron
Sample weight	0.5 gm.
Stirring speed	900 rpm.
Leaching medium	0.5 M $FeCl_3.6H_2O$ in 0.5 M HCl.

The experiments were carried out at a high stirring speed (generally higher than 750 rpm.) to ensure a turbulent regime in the system. Mass transport in the solution may become important otherwise, and the results will be masked by that variable.

The curves are clearly continuous implying that the leaching is a single process. In other words, if the leaching occured by a certain mechanism at the begining, the same mechanism continued right to the end. From the kinetic rate curves it was possible to obtain a value for the critical increment energy. The rate of the reaction was taken as the percent copper dissolved in a given time.

Fig. 30 shows a plot of the logarithm of percent copper dissolved in the first 50 hours and the next 50 hours

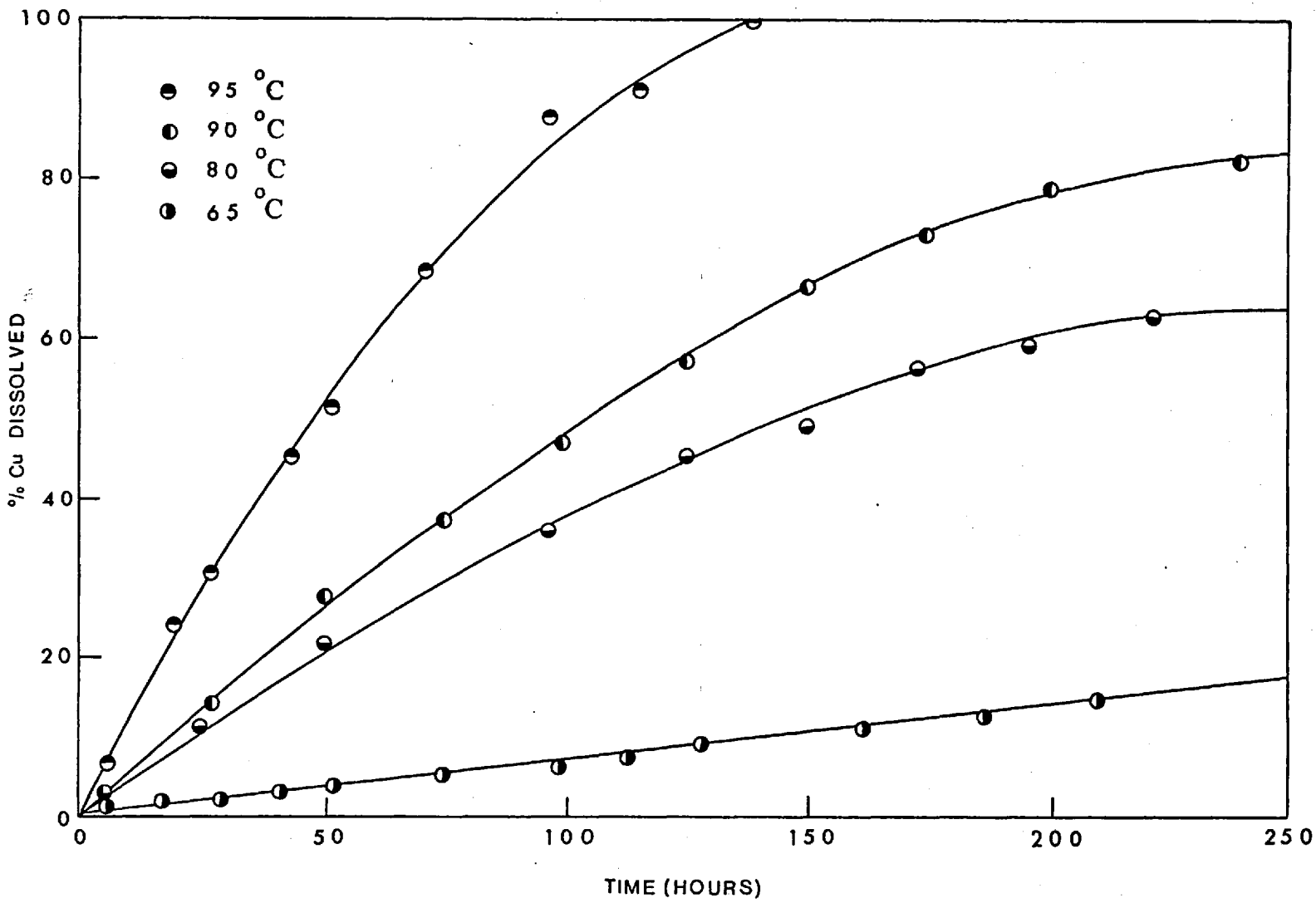

Fig. 29 Effect of temperature on the leaching of normal stannite.

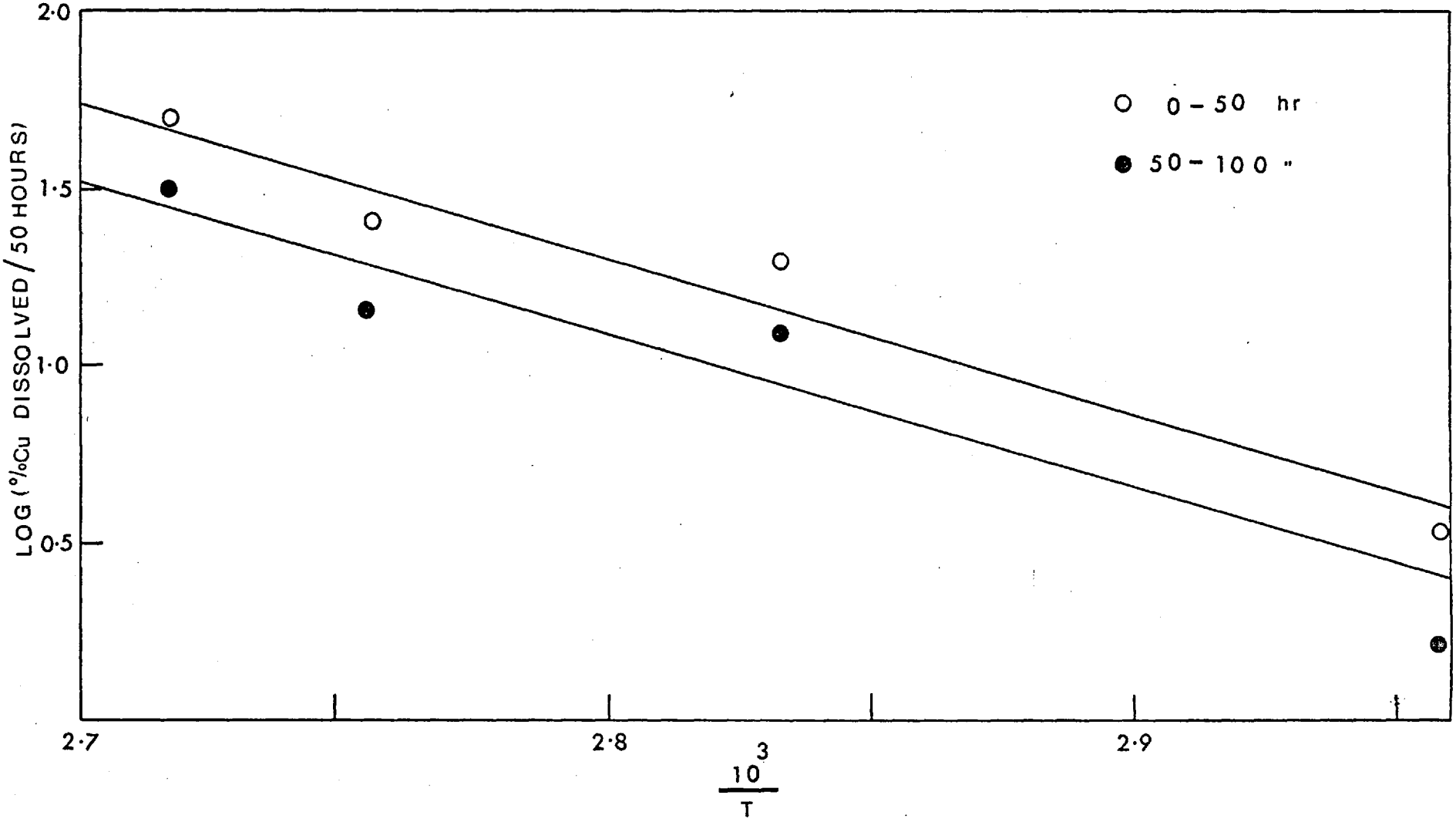

Fig. 30 Arrhenius plots for 0-50 and 50-100 hours.

Temp. °C	Temp. °K	$\frac{1}{T}$	0 - 50 Hours		50 - 100 Hours		100 - 140 Hours	
			%Cu at 50 Hours	Log(%Cu)	%Cu/50h	Log(%Cu)	%Cu/50h	Log(%Cu)
65	338	0.00295857	3.4	0.53148	3.0	0.4771	2.4	0.3802
80	353	0.00283286	20.0	1.30103	16.4	1.2148	10.6	1.0253
90	363	0.00275480	25.5	1.40654	21.5	1.3324	14.5	1.1613
95	368	0.00271739	50.0	1.69897	33.0	1.5185	17.0	1.2304

Table : 21 Data for Figures 30 and 31.

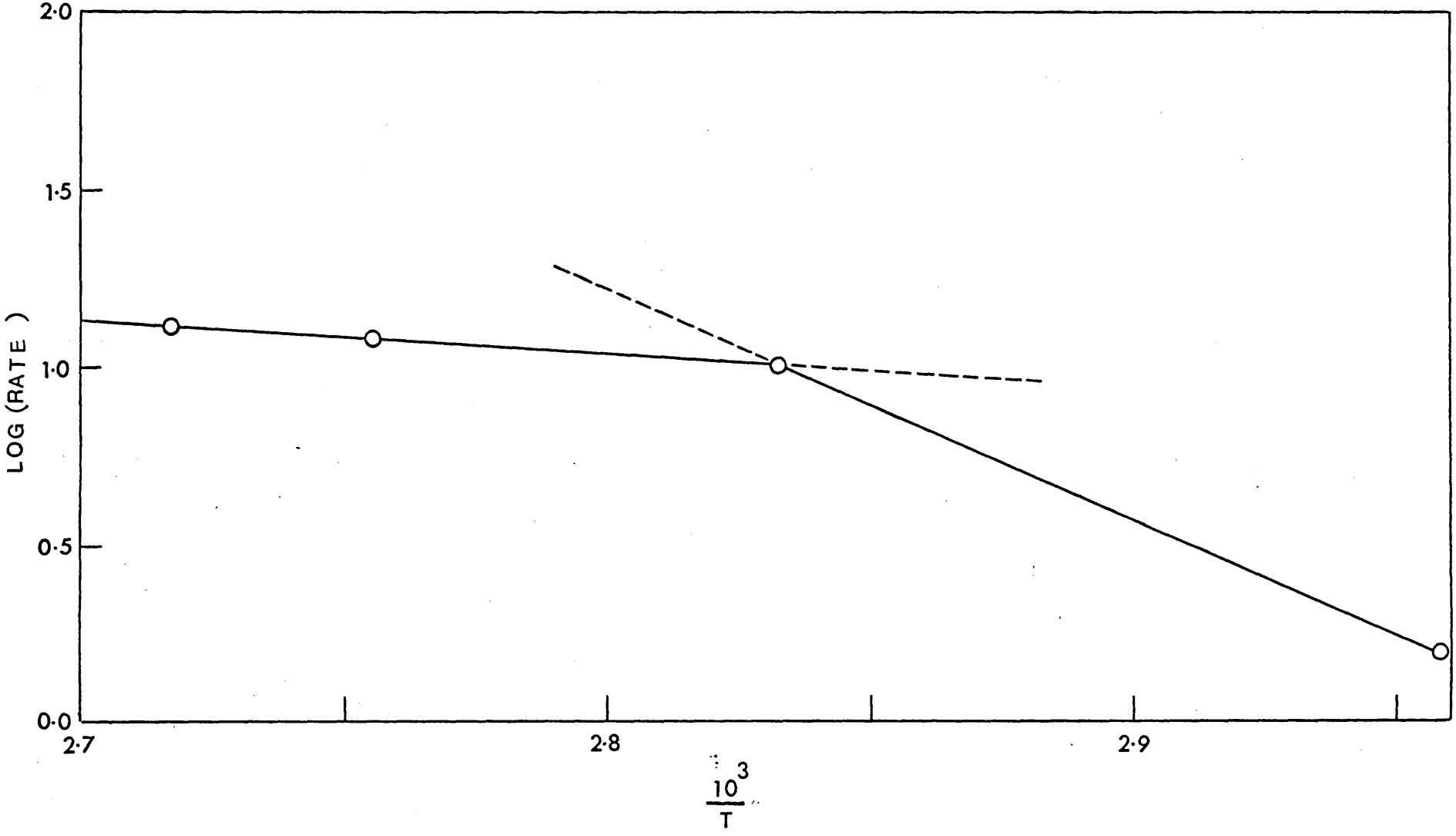

Fig. 31 Arrhenius plot for 100-140 hours.

against $\frac{1}{T}$. Both lines have the same gradient, from which critical increment of energy was calculated as 22 kcal/mole.

The Arrhenius plot for the region 100 - 140 hours is shown in Fig. 31 . It clearly shows two distinct lines. At higher temperatures the apparent activation energy is about 8 kcal/mole. Since rate control by mass transport in solution is inconceivable at the high stirring speed employed, this must mean mass transport in the solid state. Electron probe microanalyses of the leach residues do not suggest diffusion within the mineral. Therefore, transport of reactants or products across the barrier of iron and tin compounds or sulphur must be responsible for the retardation of the process at high retention times.

Therefore the apparent activation energy of 22 kcal/mole must correspond to the fundamental process in the leaching of stannite.

4.1.2 Particle Size.

Fig. 32 shows the effect of decreasing particle size on the dissolution rate of stannite at 95°C.

Obviously it has a pronounced effect on the rate and therefore attempts were made to correlate the leaching rate and particle size more quantitatively.

Reduction of particle size results in an increase of surface area. Therefore it was felt desirable to evaluate the true surface area of a given mass of the mineral screened to a known particle size. The most satisfactory method of doing this is by gas absorption techniques. Unfortunately this requires comparatively large samples (5 to 10 grams) and therefore this method was not considered. Estimation of the area by microscopic means gives only the projected area, and this may differ from the true area by a very large factor. therefore the following theoritical treatment was adopted.

The mineral sample, screened to a standard size is assumed to consist of n uniform spheres of radius r. Then the mass of the mineral sample would be

$(3/4\,\pi\, r^3)n\rho$ where ρ is the density .

The total surface area of the mineral sample is :

$(4\,\pi\, r^2).n$

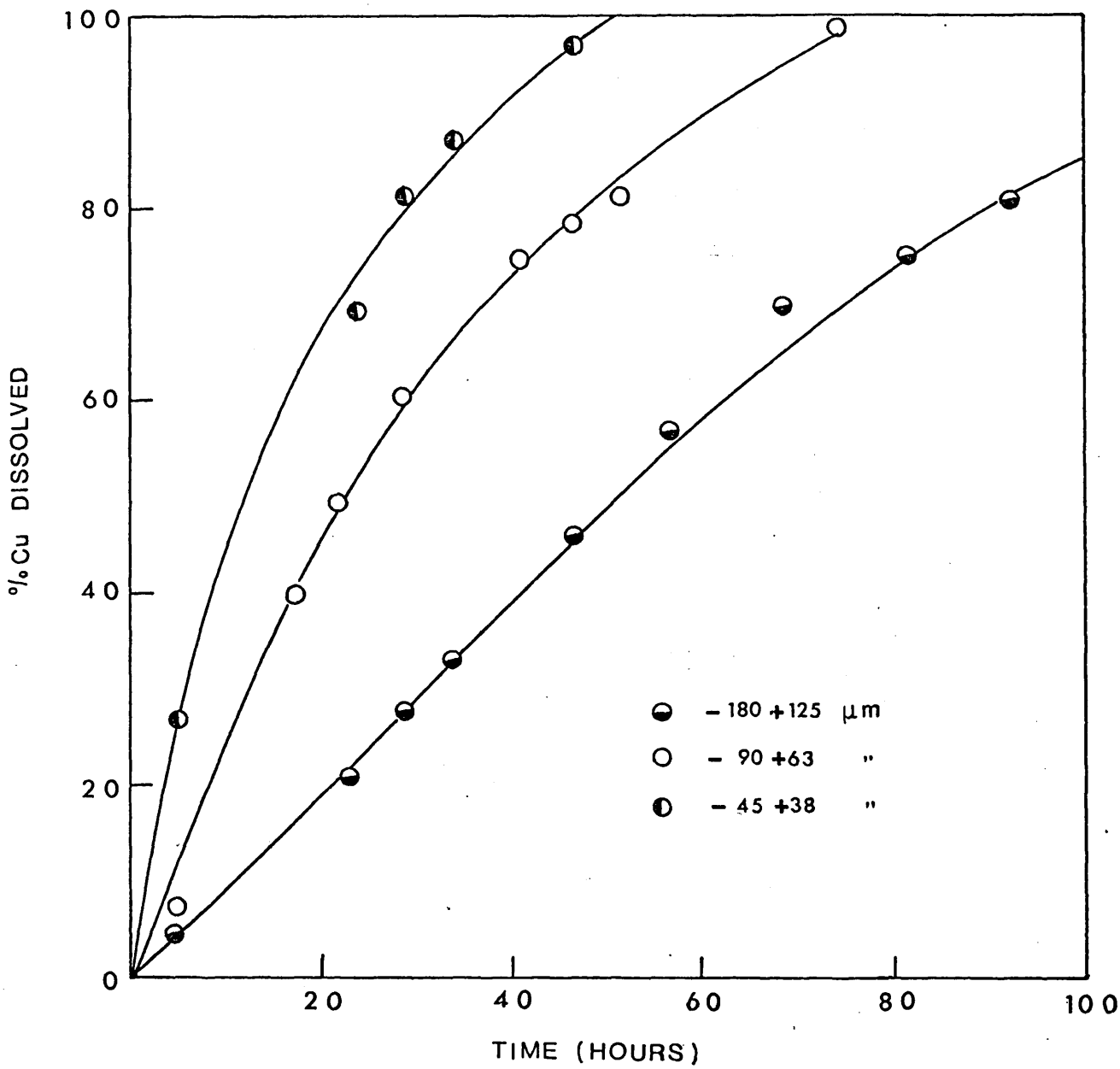

Fig. 32 Effect of Particle Size on the Rate of Leaching of Normal Stannite.

Therefore the surface area per unit mass is :

$$\frac{4\pi r^2 n}{4/3\,\pi r^3 n} \quad \text{which is proportional to } \frac{1}{r} .$$

The average diameter of particles is assumed to be the mean of the two sieve sizes. For example, particles screened to -45 + 38 micron would have a mean diameter of $\frac{45 + 38}{2}$ micron.

If the leaching rate is directly proportional to the surface area, a plot of $\frac{1}{r}$ versus the rate should give a straight line.

Fig. 33 shows such a plot, which clearly is a straight line passing through the origin. (A similar result was obtained by Wadsworth and co-workers[33] for the initial stage leaching of chalcopyrite in oxygenated sulphuric acid solutions).

This strongly suggests a surface reaction as the rate controlling process.

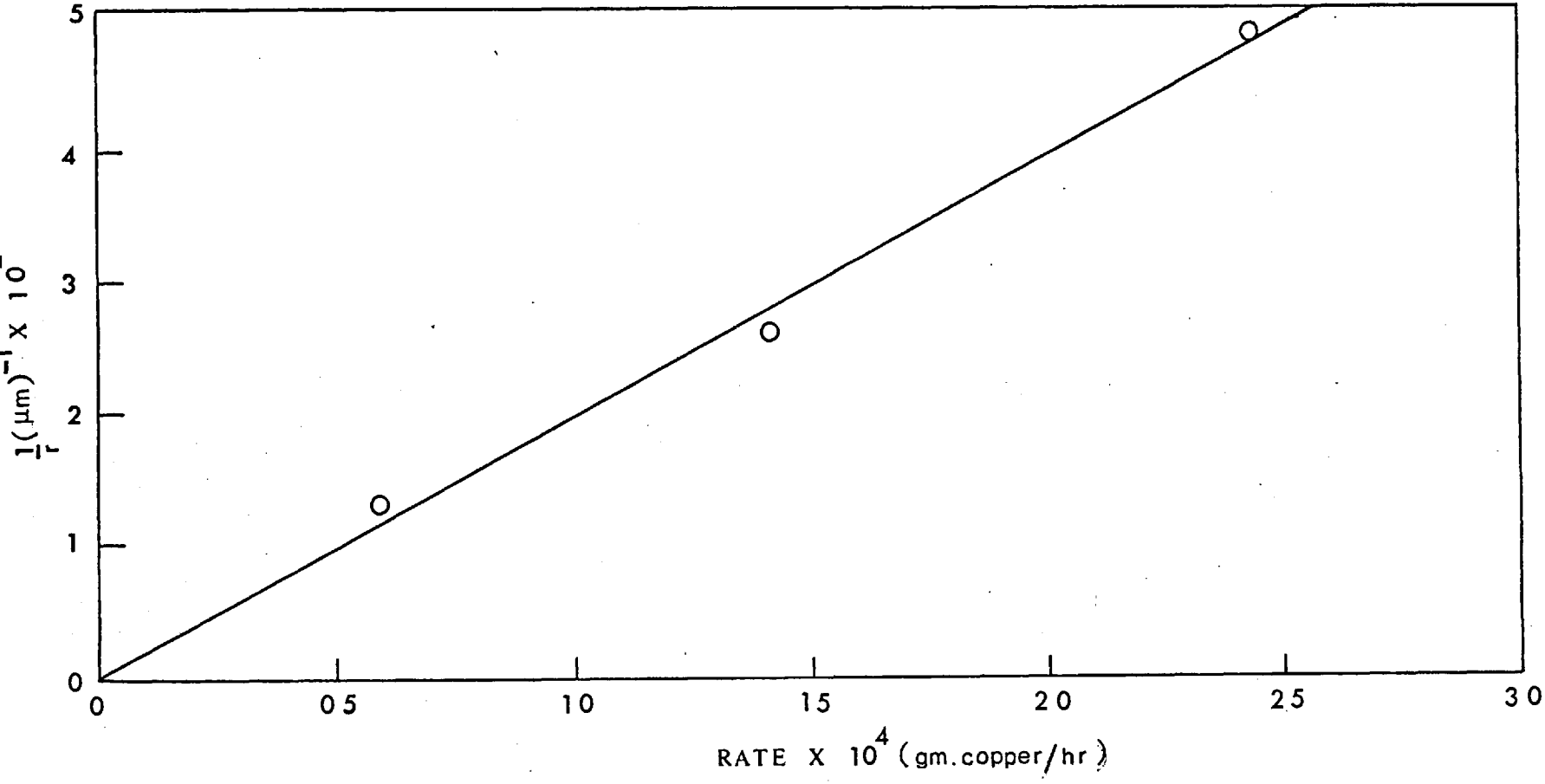

Fig. 33 Plot of inverse of mean particle diameter against the leaching rate.

4.1.3 Ferric Ion Concentration.

Stannite leaching depended on the ferric ion concentration over the entire range studied, 0.001 M to 0.5 M . Results obtained at 95°C are shown in Fig. 34

Iron hydrolysis was considerable at higher ferric ion concentrations, but this hardly affects the results for two reasons. First, the rates are calculated from the first few hours of leaching, when the hydrolysis is neglegible. Second, even after two weeks of leaching with 0.5 M Fe^{+3} , the ferric ion concentration was not altered by more than 4% of the nominal value. Curves obtained for very low ferric ion concentrations could have been improved by having a large volume of the reagent, say 2000 ml., to counteract the ferric ion depletion. Regrettably this was not practical with the present apparatus.

It is interesting to note that below 0.005 M Fe^{+3} concentration the effedt of this variable is less pronounced on the leaching process. In fact 0.5 M hydrochloric acid (purity in Sec. 2.5) leaching of stannite proceeds at about the same rate.(Sec. 4.5). An explanation is also offered in the same section.

A plot of $\log(Fe^{+3})$ versus the log(rate) gave the value 0.55 for the order of the reaction with respect to the ferric ion. The excellent linearity of(Fig. 35) the plot strongly suggests that the two are related.

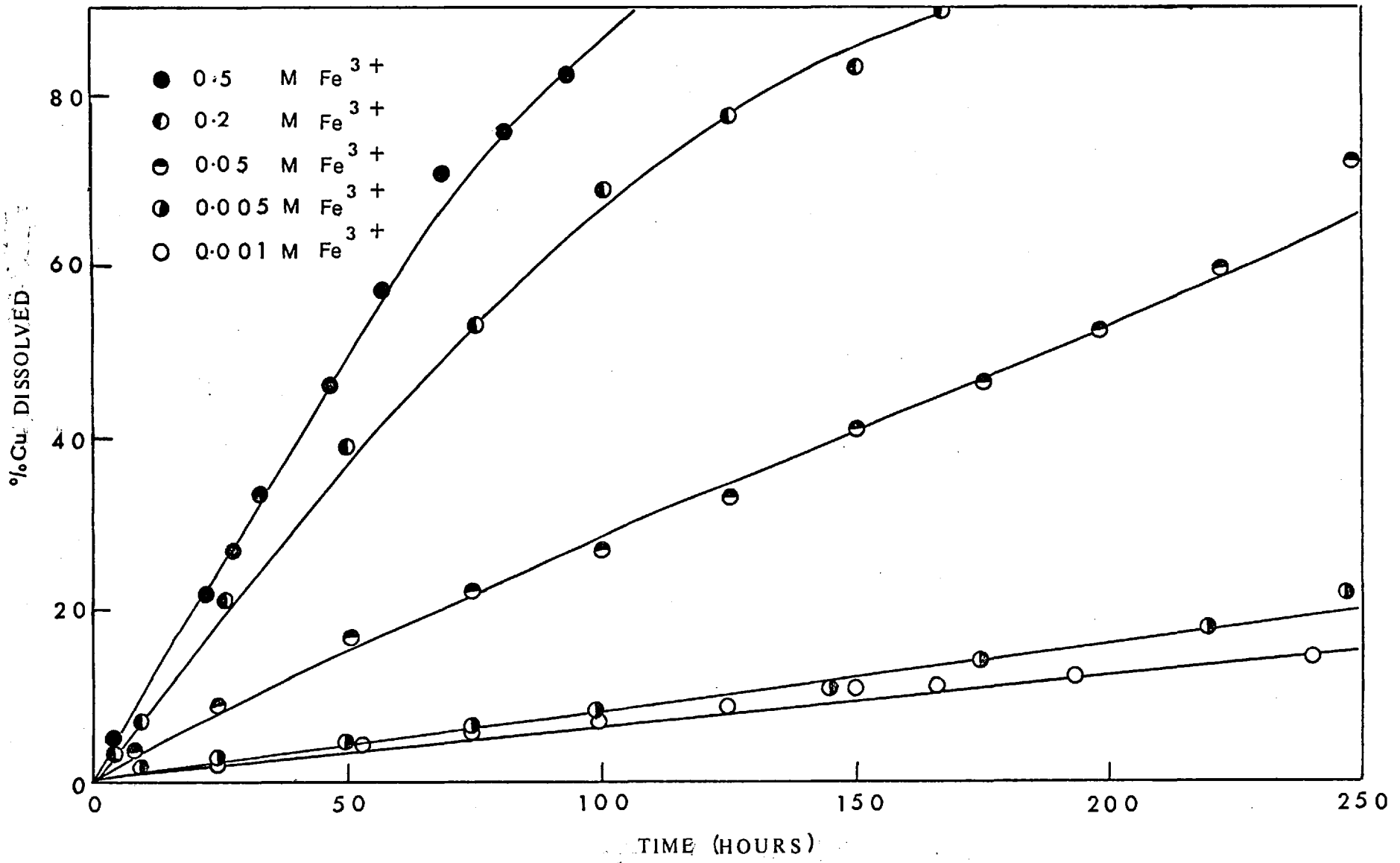

Fig. 34 Effect of Fe^{+3} on the rate of leaching of normal stannite.

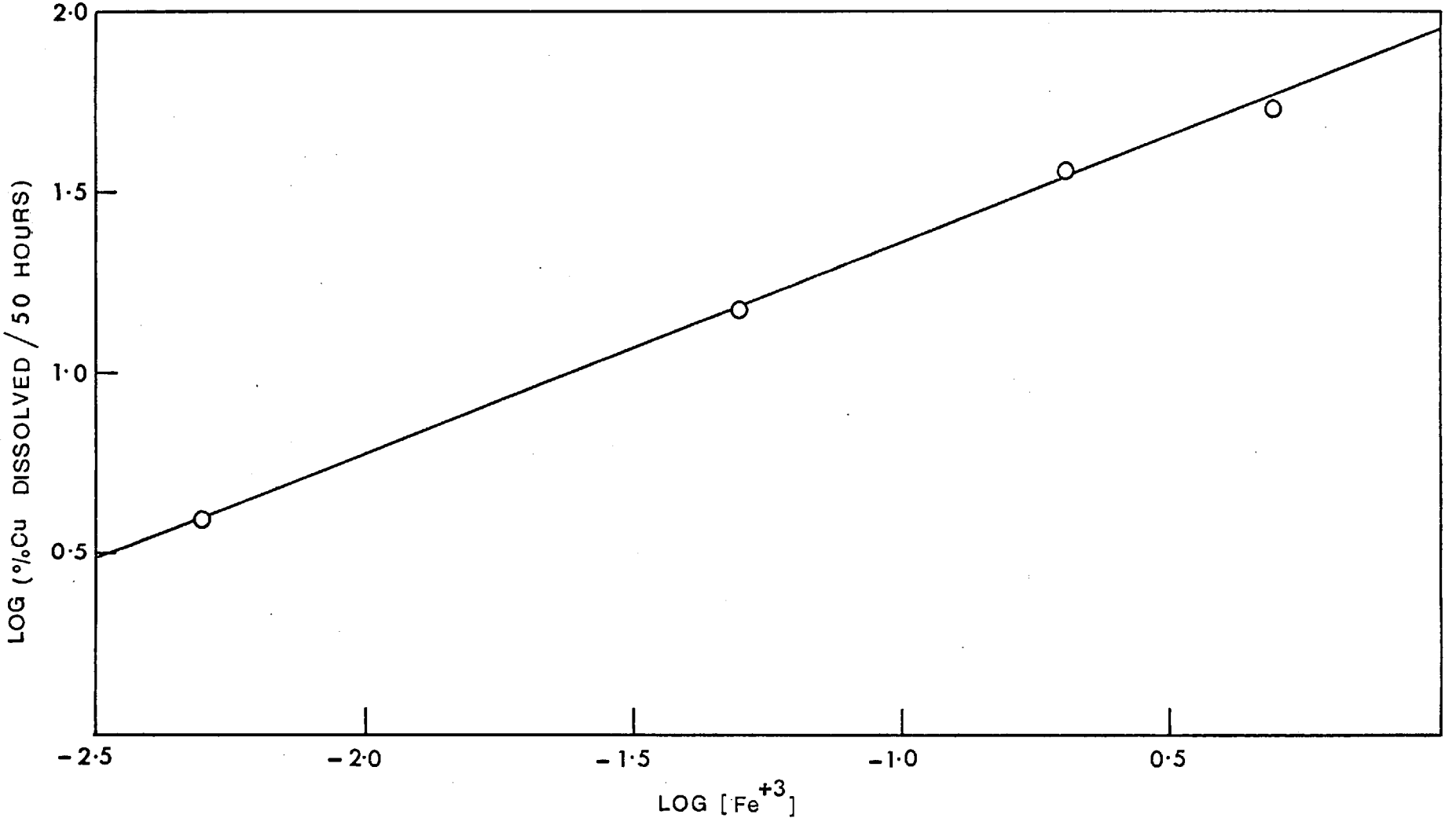

Fig. 35 Plot of log(rate) against log(Fe^{+3}) to find the order of reaction.

Therefore almost certainly the fundamental process in the leaching of stannite is a chemical interaction of ferric ion at the surface of the mineral.

4.1.4 Sample Weight.

Fig. 36 illustrates the effect of doubling the sample weight and shows that the percent dissolution is independent of the sample weight.

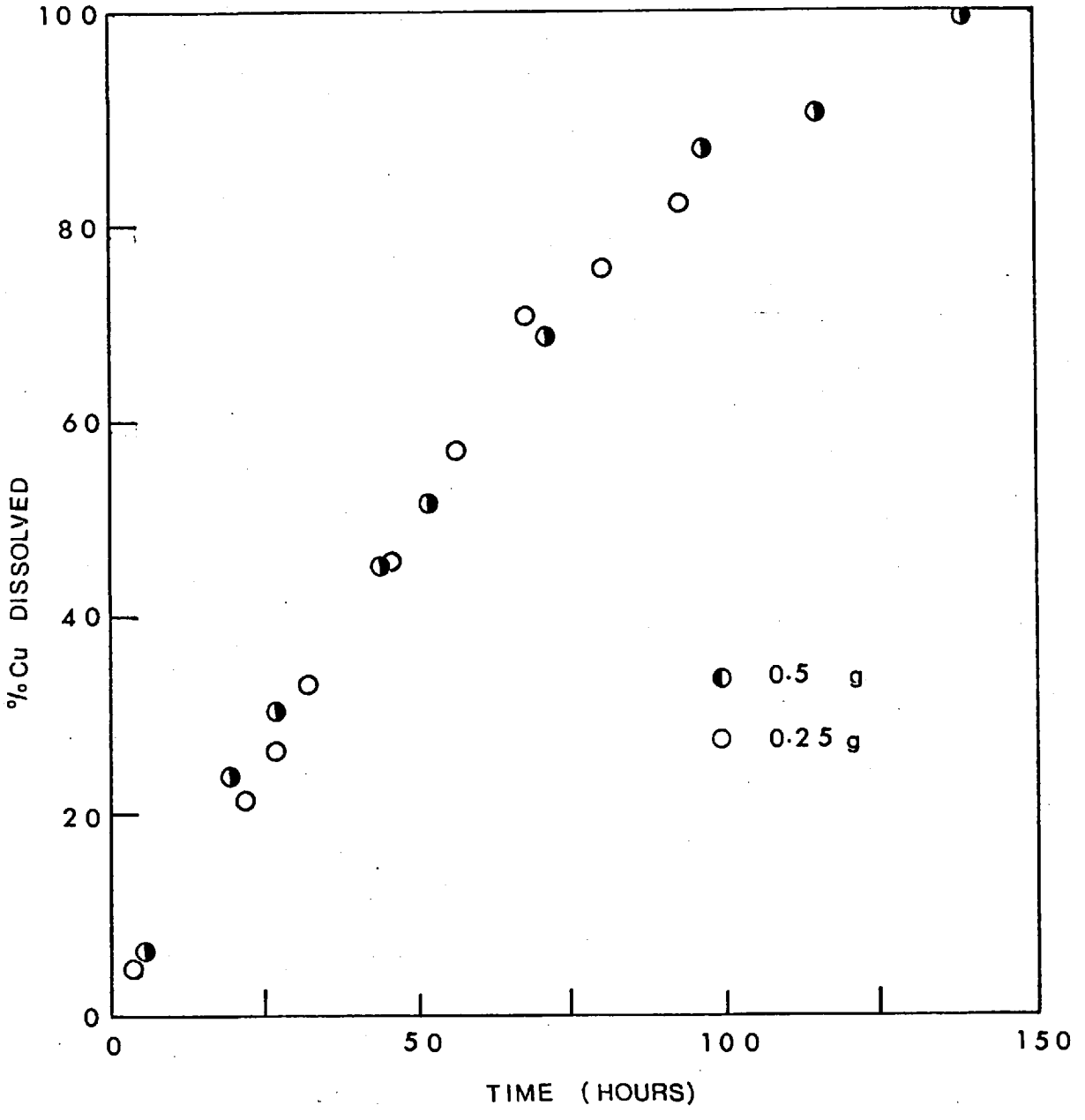

Fig. 36 Effect of sample weight on the rate of leaching of normal stannite.

4.1.5 Stirring Speed.

The effect of stirring speed on the rate of leaching was studied at 95°C, with the mineral screened to - 45 + 38 micron. This size fraction was chosen to ensure particles in suspension at low stirring speeds.

The results are shown in Fig. 37 . Clearly the rate of dissolution of normal stannite is independent of the stirring speed, which means that the transport of ferric ions from the solution to the mineral surface is not the slow step in the leaching process.

Therefore the rate determining step is either a solid state diffusion or a chemical reaction between the ferric ions adsorbed on the surface and the mineral. The latter view is supported by :

1. The increase of the rate according to the 0.55 power of ferric ion concentration.
2. Direct dependence of the rate on the surface area.
3. Independence of the rate on the stirring speed.

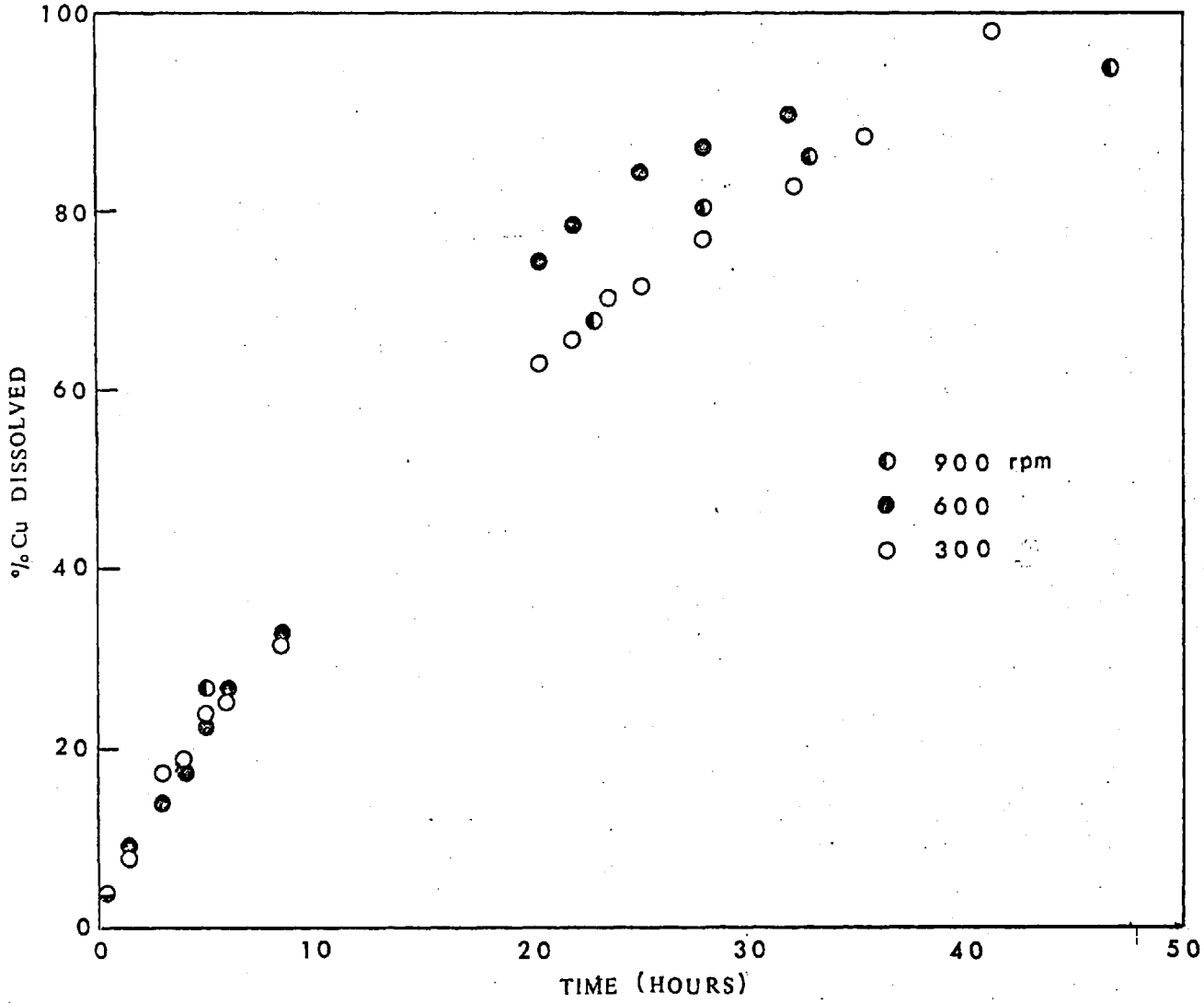

Fig. 37 Effect of stirring speed on the rate of leaching of normal stannite.

4.2 HYDROGEN PEROXIDE LEACHING.

It was necessary to know if a preferential leaching of some elements occured and a solvent not containing iron had to be sought for this.

Ferreira successfully studied the leaching of chalcopyrite using acidic hydrogen peroxide solutions and therefore the same solvent system was chosen for stannite.

The leaching solution was prepared by adding 50 ml of 20 volume hydrogen peroxide and 150 ml of 0.5 M hydrochloric acid. Hydrochloric acid was used to avoid the initial addition of sulphate.

Leaching was carried out as described in Sec. 2.2 and samples were analysed for copper, iron and sulphate by atomic absorption spectrophotometry.

The results are presented in Table B-15 and Fig. 38

Fig. 38 is a plot of percent iron dissolution against percent copper dissolved. The graph is a straight line passing through the origin with an inclination of 45^{o} upto about 50% copper dissolution. After that the iron content in the solution begins to lag behind. This shows that initially both elements are leached at the same rate and after some time either iron dissolution slows down or some dissolved iron is removed from the solution by precipitation.

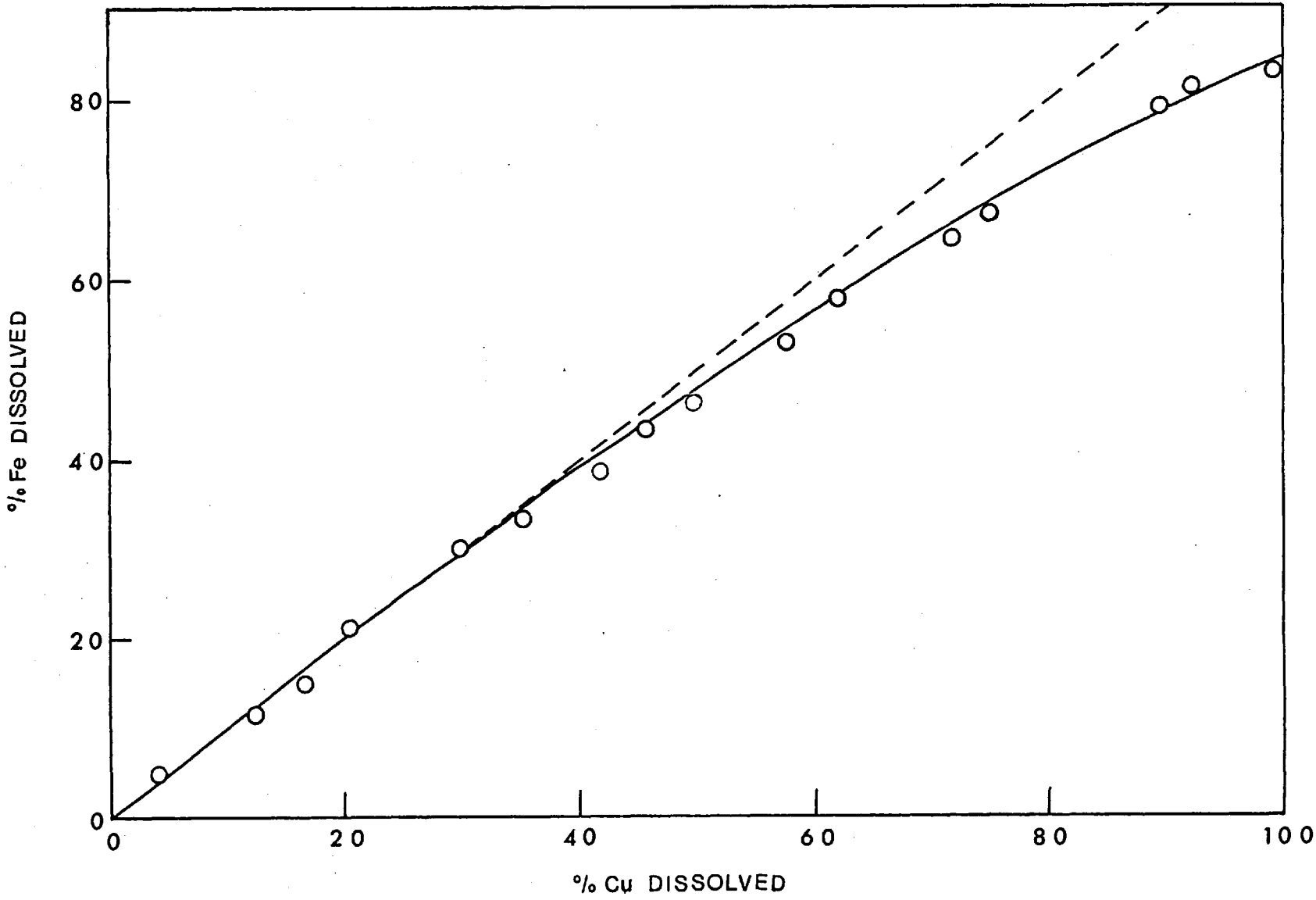

Fig. 38 Relative rates of copper and iron extraction in the leaching of normal stannite (hydrogen peroxide leach).

In addition to elemental sulphur, an amorphous, greyish white fine precipitate was obtained. This did not give a X-ray powder photograph. Atomic absorption analysis of a solution of this substance in aqua regia showed it to contain about 5% iron. Although a rigorous chemical analysis was not carried out comparison of the physical properties of this product with those of the prepared compound described in section 4.1 suggests that this material is probably SnO_2 or $Sn(OH)_2$ with co-precipitated Fe_2O_3 . It must be noted that even pure SnO_2 does not give a Guinier photograph if the powder is too fine.

The observations made in an arbitrary test are interesting.

A few milligrams of the white substance was placed in a small silica tube which was vacuum sealed. The colour of the substance immediately turned black on heating. After heating the tube at 500°C for several hours it was opened, whereupon a strong odour of hydrogen sulphide was evident. The black mass produced an extremely complex Guinier photograph almost impossible to analyse. However, some lines were identified as belonging to Fe_2O_3 .

Therefore it is inferred that the bending of the iron dissolution curve is due to iron precipitation and that copper and iron are extracted at the same rate upto 100% dissolution.

In contrast to ferric chloride leaching, hydrogen peroxide leaching produced sulphate ion in substantial quantities. 26.1% of the sulphur was found in the form of sulphate at 100% copper dissolution. (In ferric chloride medium SO_4^{-2} was absent). The detection of sulphate ion in leach liquors calls for a closer examination of the leaching process. Two possible mechanisms may be considered.

1. Stannite leaching in hydrogen peroxide consists of two simultaneous processes. A direct production of elemental sulphur accompanied by a direct production of sulphate, thus :
   a) $Cu_2FeSnS_4 \longrightarrow S^o$ + other products
   b) $Cu_2FeSnS_4 \longrightarrow SO_4^{-2}$ + other products

2. The primary leaching reaction is a single process producing elemental sulphur which is then converted to sulphate by the oxidising medium.

The feasibility of the second process was checked by an independent method.

Two grams of elemental sulphur was placed in a 50 ml round bottomed flask containing a solution of hydrogen peroxide in hydrochloric acid mixed in the same ratio as for the leaching. This was heated on a water bath for about 8 hours. On adding crystals of barium chloride to the solution a white precipitate was obtained.

This evidence, indicative but not conclusive, suggests that process 2 is more close to reality than process 1.

4.3 ANALYSES OF LEACH RESIDUES.

4.3.1 Atomic Absorption Spectrophotometry and Electron Probe Micro Analysis.

Partially leached residues, after washing thoroughly with 0.5 M hydrochloric acid and acetone were dried at room temperature. The mineral particles were sorted from other products such as elemental sulphur, under a low power stereo microscope.

Test solutions, prepared by the procedure described in section 2.4.1 were analysed for copper, iron and tin by atomic absorption spectrophotometry.

The results are tabulated in Table 22

% Cu Dissolved	%Cu	%Fe	%Sn	%S (by diff.)
55.0	32.9	13.5	26.8	26.8
66.5	34.1	12.9	25.5	26.3
79.2	27.8	11.8	26.7	33.7*
92.9	31.5	12.2	27.2	29.1

* By EPMA

Table 22 . Analyses of Leach Residues.

The values show that there is no change in the overall chemical composition of the mineral during leaching.

Electron probe microanalysis was carried out on a partially leached residue (80% copper removed) and the traces for Fe , Cu , Sn and S showed exceptional homogeneity.

These results are not consistent with a process in which solid state diffusion is occuring. If diffusion took place to any appreciable degree, then one would expect to find compositional variations across a grain (as in Cu_2S or Cu_5FeS_4) unless all the constituents migrated at the same rate. This clearly cannot be the case, because it is well known that the sulphur diffusion is extremely slow. Although data on the diffusion of tin in sulphides are not available, observations recorded in section 2.1 suggest that tin diffusion also is very slow compared to that of copper and iron.

Therefore the leach residues must be rich in sulphur and tin compared to the original mineral, if solid state diffusion took place. Since the results do not suggest this, solid state diffusion may be excluded as a rate controlling process.

4.3.2 X-ray Diffraction.

Leach residues after washing with HCl were analysed by X-ray diffraction to follow possible phase changes.

Guinier photographs are presented in Fig. 39

All the photographs are identical. No lines appeared or dissappeared upto 100% copper dissolution. Therefore it is concluded that no phase change occured within the solid during leaching.

From the Guinier photographs the lattice constants were calculated using the standard formula :

$$\frac{1}{d^2} = \frac{h^2 + k^2}{a^2} + \frac{l^2}{c^2}$$

The tetragonal unit cell parameters a and c were calculated from all the lines and the 'best' values were selected. Typical results are shown in Table 23 .

The results given in Table 23 indicate that there may be some fluctuation of the lattice parameters with percent copper extraction. Since there was no uniformity in the results, a diffractometer technique was adopted to compare the lattice parameters of stannite and a partially leached (28% copper extracted) stannite residue.

Reflections occuring at high Bragg angles ($2\theta > 80^{o}$) were chosen for the analysis. At these high angles α_1 α_2 resolution was observable and only those peaks caused by the reflection of α_1 were considered.

A : Stannite

B : 1-2% Cu dissolved

C : 13.5% "

D : 13.8% "

E : 27.8% "

F : 41.1% "

G : 50.7% "

H : 57.0% "

I : 66.5% "

J : 81.9% "

K : 85.7% "

L : 90.0% "

Fig. 39 Guinier photographs of leach residues.

%Cu Dissolved			1 - 2	13.48	27.76	50.69	57.00	66.49	80.00
	Stannite								
	A	B							
a_o	5.442	5.428	5.445	5.438	5.426	5.443	5.434	5.446	5.431
c_o	10.756	10.7396	10.756	10.743	10.712	10.734	10.734	10.777	10.748

Table : 23 Lattice parameter data of the leach residues calculated from Guinier photographs.

The peak positions were accurately determined by the procedure described in section 2.4.4.3 .

In strict accordance with the recommendations in the 'International Tables for X-Ray Crystallography'[98] values for the lattice parameter a were calculated from reflections of low h , k indices (006 for example). Similarly c values were obtained from reflections with low l indices. The reason why this should be so is clear when one considers the final expressions for a and c .

ie. $$a = d\,c\,\sqrt{\frac{h^2 + k^2}{c^2 - l^2}}$$

and $$c = \frac{a\,l\,d}{\sqrt{a^2 - (h^2 + k^2)}}$$

where d is the interplaner distance between the planes defined by the Miller indices h k l .

If reflections of high l were used to calculate c the errors in d will be multiplied directly resulting in a high c value. Likewise, high h and k increase the error in a, although to a lesser extent.

The selected values of a and c were plotted against cos θ.cot θ . Such plots are presented in Figs. 40-43.

The values of a and c calculated from each line of the powder pattern are presented in Tables 24-26.

DETERMINATION OF LATTICE PARAMETERS

USING DIFFRACTOMETER DATA.

Table : 24 For Stannite.

2θ (°)	d (Å)	h k l	c (A)	a (A)	cosθ.cotθ
88.040	1.10846	2 4 4	10.74590	5.44469	0.74389
88.750	1.10142	2 2 8	10.74636	5.46336	0.73054
96.225	1.03469	1 1 10	10.74252	5.55302*	0.59880
106.575	0.96087	4 4 0	-	5.43550	0.44579
107.450	0.95546	0 4 8	10.73705	5.44780	0.43422
114.350	0.91664	1 5 6	10.73767	5.44413	0.34968
115.450	0.91104	1 3 10	10.73862	5.45856	0.33836
127.450	0.85904	3 0 11	10.72871	5.44100	0.21985
		(0 6 4)			
130.050	0.84974	0 2 12	10.73370	5.45815*	0.19707
		(5 4 1)			
137.180	0.82738	3 5 6	10.72878	5.44241	0.14313
		(4 5 3)			

* High l indices.

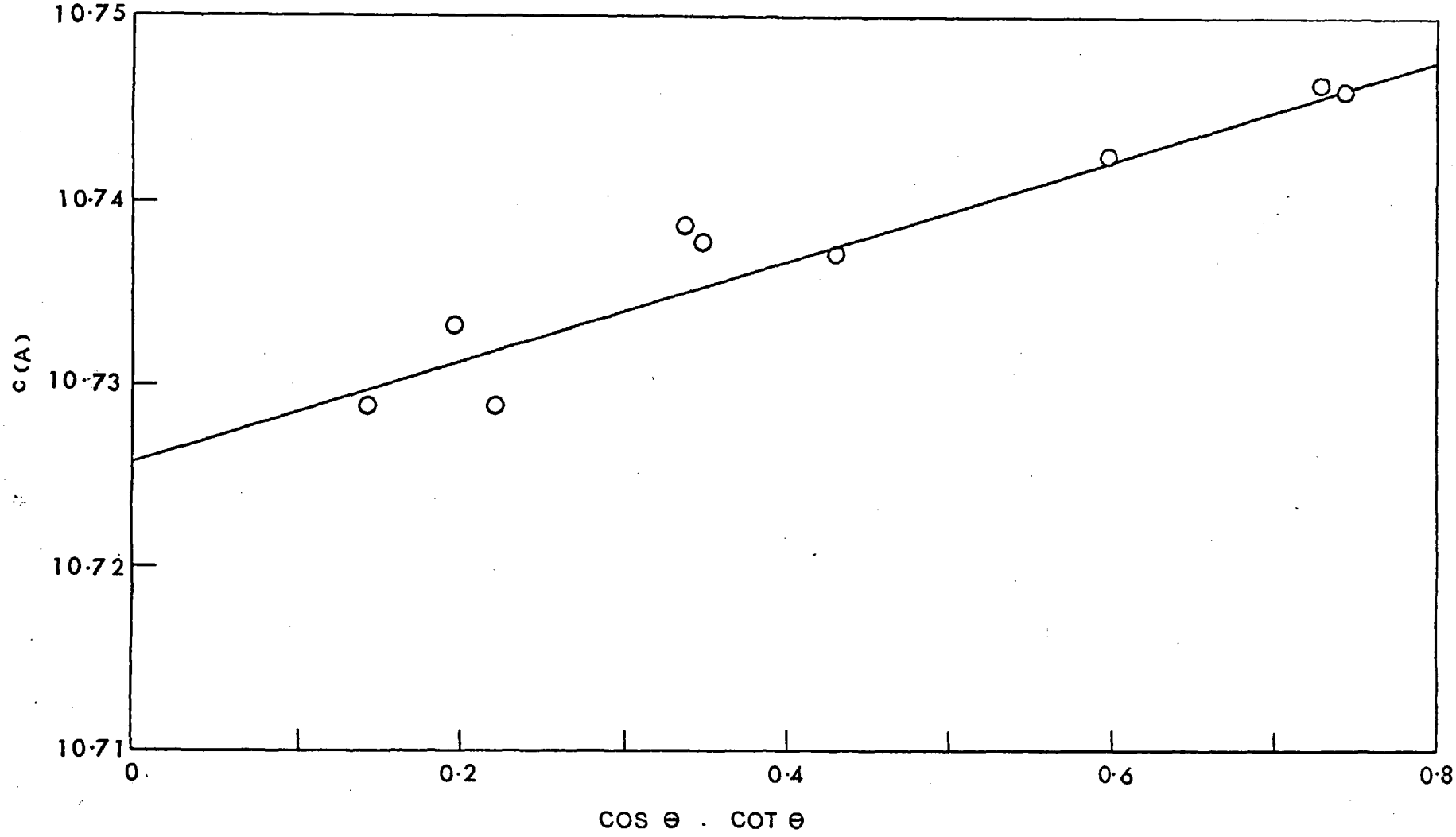

Fig. 40 Plot of lattice parameter 'c' against cosθ.cotθ for normal stannite.

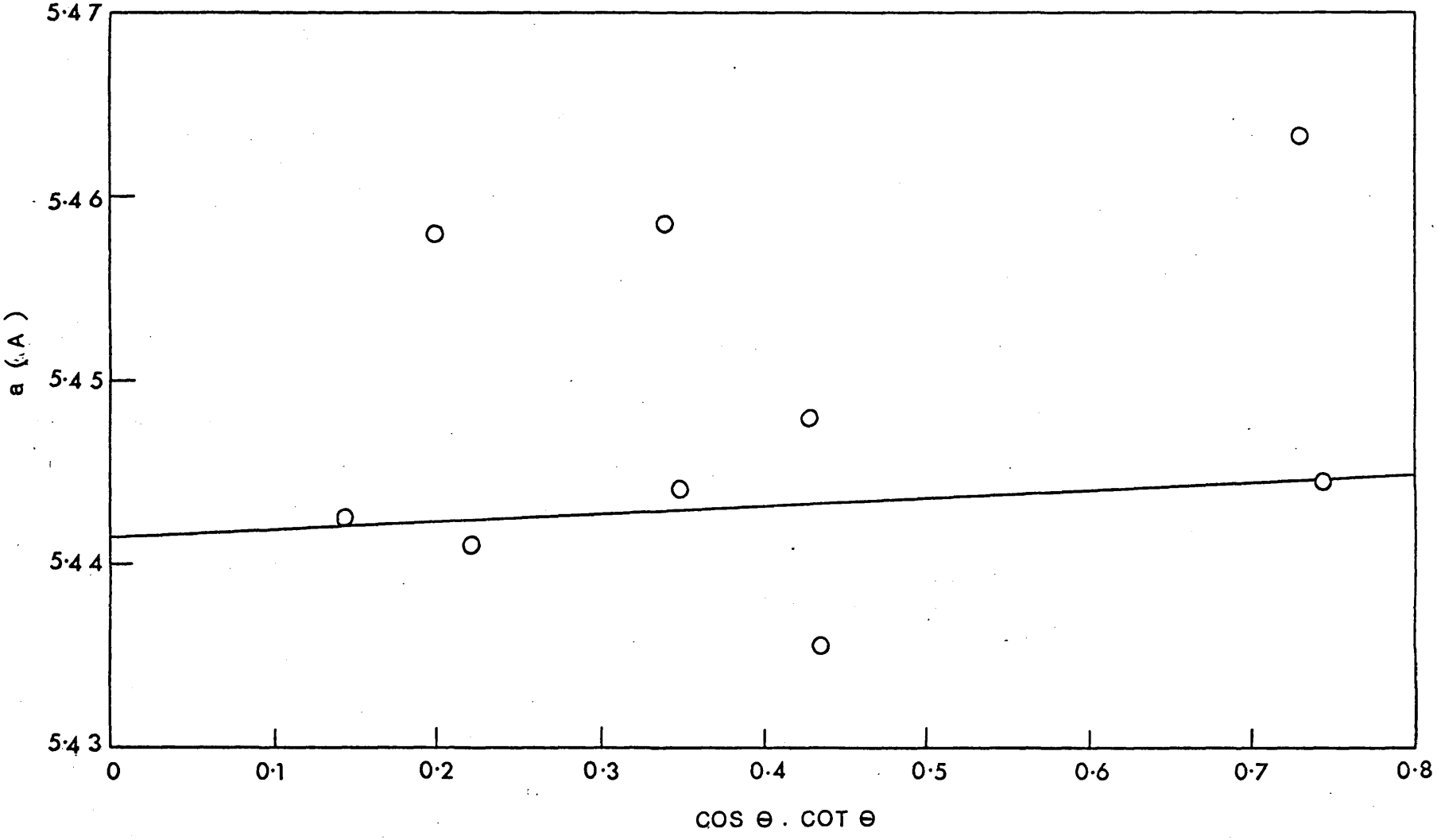

Fig. 41 Plot of lattice parameter 'a' against cosθ.cotθ for normal stannite.

DETERMINATION OF LATTICE PARAMETERS

USING DIFFRACTOMETER DATA.

Table : 25 For Leach Residue. (27.8% Copper Dissolved)

2θ (°)	d (A)	h k l	c (A)	a (A)	cosθ.cotθ
88.053	1.10834	2 4 4	10.73907	5.44339	0.74389
88.805	1.10088	2 2 8	10.73852	5.45515	0.72950
96.198	1.03491	1 1 10	10.74498	5.57017	0.59925
106.700	0.96009	4 4 0	-	5.43109	0.44412
107.463	0.95538	0 4 8	10.73528	5.44688	0.43406
114.375	0.91651	1 5 6	10.73187	5.44308	0.34939
115.450	0.91104	1 3 10	10.73862	5.46072	0.33747
127.440	0.85907	3 0 11	10.72919	5.44121	0.21863
		(0 6 4)			
130.000	0.84991	0 2 12	10.73608	5.45924	0.19766
		(5 4 1)			
137.200	0.82726	3 5 6	10.72508	5.44157	0.14291
		(4 5 3)			

Material	c (A)	a (A)
Stannite	10.72599	5.4415
Leach Residue (27% Cu Removed)	10.72598	5.4414

Table : 26 Comparison of Lattice Parameter Data.

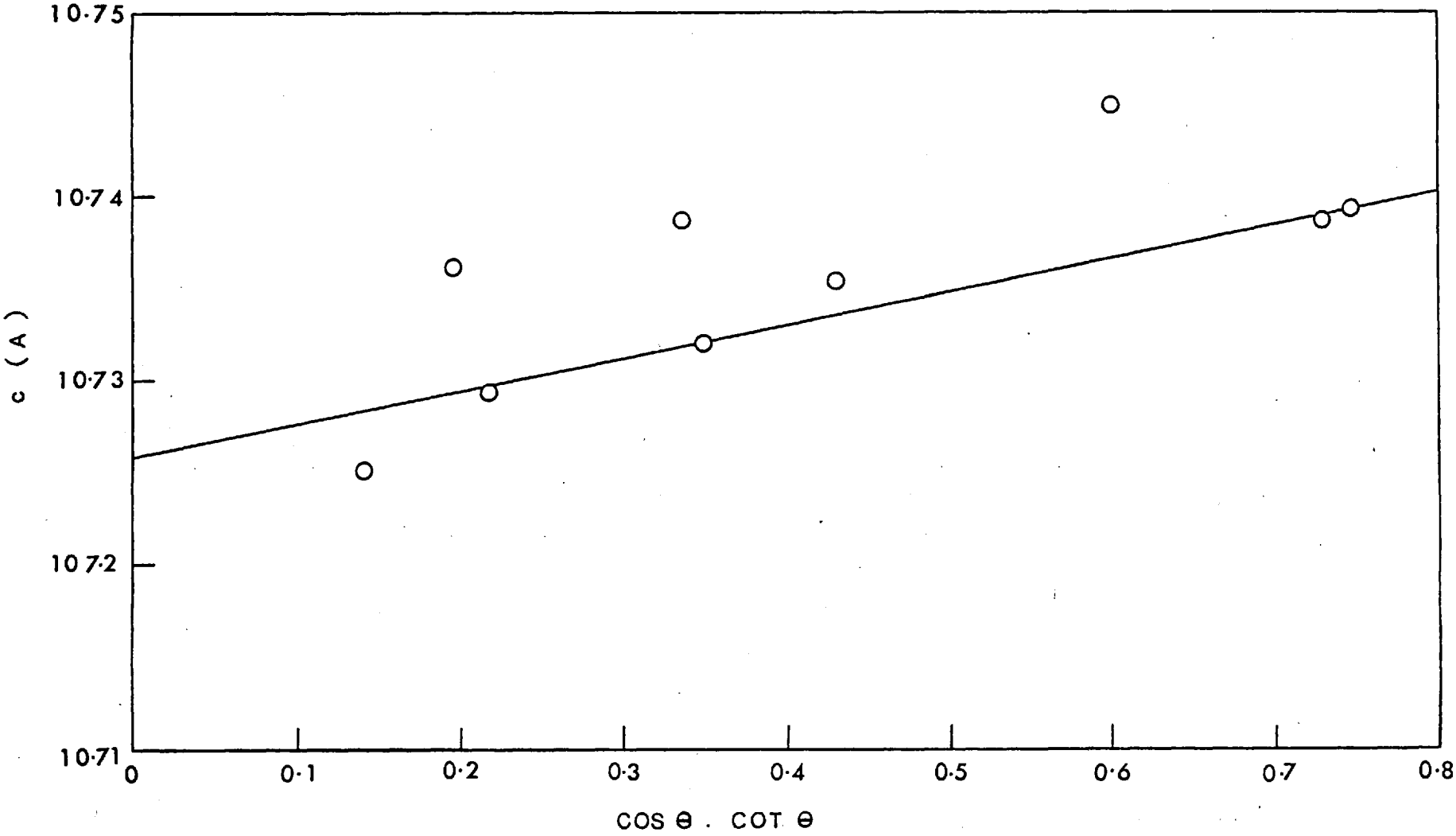

Fig. 42 Plot of lattice parameter 'c' against cosθ.cotθ for the leach residue (27.8% copper dissolved) normal stannite.

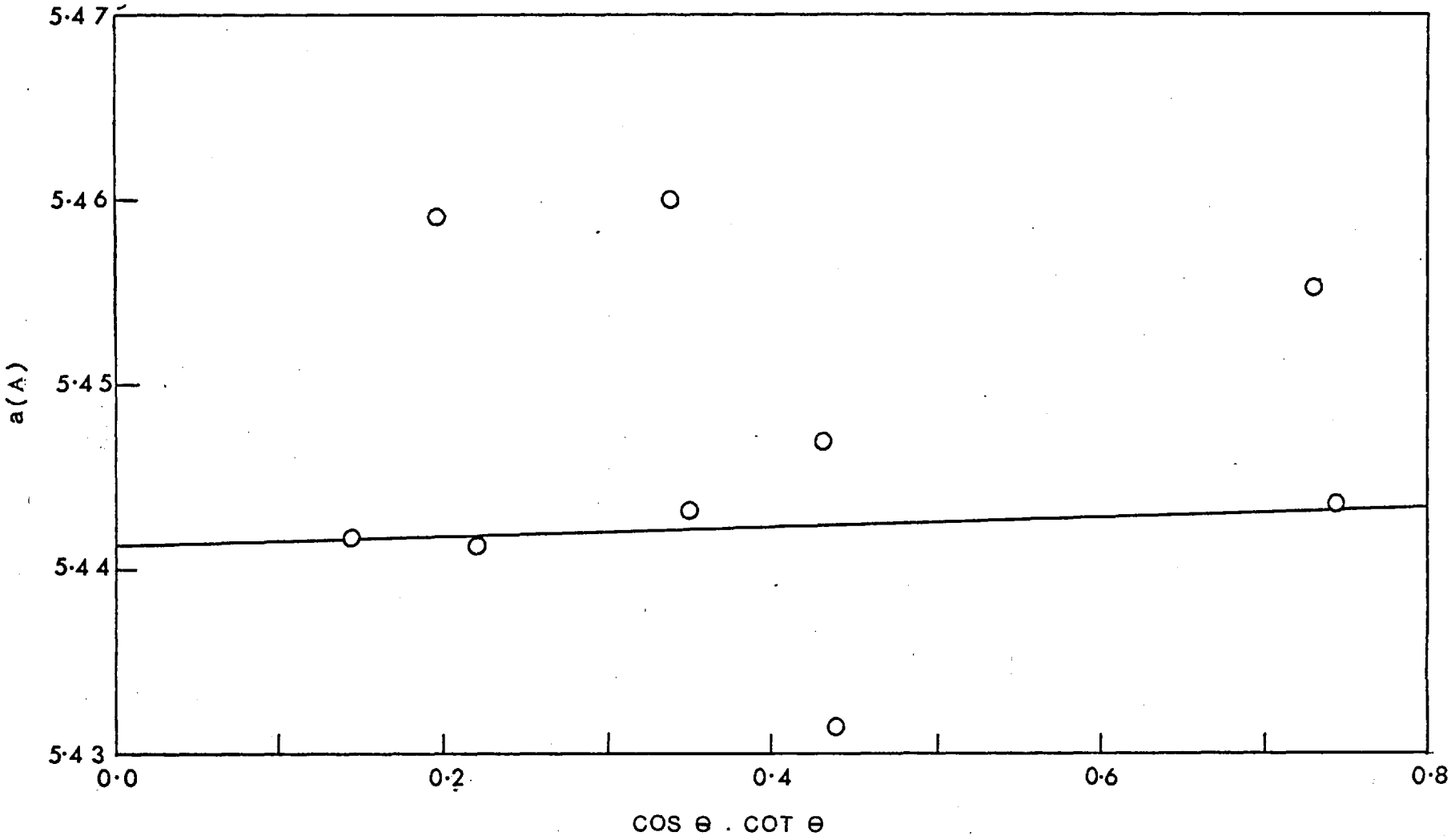

Fig. 43 Plot of lattice parameter 'a' against cosθ.cotθ for the leach residue of normal stannite (27.8% copper dissolved).

This shows that there is no change in the lattice parameters during leaching.

Ugarte conclusively showed that the initial stage of leaching of bornite is controlled by the solid state diffusion of the copper ions. This, he showed, was accompanied by a marked contraction of the unit cell. (Figs 2 & 3).

Similar observations were recorded by Ferreira in the leaching of β-chalcopyrite. Here also solid state diffusion was thought to be rate controlling.

It is reasonable to assume therefore that the constancy of the lattice parameters indicated the absence of a solid state diffusion in the leaching of stannite.

Since the crystal structure is not affected to any degree, it must be concluded that the stannite leaching is a surface process. Experiments carried out with different particle sizes confirm this.

The apparent activation energy ($\sim$ 22 kcal/mole) strongly suggests a chemical reaction for the surface process.

4.4 EXAMINATION OF LEACH RESIDUES - OPTICAL AND SCANNING ELECTRON MICROSCOPY.

Polished sections of the partially leached residues were examined by the optical microscope to observe possible phase changes and to investigate the mode of attact that occured during leaching.

Close examination of the samples, even under polarised light with crossed nicols, failed to reveal the presence of a new phase.

It was not possible to derive firm conclusions regarding the mode of attack, from a few random specimens.

Therefore, six leach residues, representing different degrees of copper dissolution, from about 13% to almost 100% , were selected for a systematic investigation. Starting from mounting the sample to the final 1 micron polish, exactly the same procedure was applied to all of them. (The extent of grinding on different sand papers was checked using an ordinary metallurgical microscope).

The photomicrographs are reproduced in Figs. 44-50

The particles in the first residue corresponding to 13% copper dissolution (Fig. 45) are almost identical to those in the unleached mineral (Fig. 44), with well defined edges having no cracks or pores.

Fig. 46 which is a photomicrograph of a residue with 41.4% copper dissolved, shows the non-uniform

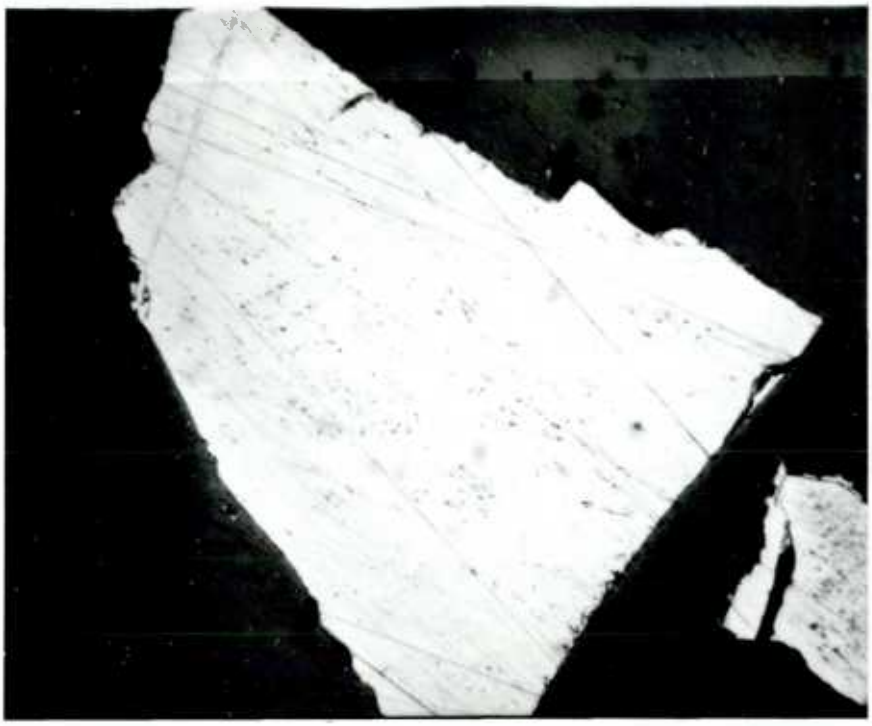

Fig. 44 Photomicrograph of normal stannite (X300)

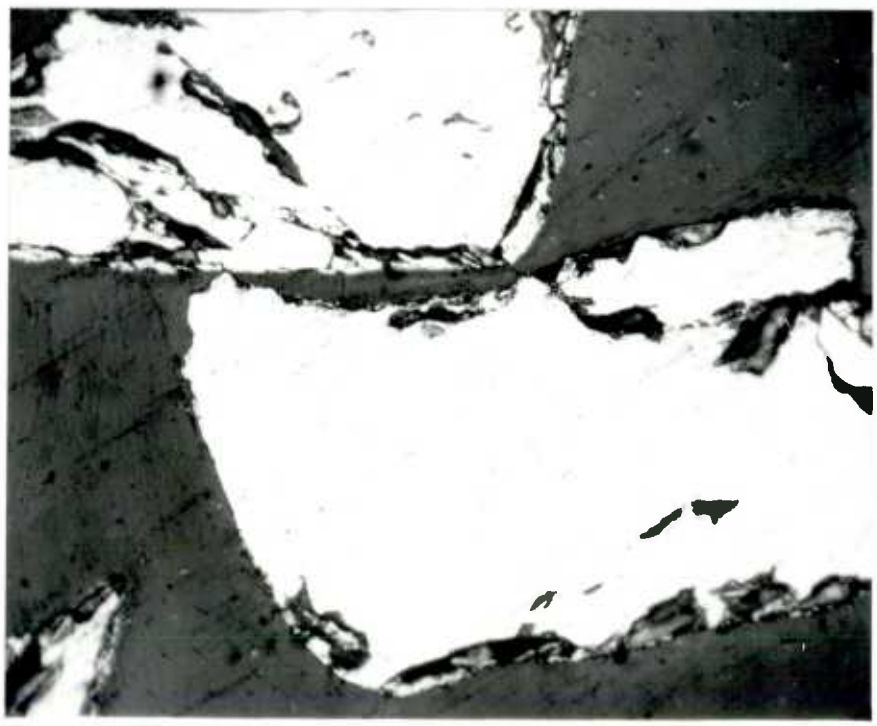

Fig. 45 Photomicrograph of leach residue 13.5% copper dissolved. (X 300)

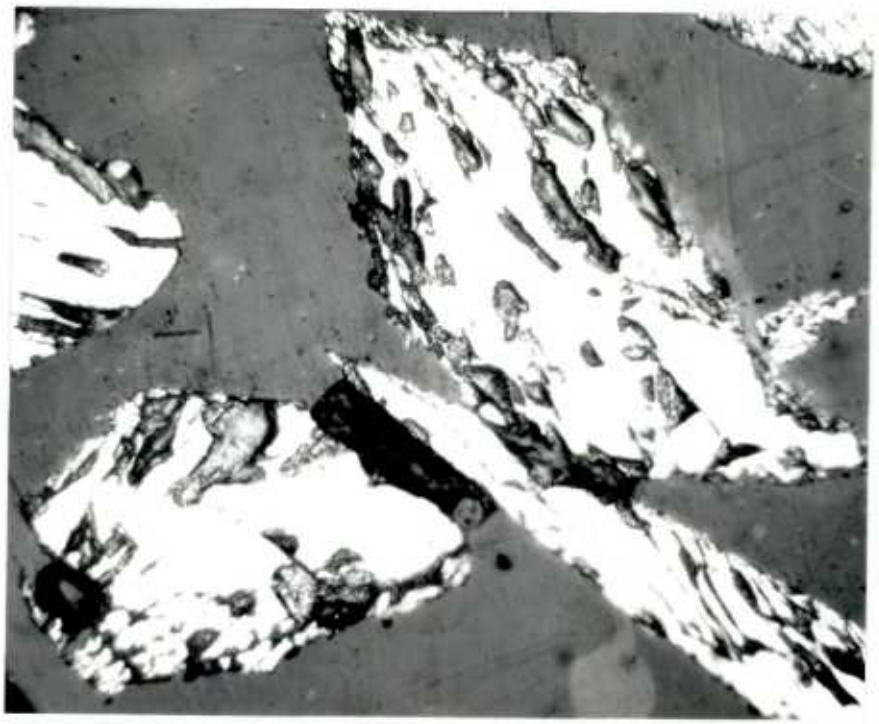

Fig. 46 Photomicrograph of leach residue 41.1% copper dissolved. (X 300)

Fig. 47 Photomicrograph of leach residue 66.5% copper dissolved. (X300)

nature of the attack. The path of attack seems to take straight lines rather than a pore formation.

When more copper is leached out, (Fig.47) the particles regain the appearence of the unleached mineral. But now they are smaller.

This alternate appearence and disappearence of 'grooves' is the most striking feature of the photomicrographs. This phenomenon continues upto 100% copper dissolution.

The preferential nature of the leaching action was confirmed by scanning electron microscopy.

A mounted stannite specimen, after polishing down to 1 micron, was allowed to remain in a stirred 0.2 M $FeCl_3$ solution for 12 hours at 80°C. This was observed with a scanning electron microscope.

Fig. 52 shows the general topography of the leached surface and it is possible to see the 'groove' where the attack is particularly heavy. A comparison of the 'groove' with the polishing scratches clearly visible in Fig. 53 , which is a photograph of the same area at a lower magnification, shows that the 'groove' is not a polishing scratch. Fig. 51 , which is a photograph of the unleached specimen brings out this difference better. In fact the polishing scratches are <u>not</u> preferentially attacked.

The mechanism of attack may be visualized by combining this information.

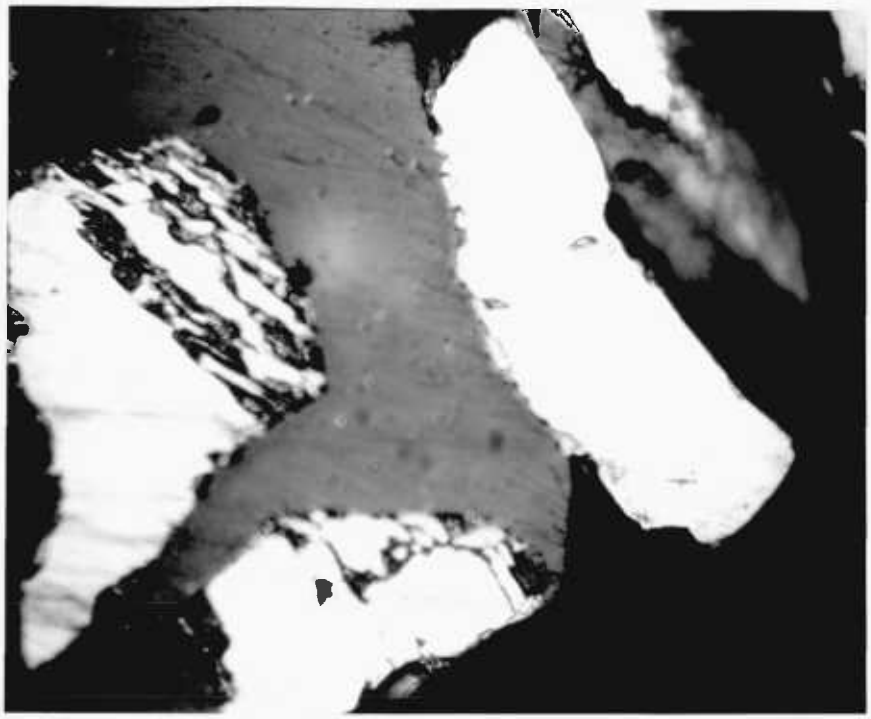

Fig. 48 Photomicrograph of leach residue 81.9% copper dissolved. (X300)

Fig. 49 Photomicrograph of leach residue 90.0% copper dissolved. (X300)

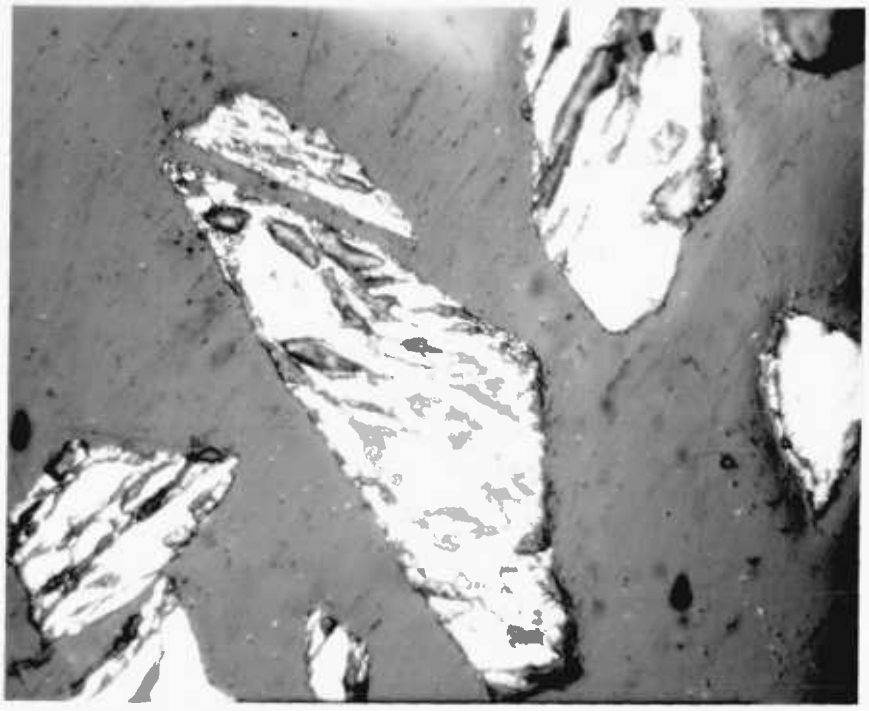

Fig. 50 Photomicrograph of leach residue almost 100% copper dissolved. (X300)

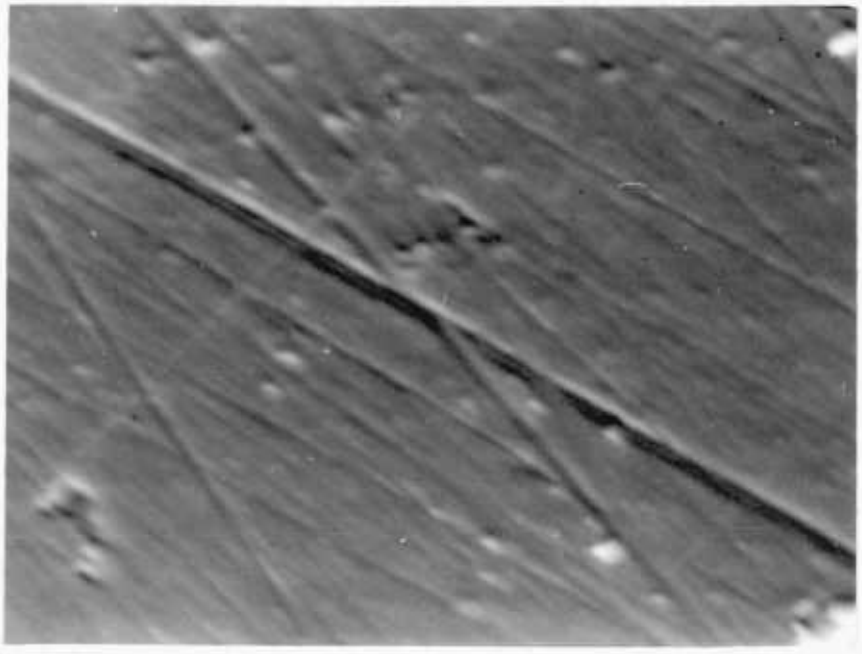

Fig. 51 Scanning electron micrograph of the unleached mineral (1 micron polish) (X5000)

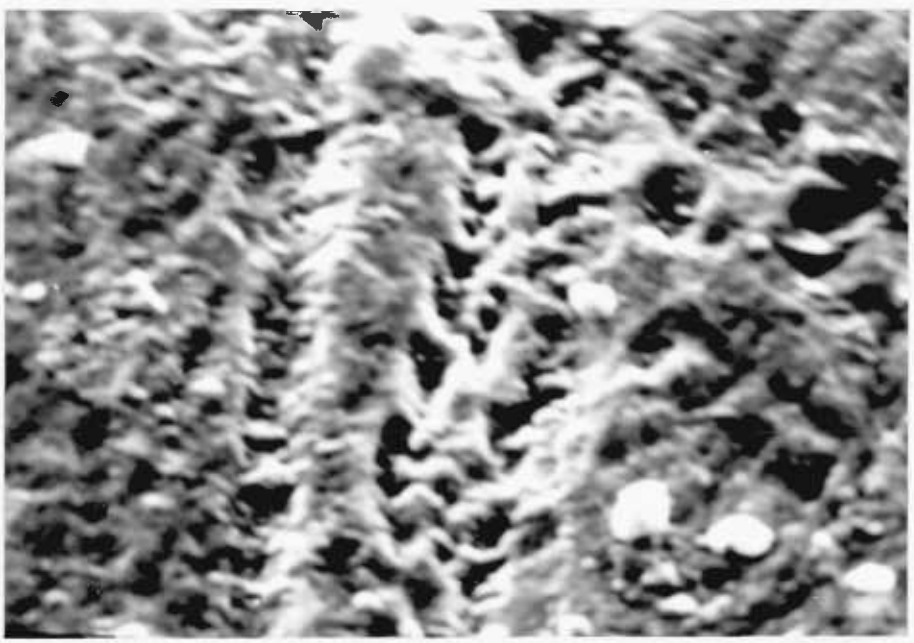

Fig. 52 Scanning electron micrograph of a partially leached specimen. (X5000)

Fig. 53 Scanning electron micrograph of the same area at a lower magnification. (X2000)

First, preferential attack occurs in certain areas resulting in 'grooves' and 'crests'. This situation is illustrated in Fig. 54b . Then attack occurs on the 'crests', levelling off the surface. Ideally a particle that has leached to this stage would be indistinguishable from unleached stannite, on the microscope.(Fig. 54d) Again the cycle is repeated by formation of crests followed by the smoothing off.

Exactly why this type of attack occurs is not clear.

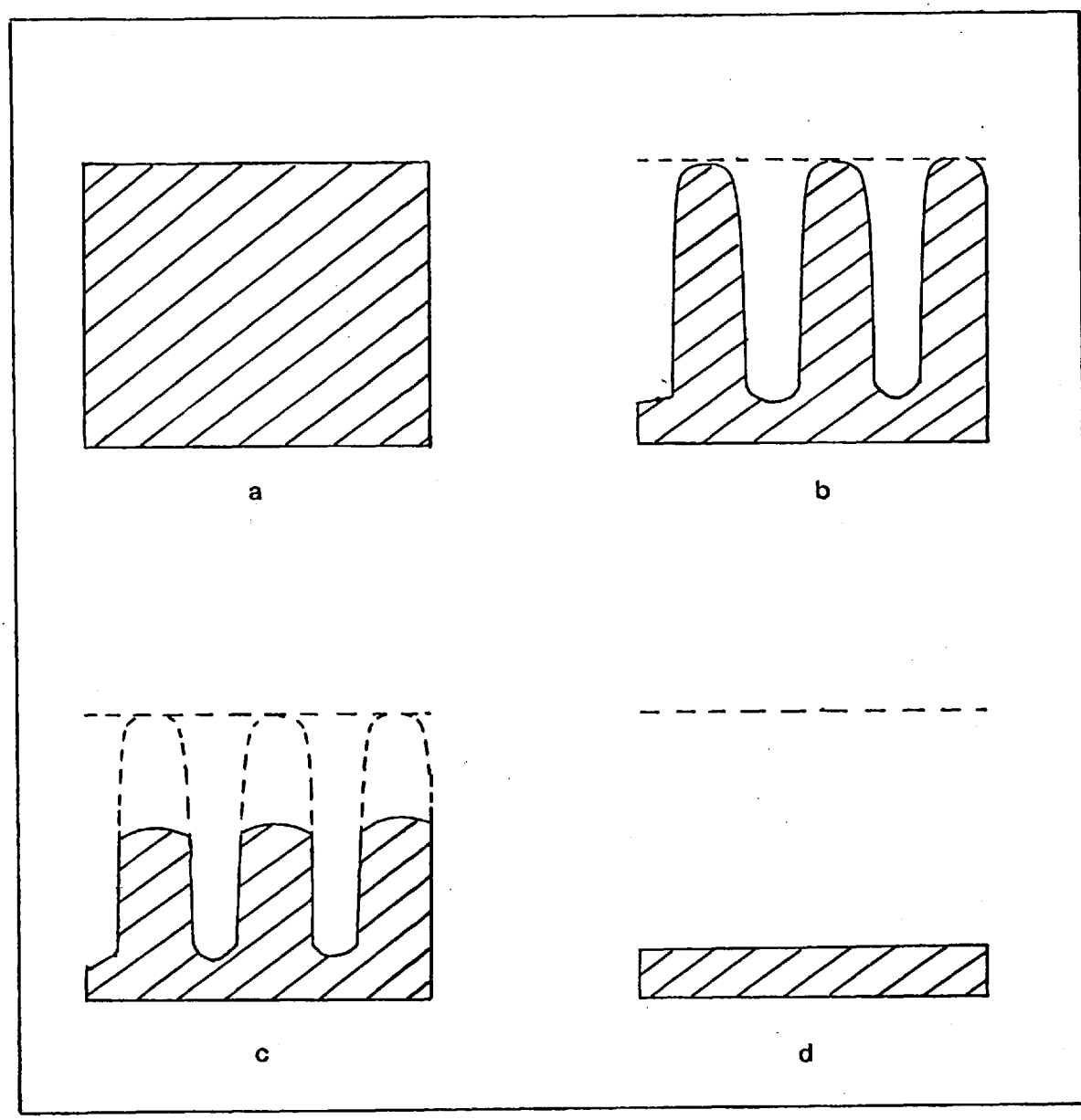

Fig. 54 Schematic representation of the mode of attack.

a. Unleached mineral.
b. Preferential attack.
c. Levelling of crests
d. Levelling complete.

4.5 HYDROCHLORIC ACID LEACHING.

Fig. 55 shows the kinetic rate curve for the leaching of stannite in 0.5 M hydrochloric acid. The same apparatus as was described in Sec. 2.2 was used. Rate curves obtained with 0.001 M and 0.005 M Fe^{+3} are also included for comparison.

A feature of interest about the three rate curves is that, all of them coincide at the early stages of leaching (below 100 hours). But, hydrochloric acid leaching proceeds faster afterwards.

Ferreira explained similar observations made in the leaching of α-chalcopyrite by considering the stability of the complex $CuCl_2^-$ thought to be formed during leaching.

Three possible attacking species may be considered to explain the leaching in hydrochloric acid solutions.

1. Atmospheric oxygen dissolved in the acid.
2. Ferric ion which may be present in the acid as an impurity.
3. Cupric ion which is produced as a result of leaching.

Clearly cupric ion cannot be the initiating species.

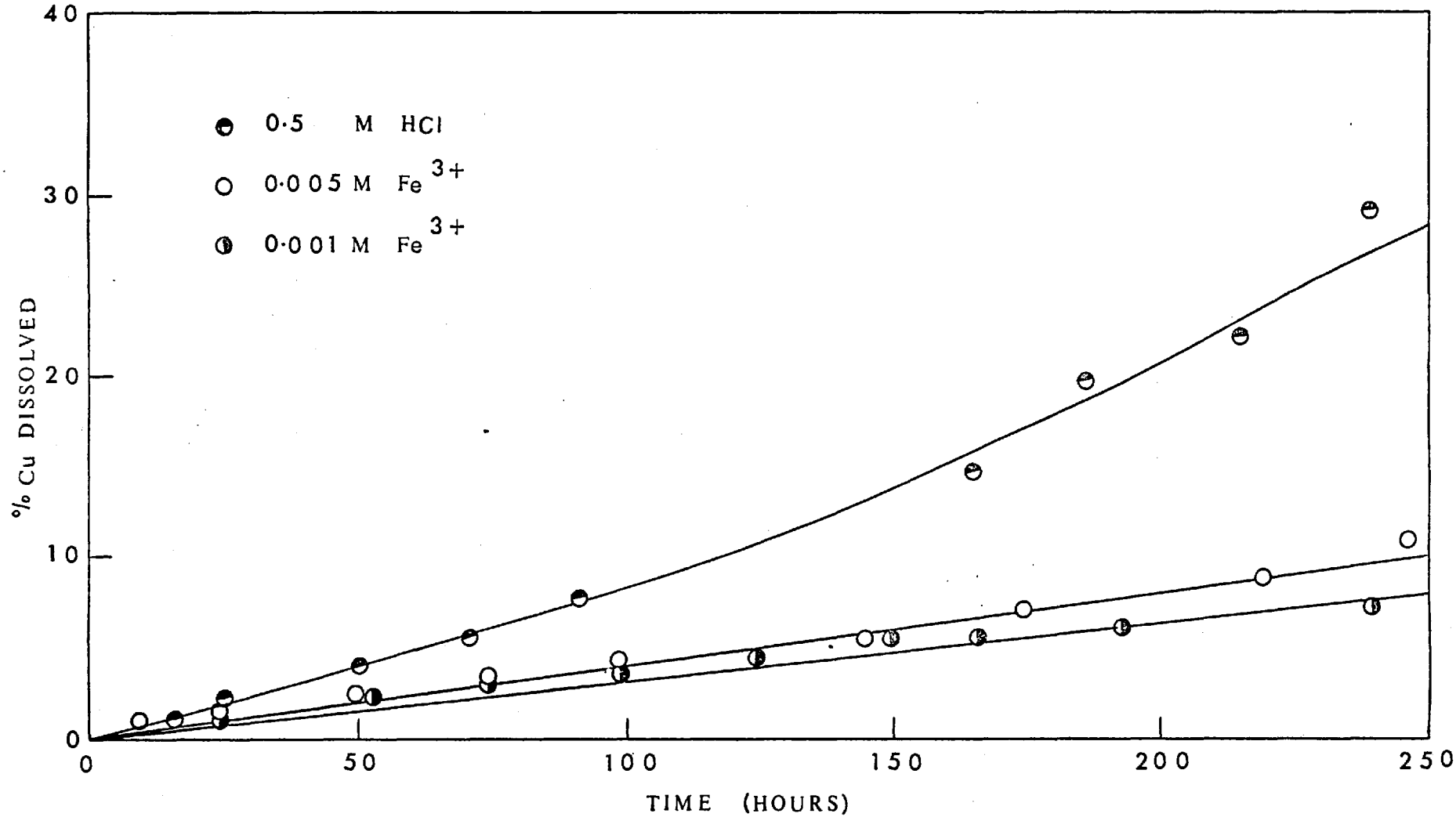

Fig. 55 Hydrochloric acid leaching of normal stannite.

The observations can be explained by making two assumptions :

1. Under the experimental conditions, dissolved oxygen is a better oxidising agent than ferric ion.

   Pourbaix gives the following E - pH relations:[100]

$$Fe^{+2} \qquad Fe^{+3} + e$$

$$E = 0.771 + 0.591 \log \frac{(Fe^{+3})}{(Fe^{+2})}$$

and

$$2H_2O \qquad O_2 + 4H^+ + 4e$$

$$E = 1.228 - 0.0591\ pH + 0.0147 \log p_{O_2}$$

The ferric chloride used had about 0.03% Fe^{+2}. Therefore $\log \frac{(Fe^{+3})}{(Fe^{+2})}$ is about 2 - 3. Then $E_{Fe^{+2}/Fe^{+3}}$ becomes 0.8792 to 0.9483 volts.

The pH of the solution was about 0.7 and p_{O_2} is 0.2 atm. or less. Then the second expression becomes :

$$E = 1.228 - 0.0591 \times 0.7 - 0.0147 \times 0.699$$
$$= 1.228 - 0.04137 - 0.01028$$
$$= 1.1764 \text{ volts.}$$

Therefore this assumption is reasonable.

2. The attacking species in $FeCl_3$ solutions are much smaller than those in the hydrochloric acid solutions (dissolved oxygen). This is reasonable because cation radius of Fe^{+3} is 0.64 A, while the bond length in the oxygen molecule is 1.42 A.

At low ferric ion concentrations the attack is primarily by dissolved oxygen. Upto a certain limit, ferric ions cannot influence this, because of their smaller size. The large oxygen molecules can maintain contact with the mineral surface. But when the ferric ion concentration exceeds the limit, they cover a large surface area and the contact between oxygen molecules and the surface will be lost, and thereafter the rate will be controlled by the ferric ion concentration.

SECTION 5

LEACHING OF CUBIC STANNITE , α- AND β-STANNITES

5.1 FERRIC CHLORIDE LEACHING.

The results obtained from the ferric chloride leaching of the four stannites are shown in Fig. 56 These experiments were carried out with samples quenched from 800°C (β - stannite), 540°C (α - stannite), 480°C (cubic stannite) and normal stannite.

The general shape of the curves is the same for all the forms. This shows the existence of a leaching mechanism common to them. As was concluded in section 3 , all of them have similar atomic arrangements and therefore this is not unexpected.

Initially cubic stannite leaches faster than α - stannite, but later the rate becomes slower than that of the latter. However, considering the closeness of the two quenching temperatures (480 and 540°C) this difference may be insignificant.

An interesting feature of the curves is the increase of overall rate with increasing quenching temperature. This is easy to understand, because, at high temperatures the crystal lattice expands making the structure more 'open'. The structure will be easily accessible to the reagent as a result, which produces higher reaction rates.

Sulpahate ion was not present in any of the leach liquors in ferric chloride leaching and no odour of hydrogen sulphide was detected. However, elemental sulphur was found in considerable quantities.

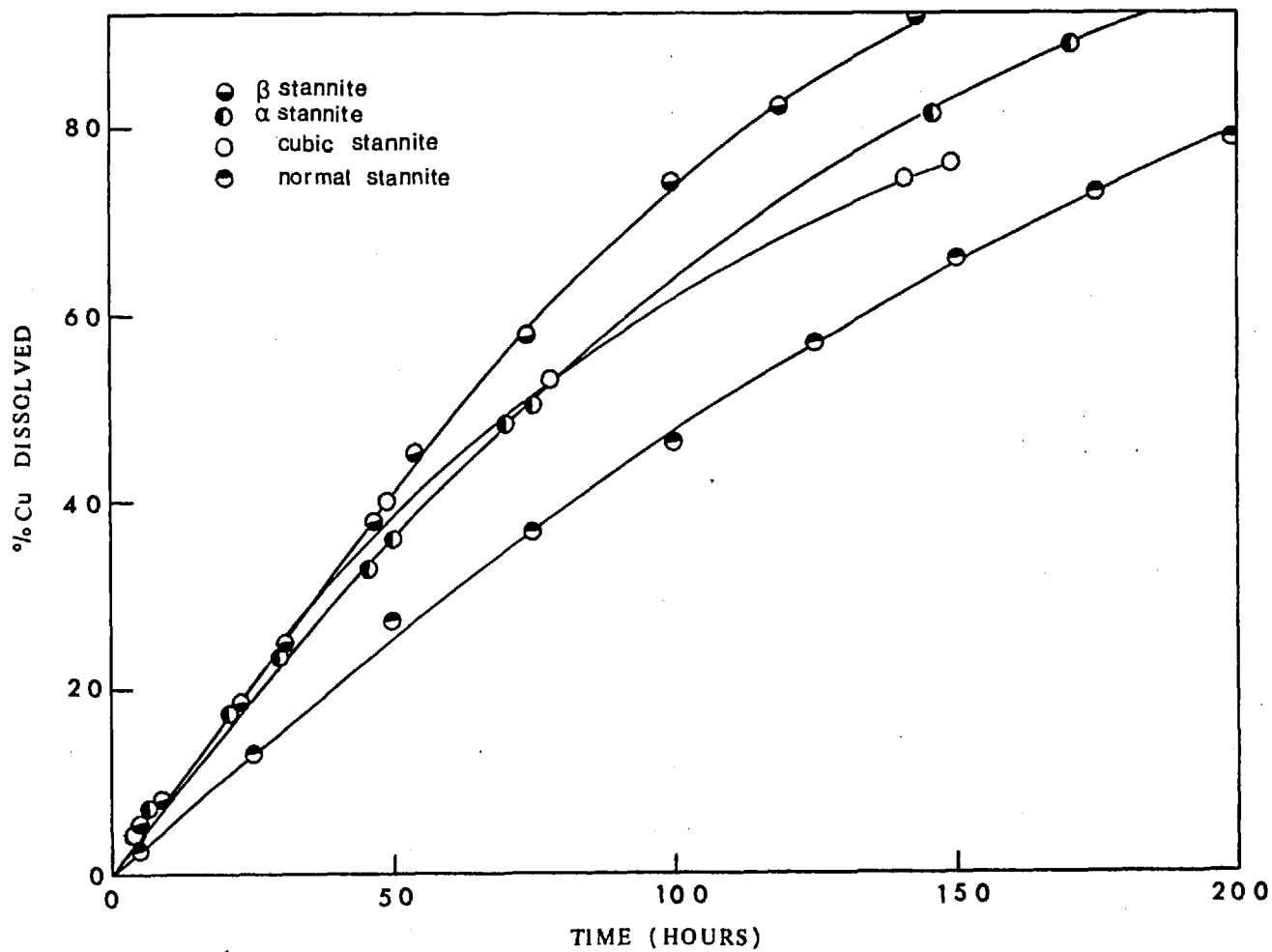

Fig. 56 Relative rates of the ferric chloride leaching of the four stannites.

5.2 THE EFFECT OF STORAGE TIME ON THE RATE OF LEACHING.

The storage time seemed to affect the leaching rate quite appreciably. Fig. 57 shows the rate curves obtained from two experiments carried out with two cubic stannite samples stored for different lengths of time, under identical conditions.

It is interesting to note that the trend observed for stannite is exactly the opposite to what Ferreira observed for β -chalcopyrite.

The examination of polished sections of synthetic stannites left in a desiccator for a long time revealed the presence of cracks. A narrow brown band was observed in the cracked region. Moreover visual examination of stannite showed a brass yellow tint, if stored in air. The colour of the corrosion product sorrounding the cracks, may be due to the formation of iron compounds. Whatever the nature of this, effectively it reduces the surface area of the mineral. As was noted in section 4.1.2 the surface area has a profound effect on the rate of leaching of stannite. Therefore, initially the rate must be slower than it would have been if the corrosion was absent. But when the corrosion products are carried away by the solution, the effective surface area is increased. Therefore the rate becomes higher than in the fresh mineral leaching.

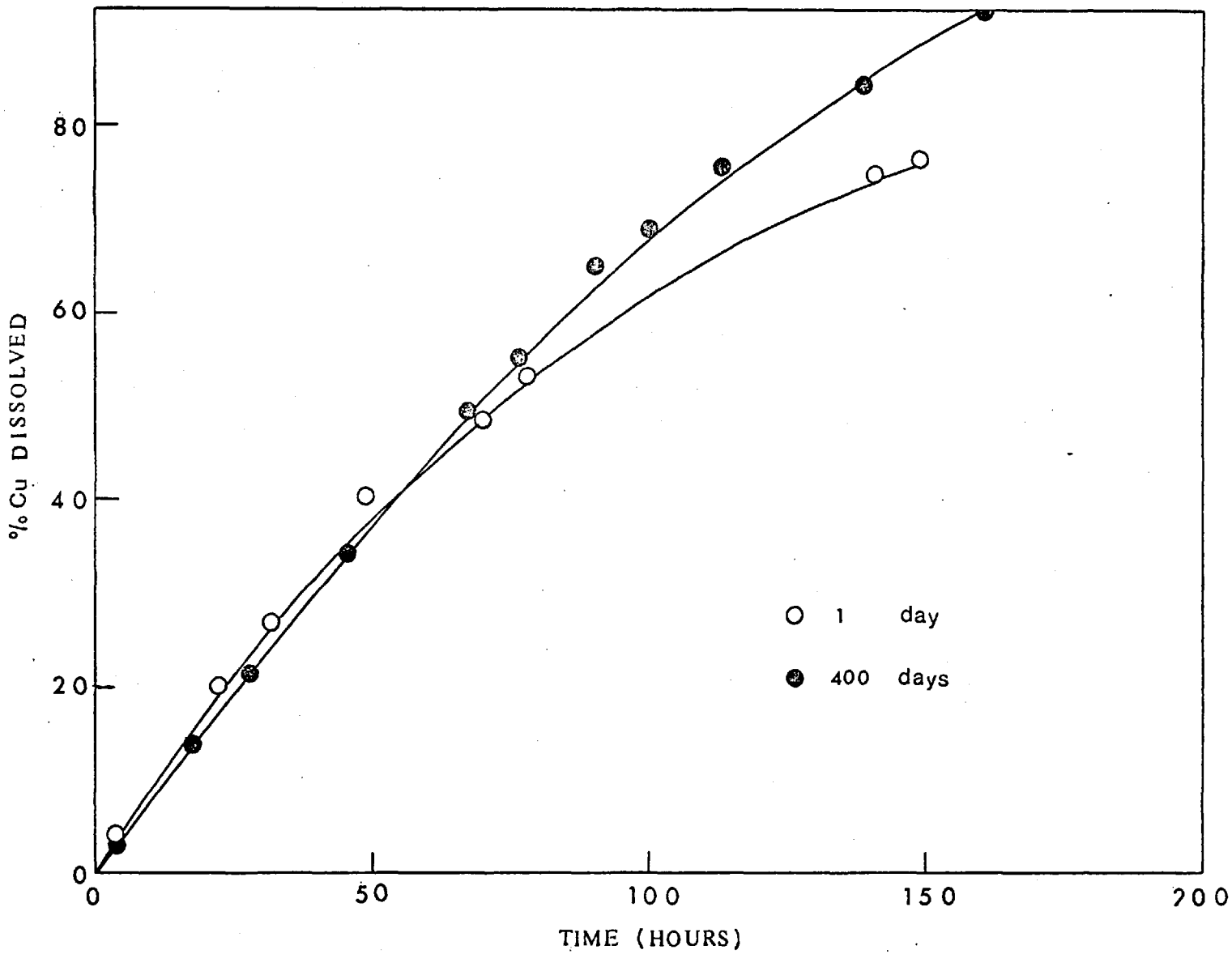

Fig. 57 Effect of Storage Time on the Leaching of Cubic Stannite.

5.3 HYDROGEN PEROXIDE LEACHING.

A hydrogen peroxide leach was carried out with α-stannite to study the relative rates of copper and extraction. The results are presented in Table B21 and Fig. 58.

A comparison of Fig. 58 with that obtained for normal stannite (Fig. 38 p179) at once brings out the similarity of the two. Initially both curves follow the ideal straight line course, which means that copper and iron are extracted at the same rate. Later they begin to deviate, and this is more noticeable for α-stannite. In section 4.2 it was explained that this was due to the precipitation of iron and does not mean preferential leaching. The apparent deviation of the two curves obtained for normal stannite and α-stannite is explained by the different extents of iron precipitation in the two cases.

The hydrogen peroxide leaching of α-stannite also produced substantial quantites of sulphate ion, like normal stannite. Fig. 59 shows the percentage of sulphur found in the form of sulphate as a function of copper extraction.

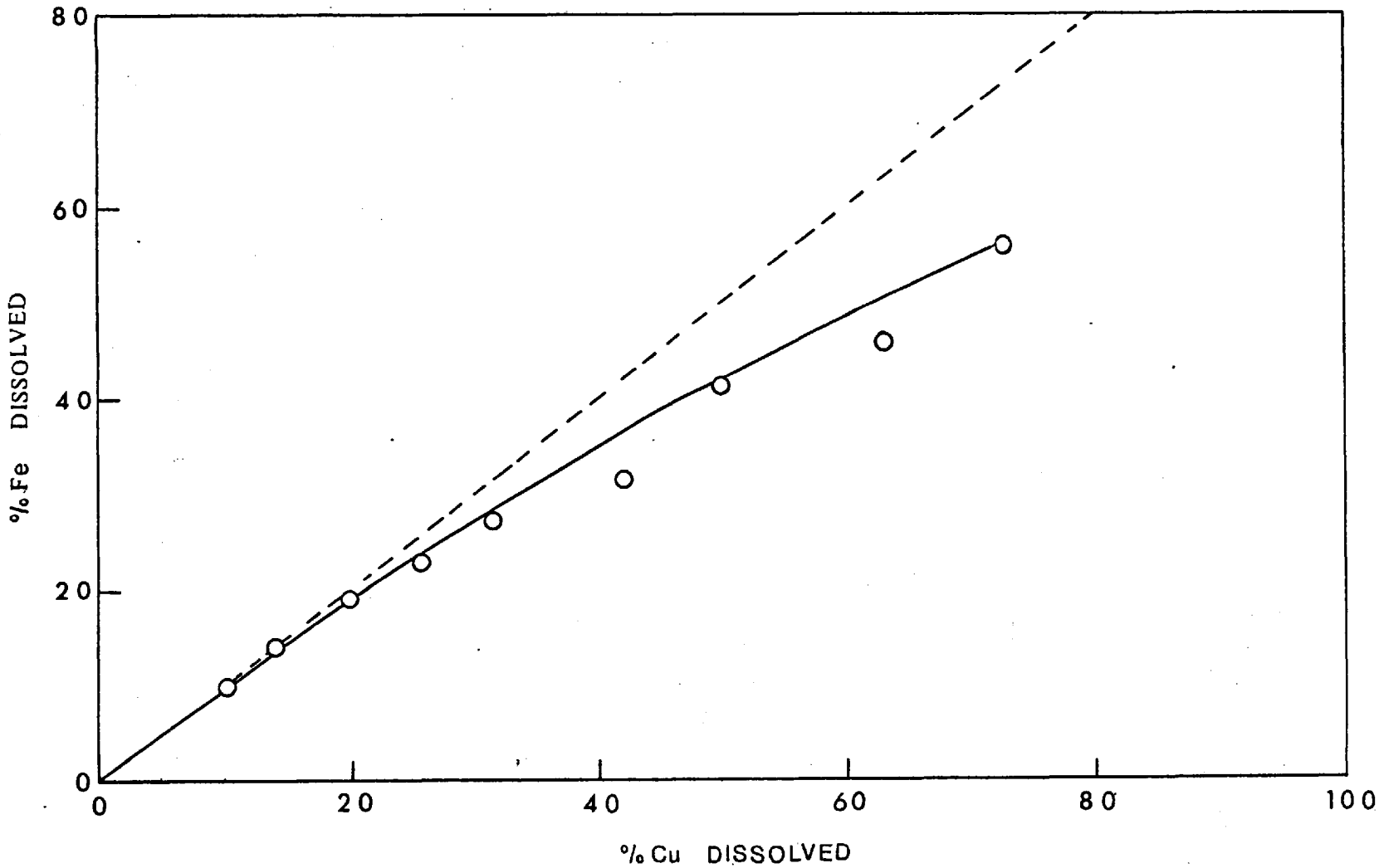

Fig. 58 Relative rates of copper and iron extraction in the leaching of α-stannite.

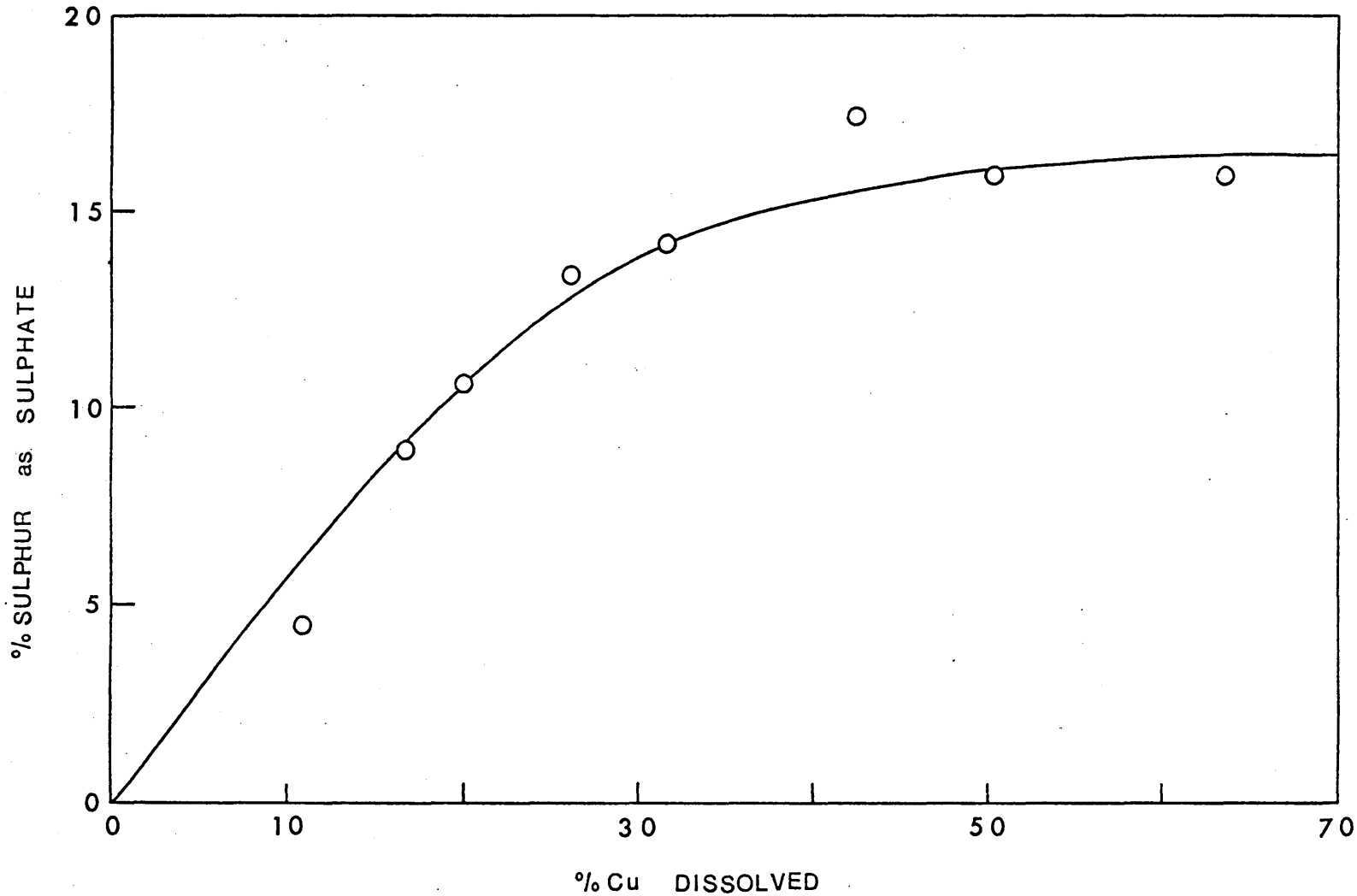

Fig. 59 Percentage sulphur found as sulphate as a function of copper dissolved.
(α - Stannite)

5.4 X-RAY DIFFRACTION OF LEACH RESIDUES.

X-ray diffraction studies of the leach residues indicated that the leaching process continued without a solid state transformation.

Fig. 60 shows a Guinier photograph of a leach residue of cubic stannite (about 80% copper removed) along with that of the unleached mineral. Clearly the two are identical. This is interesting when one realises that β-chalcopyrite (cubic) transforms to α-chalcopyrite (tetragonal) during leaching. α-stannite leach residues also produced Guinier photographs identical to those of the unleached mineral (Fig. 60). These results also show that both cubic stannite and α-stannite undergo leaching without a change in the lattice parameters.

Sufficient material was not available to undertake a systematic microscopic examination of the leach residues. The few specimens examined did not show a second phase.

From the results described so far, it is evident that the same mechanism is operating in the leaching of all the four minerals studied. Therefore remarks made in sections 4 and 6 for the leaching of normal stannite are assumed to be equally valid for the leaching of cubic and α- and β- stannites.

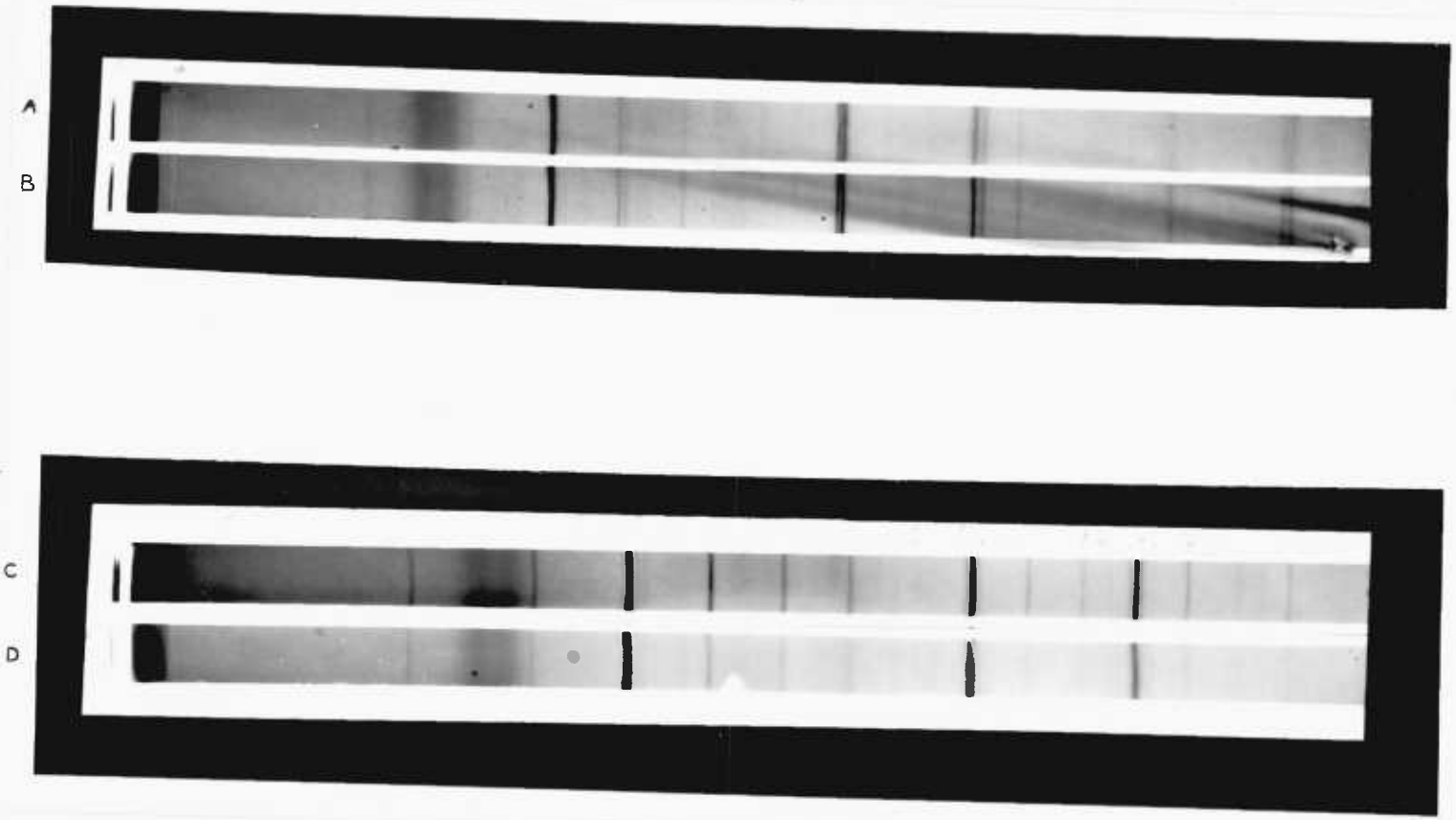

Fig. 60 Guinier photographs of unleached and leached stannites.

A : α-stannite (unleached). C : Cubic stannite.

B : α-stannite (partially leached). D : Cubic stannite (partially leached).

SECTION 6

GENERAL DISCUSSION

In sections 4 and 5 it was mentioned that the leaching of stannite is primarily a chemical reaction. The arguments for this hypothesis are discussed in this section in relation to the copper sulphides in general.

The minerals for which solid state diffusion is positively identified as the rate determining process are chalcocite (Cu_2S), bornite (Cu_5FeS_4) and β -chalcopyrite. In all these only a part of the copper was mobile. In bornite it was the 'ionically bound' copper that was easily removed while in β -chalcopyrite it was the excess copper over the stoichiometric $CuFeS_2$. Therefore it is unlikely that an ordered crystal structure of a non-ionic mineral with stoichiometric composition should undergo diffusion at the low temperatures considered ($<100^{o}C$). Synthetic stannite satisfies all these requirements and therefore either extremely slow rates or a total non-existence of solid state diffusion is not unexpected.

Jost[96] mentions a few empirical relations concerning the mechanism of migration in ionic crystals. The first of which is "In compounds of ions of different valency ususally the mobility of the ion with the smaller charge is the highest. Thus in Ag_2S , Cu_2S , Ag_2Se , etc., the mobility of the cations is by many orders of magnitude higher than that of the anions. In $PbCl_2$, $BaCl_2$ etc., only a mobility of the anions could be observed."

It is generally agreed that the cation valencies of stannite are Cu^{+} , Fe^{+2} , and Sn^{+4} . Although stannite

is not strictly ionic, the degree of ionicity is appreciable*. Therefore if Jost's rule is applicable to stannite, copper should be diffusing faster than Fe , Sn and S. That means a preferential leaching of copper must be observable if the diffusion is fast enough. Since the results did not suggest this, it must be concluded that solid state diffusion did not occur at a measurable rate.

Gerlach found that the specific conductivities of natural chalcopyrite and synthetic stannite are 0.021 $\Omega\ cm^{-1}$ and 0.0071 Ωcm^{-1} at 20°C. Jost states (p 144 Ref.96) in no ambigous terms, that electrolytic conduction and diffusion are directly related both being due to lattice defects. This means that diffusion must be more pronounced in chalcopyrite than in stannite. Therefore if diffusion was rate controlling, chalcopyrite must leach faster than stannite.

Gerlach's[66] observation that stannite leached about five times faster than chalcopyrite in O_2/H_2SO_4 systems, rules out diffusion in the slow step in leaching in this medium.

Solid state diffusion has been identified in the leaching of chalcopyrite only once in ferric ion leaching. (Diff. of excess copper in β-chalcopyrite). Although the exact mechanism of chalcopyrite leaching in such systems remains debatable, evidence in support of a chemical reaction is considerable.

*Goncharov found that stannite lies in the 'Fe^{+2} ionic' line (section 1.4)

Therefore differences of leaching between stannite and chalcopyrite must be attributed to the differences in interatomic forces operating in the two minerals. The present knowledge about the bonding in sulphide minerals is extremely confused and therefore, some well established differences between the two minerals are presented without further comments.

1. Although the crystal structures of chalcopyrite and stannite are very similar there is an important difference. In stannite, copper atoms occupy planes by themselves, whereas in chalcopyrite they do not. It is not known whether there are copper - copper bonds in stannite, making the copper less mobile. (Pauling[69a] suggests that the metallic lustre of some sulphide minerals is due to the presence of metal-metal bonds. Stannite has a very marked metallic lustre).

2. The oxidation state of iron in the two minerals is different. It is generally agreed that in chalcopyrite iron is in the ferric state, while in stannite, iron is ferrous.

3. Mossbauer studies indicate that iron is 'ionic' in stannite and not so in chalcopyrite.

4. The electronic environment around the iron nuclei is markedly different in the two minerals. In chalcopyrite it is symmetrical as is shown by Mossbauer studies (quadrupole splitting almost zero) while in stannite

the electronic environment around the iron nuclei is non-symmetrical (Quadrupole splitting 2.9 mm sec^{-1}. Burns believes that this is due to the localisation of the 6^{th} 3d electron in an e orbital of Fe(II)).

5. In stannite the Fe-S distance is anomalously high. (2.36 A compared to 2.257 A in chalcopyrite).

An important result which suggested a chemical reaction as the rate controlling step is the dependence of the rate on the ferric ion concentration. The order of the reaction with respect to the ferric ion was 0.55 . If the transport of ferric ions from the bulk to the solid-liquid interface was rate controlling the expected reaction order is 1. On the other hand, the rate would have been independent of the ferric ion concentration, if diffusion in the solid was rate determining.

Several leaching reactions are known to have orders less than 1 with respect to the oxidant. Particularly interesting are the findings of Dutrizac and MacDonald[3] who obtained values of 0.55 and 0.6 for the leaching of enargite and cubanite respectively in acidic ferric sulphate solutions. The orders of reaction reported for some selected systems are given in Table 27 below.

Mineral	Oxidant	Order With Respect To	
Enargite Cu_3AsS_4	$Fe_2(SO_4)_3$	0.55	Fe^{+3}
Cubanite $CuFe_2S_3$	$Fe_2(SO_4)_3$	0.6	Fe^{+3}
Pentlandite $(Ni , Fe)_9S_8$	$Fe_2(SO_4)_3$	0.20	Fe^{+3}

Table : 27

If the ferric ion in the solution reacted directly with stannite (or any other mineral) one would expect an order greater than 1.

It was shown in section 4.1.2 that the stannite leaching in acidic ferric chloride has a direct dependence on the surface area.

Therefore the observed order of the reaction could be explained by assuming that the slow step in the leaching of stannite involved an interaction between the ferric ions adsorbed on the surface and the mineral.

The adsorption of ions in solution by solids often follow the empirical Freundlich adsorption isotherm :

Viz. $\text{Log} \left(\frac{x}{m} \right) = \log k' + n \log c$

where x = number of moles adsorped

m = mass of the solid

c = bulk concentration

n and k' are constants ($n < 1$).

It is likely that the adsorption of ferric ions by stannite followed the same isotherm. This was not confirmed however.

Then, the leaching process may be schematically represented by :

$$Fe^{+3}_{\text{adsobed}} + \text{stannite} \longrightarrow \text{products}$$

It is useful to recall at this stage , that in the leaching of some copper sulphide minerals in acidic ferric salt solutions, the rate directly depended on the ferric ion concentration upto a certain limit and then became independent. (Synthetic bornite for example; Ugarte[45]) This is because, in these, two processes contribute to the overall rate.

1. Diffusion of Cu ions in the solid.

2. Electron transfer with the Fe^{+3} ions at the surface.

The diffusion of copper ions in the solid is generally fast, and therefore there will be a high population of copper ions at the surface at anytime. At low Fe^{+3} concentrations, therefore, the rate will be controlled by the availability of Fe^{+3} ions resulting in first order kinetics. However, the number of copper ions diffusing to the surface is limited by the structure of the mineral. When sufficient ferric ion is available to react with all that, the effect of increasing the ferric ion concentration would be minimal on the overall rate.

Next the position on the solid surface at which the attack is initiated must be considered.

It is reasonable to assume that the Fe-S bond is a weak spot in the structure (generally a long bond length implies a relatively weak bond). If this was true, one might be able to detect high iron contents in the leach liquor in the first stages of leaching.

The results obtained from the hydrogen peroxide leaching of normal stannite and α -stannite are presented in Table 28 below.

Time(Hr.)	%Cu	%Fe	Time(Hr)	%Cu	%Fe
1	4.58	4.82	.25	10.22	9.96
2	4.19	4.88	1.00	9.92	9.22
3	4.36	4.56	3.00	10.41	10.49
4	4.44	4.61	4.00	11.30	10.94
21	12.67	11.58			
22	11.70	10.55			

Normal stannite α - stannite.

Table : 28

However, these were not taken very seriously for two reasons. First, the sensitivity of atomic absorption spectrophotometry was better for copper than for iron. Second, the acid contained traces of iron as an impurity. (section 2.5)

Gerlach and co-workers observed that, in a leach run with synthetic stannite carried out at 110°C, even before admitting oxygen gas, 10% of the iron was already in solution.

These observations seem to support the ideas presented in the preceding paragraphs.

The high apparent activation energy , which was taken to indicate a chemical process, deserves comment.

Peters and Loewen[11] noted that for chalcopyrite, the apparent activation energy obtained from oxygen-acid leaching is about half that reported for ferric ion leaching.($\sim$ 10 and 20 kcal). The low value for acid ppressure leaching was interpreted as the activation energy of the reaction :

$$O_2 + 4H^+ + 4e \longrightarrow 2H_2O$$

For covellite leaching also, a parallel trend exists between the two apparent activation energies. (section 1.1.1)

Gerlach and co-workers reported a value of 11 kcal/mole for oxygen-acid leaching of synthetic stannite while for ferric chloride leaching the value found in this work is about 22 kcal/mole. The same workers believed that the leaching using gases involved a slow step of gas adsorption on the solid surface. The value 11 kcal/mole therefore represents the activation energy of gas adsorption. This seems more realistic, since it is inconcievable that a chemical reaction should have such a low activation energy as was suggested by Peters and Loewen.

SECTION 7

CONCLUSIONS

7.1 SUMMARY OF RESULTS.

Four forms of stannite were synthesised. The primary product, normal stannite $Cu_{2.07}Fe_{1.02}SnS_{3.99}$ was synthesised starting from the elements Cu , Fe , Sn and S and the other three were obtained as thermal transformation products. The following transformation sequence was established by high temperature X-ray diffraction and quenching experiments.

Normal Stannite (Tetragonal) $\xrightarrow{285^{o}C}$ Cubic Stannite (Cubic)

Cubic Stannite (Cubic) $\xrightarrow{500^{o}C}$ α -Stannite (Tetragonal)

α -Stannite (Tetragonal) $\xrightarrow{700^{o}C}$ β -Stannite (Tetragonal)

A crystal structure for cubic stannite was proposed and a plausible mechanism for the transformation of normal stannite to cubic stannite is suggested.

The leaching of all four forms followed a common mechanism. The slow step involved a chemical reaction between the surface adsorbed ferric ions and the mineral. It was suggested that the reaction started by a cleavage of the Fe-S bonds.

Schematically, the overall leaching reaction may be described by :

$$Cu_2FeSnS_4 + 8Fe^{+3}_{ads} \longrightarrow 2Cu^{+2} + Sn^{+2} + 9Fe^{+2} + 4S^{o}$$

Part of the tin extracted was precipitated, presumably in the form of SnO_2 with adsorbed Fe_2O_3 .

During leaching the solid maintained constant lattice parameters and did not undergo solid state transformations. The attack was preferential, (but a galvanic action is not suggested).

Leaching of normal stannite carried out in hydrochloric acid in air, proceeded considerably fast.

Cubic stannite leaching was affected by the storage time, and this was explained by the effective changes of surface area due to surface oxidation.

Higher the quenching temperature from which the minerals were prepared, higher was the leaching rate. This was explained as being due to the expansion of the crystal lattice with rising temperature, enabling easy access by the reagent.

7.2 COMPARISON OF THE PRESENT STUDY WITH PREVIOUS WORK.

No published X-ray powder pattern for stannite agreed perfectly with that of normal stannite found in this work. The very strong doublet at d = 1.925 and 1.913 A was found only in the synthetic sample of Bente[74] (d = 1.927 and 1.909 A).

Franz's X-ray powder pattern of cubic stannite[70] is identical to the one obtained in the present work. Also, the temperature at which it was synthesised lies in the range of stability found for this phase. However, his interpretation is not accepted in this work.

The only available diagram for α-stannite is that of Franz. The agreement is good considering that he discarded some lines as weak.

For β-stannite no X-ray data exists. Springer[71] reported that the lines 4.85 , 2.99 , 2.3718 , 2.010 and 1.787 A were present in β-stannite but not in α-stannite. In the present work also the same lines were present in β-stannite but not in α-stannite.

It is interesting to note that the X-ray powder diagram published in the ASTM file for naturally occuring stannite is close to β-stannite found in this work.

The $\alpha \rightarrow \beta$ transition temperature reported by Springer, 680°C, agrees well with the present work.

The observations made in this study do not support the temperature, $706^{o}C$, reported by Moh's school for the tetragonal $\longrightarrow$ cubic transformation. No cubic phase was found above about $525^{o}C$.

The leaching results cannot be compared directly with the only published work (Gerlach et al. 1972), because, the conditions are totally different. However, some points are worth noting.

Their work agrees with the present work in that stannite leaches faster than chalcopyrite. Also, initially both copper and iron were extracted at the same rate (except at $110^{o}C$ when Fe extracted faster), but later iron extraction curves lagged behind. The same explanation given in this work, the precipitation of some iron with tin was presented. However, they believed the precipitate to be (Sn , Fe)(O , OH). In the present work the precipitate is assumed to be SnO_2 with adsorbed Fe_2O_3 .

The present work also agrees reasonably with the findings of Gruner and Lin[65] , that hydrochloric acid alone attacks stannite at appreciable rates.

APPENDIX A.

AN ATTEMPT TO USE ELECTRON MICROSCOPY TO STUDY THE LEACHING OF COPPER SULPHIDES.

The present work clearly demonstrated the need to develop novel techniques to study leaching. As a first step, the possibility of using electron microscopy was investigated.

Covellite was chosen for this because its leaching is remarkably similar to that of stannite. However, this was soon abandoned owing to the difficulties of synthesising homogeneous samples.

The next choice was chalcocite. The first stage of its synthesis was carried out by the procedure used by King. It was brought to melting by a different process. The silica tube containing the primary product was placed inside a second silica tube, which was sealed after filling with argon. The unit was then placed in a muffle furnace at $1100^{o}C$. After about 20 miniutes the product was cooled in the furnace.

Thin sections were prepared from the homogeneous product thus obtained, following standard procedures.

After thinning the sections to below 50 micron by polishing, further thinning was done using an ion beam thinning machine (Edwards - IBMA - 1). Lowest practical thinning rates had to be used (typically 0.4 mA and 4.5 kV) because of the instability of the specimen. (At higher thinning rates only copper remained after some

time !). The samples were extremely brittle and as a result the minimum thickness achievable was about 2000 - 3000 A. (For satisfactory results the thickness should be less than 1000 A).

Specimens so obtained were examined using AIME - 6G 100 kV electron microscope. The specimens, which were too thick in the first place, dissociated immediately on hitting the electron beam.

APPENDIX B.

KINETIC RESULTS.

1. Reproducibility.

The experimental conditions for the two experiments were:

HCl	:	0.5 M
Fe^{+3}	:	0.5 M
Stirring speed	:	900 rpm.
Sample weight	:	0.5 gm.
Particle size	:	-180 + 125 micron
Temperature	:	$90^{o}C$

Table : B1

Time (Hrs)	%Cu Dissolved	%Sn Dissolved
1	1.26	1.34
3	2.85	2.27
5	4.11	3.07
7	5.60	4.80
26	13.00	11.27
30	14.41	12.56
34	16.86	15.98

.....contd/

Table : B1 contd.....

50	25.09	22.53
55	27.99	22.44
58	29.69	24.07
75	38.35	30.10
80	41.19	33.63
101	48.12	39.30
105	48.77	39.55
125	57.51	45.49
145	67.35	51.44
151	70.96	47.72
169	80.63	54.29
175	80.90	55.70

Table : B2

Time (Hrs)	% Cu Dissolved	% Sn Dissolved
1	00.894	00.803
5	02.219	01.609
7	03.015	02.085
25	10.290	07.065
31	14.048	09.739
50	27.038	18.077
75	36.421	24.686
100	46.114	30.632
125	56.818	34.555
150	65.366	35.397
175	72.321	35.530
191	74.126	33.247
200	78.045	

2. Temperature.

The experimental conditions were :

HCl	:	0.5 M
Fe^{+3}	:	0.5 M
Stirring speed	:	900 rpm
Sample weight	:	0.5 gm.
Particle size	:	-180 + 125 micron

Table : B3

Temperature : $95^{o}C$

Time (Hrs.)	% Cu Dissolved
6.00	5.908
20.00	23.453
27.25	30.111
44.00	44.982
51.25	50.886
71.00	67.762
97.00	87.049
116.00	90.182
140.00	100.000

Table : B4

Temperature : 80°C

Time(Hours)	% Cu Dissolved
1.00	0.28
3.00	1.12
5.00	2.17
7.00	2.45
19.00	8.89
25.25	11.60
29.75	13.70
47.75	20.74
97.25	34.95
124.50	44.32
144.25	46.01
150.25	47.60
173.25	55.51
198.25	58.12
222.00	62.59

Table : B5

Temperature : 65°C

Time (Hrs)	% Cu Dissolved
5.00	0.656
17.00	1.026
28.75	1.657
41.25	2.326
52.25	2.996
74.50	4.331
91.00	4.847
98.75	5.365
113.25	6.216
137.45	8.214
162.00	9.713
187.00	11.226
210.00	13.480

3. Particle Size

The experimental conditions for the variation of particle size were :

HCl	:	0.5 M
Fe^{+3}	:	0.5 M
Stirring speed	:	900 rpm.
Sample weight	:	0.25 gm.
Temperature	:	95°C

Table : B6 Particle Size : - 90 + 63 micron

Time (hrs)	%Cu Dissolved
5.00	07.448
17.00	39.415
22.00	48.947
28.75	60.733
41.25	75.097
46.50	78.155
52.25	80.442
74.75	86.207
91.00	86.324
98.75	85.725
113.25	87.732

Table : B7 Particle Size : -45 + 38 micron

Time (Hrs)	% Cu Dissolved
5.00	26.699
23.00	67.912
28.00	80.964
33.00	86.279
47.00	95.343
57.00	94.787
69.00	96.731
81.00	98.078

Table : B8 Particle Size : -180 + 125 micron

Time (Hrs)	% Cu Dissolved
5.00	2.262
9.00	3.467
25.00	8.804
51.00	16.501
74.75	21.700
100.75	26.118
125.00	31.601
150.00	41.047
174.00	46.119
198.00	51.955
221.00	59.707
247.50	62.366
269.75	62.890

4. Ferric Ion Concentration.

The experimental conditions were :

HCl	:	0.5 M
Stirring Speed	:	900 rpm.
Sample Weight	:	0.25 gm.
Particle Size	:	- 180 + 125
Temperature	:	95°C

Table : B9 Ferric Ion Concentration : 0.001 M

Time (Hrs)	% Cu Dissolved
5.00	1.039
25.25	2.119
53.00	3.913
75.00	5.192
95.00	6.255
100.00	6.503
105.00	6.996
118.00	7.655
125.00	8.096
142.00	9.709
150.00	10.111
166.00	10.363
193.50	11.343
240.00	13.498
266.00	13.684
290.00	13.727

Table : B10 Ferric Ion Concentration : 0.005 M

Time (Hrs)	% Cu Dissolved
5.00	0.666
10.00	1.054
23.00	1.817
25.00	1.885
30.00	2.132
50.00	3.503
58.50	3.961
75.00	5.317
98.50	7.318
145.00	7.325
175.00	13.561
220.00	17.507
147.00	21.676
292.00	27.762

Table : B11 Ferric Ion Concentration : 0.050 M

Time (Hrs)	% Cu Dissolved
5.00	2.262
9.00	3.467
25.00	8.804
51.00	16.501
74.75	21.700
100.75	26.118
125.00	31.601
150.00	41.057
174.00	46.119
198.00	51.955
222.00	59.707
247.50	62.366
269.75	62.890
290.25	66.492

Table : B12 Ferric Ion Concentration : 0.20 M

Time (Hrs)	% Cu Dissolved
5.00	2.819
10.00	6.580
25.00	20.926
50.00	38.359
75.00	52.886
100.00	68.762
125.50	77.470
150.00	82.707
167.00	90.022

5. Stirring Speed

The experimental conditions were :

HCl	:	0.5 M
Fe^{+3}	:	0.5 M
Sample weight	:	0.12 gm.
Particle size	:	- 45 + 38 micron
Temperature	:	95°C

Table : B13 Stirring Speed : 600 rpm.

Time (Hrs)	% Cu Dissolved
0.50	3.748
1.50	8.765
3.00	13.805
4.00	17.621
5.00	22.707
6.00	26.566
7.75	32.943
20.50	74.610
22.00	78.450
25.00	84.490
28.00	86.956
32.25	90.412
44.00	100.000

Table : B14 Stirring Speed : 300 rpm.

Time (Hrs)	% Cu Dissolved
0.50	3.894
1.50	7.808
3.00	16.932
4.00	18.314
5.00	23.597
6.00	25.012
7.75	31.623
20.50	62.932
22.00	65.839
25.00	71.354
28.00	76.894
32.25	82.462
44.00	100.000

6. Hydrogen Peroxide Leaching.

The experimental conditions were :

Solvent	:	150 ml. of 0.5 M HCl plus 50 ml. of 20 volume H_2O_2 .
Temperature	:	80^oC
Stirring Speed	:	900 rpm.
Particle Size	:	- 180 + 125 micron
Sample Weight	:	0.4054 gm

Table : B15

Time (Hrs)	% Cu Dissolved	% Fe Dissolved
1.00	4.58	4.82
2.00	4.19	4.88
3.00	4.36	4.56
4.00	4.44	4.61
21.00	12.07	11.58
22.00	11.70	10.55
23.00	11.61	11.05
24.00	11.73	10.39
25.00	12.05	11.26
26.00	12.35	12.14
27.50	11.96	11.49
45.00	16.79	14.95
46.00	17.28	14.99
68.00	20.32	21.02

contd...../

.....contd

70.00	21.42	21.31
72.00	21.16	21.10
75.00	21.52	21.30
140.00	27.39	26.50
144.00	28.01	26.99
148.00	28.18	27.23
164.00	30.67	29.03
172.00	30.06	29.94
188.00	34.46	34.64
192.50	34.91	33.13
	41.61	13.09
	45.89	43.04
	49.41	45.59
	52.98	47.38
	57.78	52.61
	64.47	57.23
	67.93	62.29
	71.51	63.94
	75.43	66.66
	90.24	78.44
	94.72	80.61
	100.00	82.57

26.105% of sulphur was found in the form of sulphate.

7. Hydrochloric Acid Leaching.

The experimental conditions were :

Solvent	:	0.5 M HCl.
Particle size	:	- 180 + 125 micron
Sample weight	:	0.25 gm.
Stirring speed	:	900 rpm.
Temperature	:	95^{o}C

Table : B16

Time (Hrs)	% Cu Dissolved
16.00	0.970
25.00	2.012
50.00	3.683
71.00	5.509
91.25	7.603
165.00	14.910
186.00	19.632
215.50	23.397
239.50	28.714
263.00	29.863
283.25	32.335
311.00	37.415
328.00	41.091

8. Ferric Chloride Leaching of β-Stannite.

The experimental conditions were :

Solvent	:	0.05 M $FeCl_3$ in 0.05 M HCl.
Stirring speed	:	900 rpm.
Particle size	:	- 180 + 125 micron
Temperature	:	$90^{o}C$
Sample weight	:	0.1425 gm. (sample quenched from $800^{o}C$)

Table : B17

Time (Hrs)	% Cu Dissolved
5.00	5.246
9.00	7.904
23.00	18.690
30.25	24.511
47.00	37.525
54.25	44.836
74.00	57.446
100.00	73.977
119.00	84.293
143.00	94.276

9. Ferric Chloride Leaching of α -Stannite.

The experimental conditions were :

Solvent	:	0.5 M $FeCl_3$ in 0.5 M HCl.
Stirring speed	:	900 rpm.
Particle size	:	- 180 + 125 micron
Temperature	:	90°C
Sample weight	:	0.49 gm.
		(sample quenched from 540°C)

Table : B18

Time (Hrs)	% Cu Dissolved
4.00	4.088
7.50	6.980
21.25	17.359
24.00	19.185
27.00	20.604
30.00	23.853
46.25	32.336
50.00	35.772
70.00	47.908
75.25	49.959
121.75	62.617
148.00	81.22
171.00	87.432

10. Ferric Chloride Leaching of Cubic Stannite.

The experimental conditions were :

Solvent	:	0.5 M $FeCl_3$ in 0.5 M HCl.
Stirring speed	:	900 rpm.
Particle size	:	- 180 + 125 micron
Temperature	:	90°C
Sample weight	:	0.4214 gm
Storage time	:	1 day
		(sample quenched from 480°C)

Table : B19

Time (Hrs)	%Cu Dissolved
5.00	5.88
24.00	20.67
30.50	27.08
51.25	42.15
70.00	47.47
72.00	50.50
74.00	47.67
76.00	52.70
78.00	52.20
141.00	74.06
149.00	75.29

11. Effect of Storage Time on the Leaching of Cubic Stannite.

Solvent	:	0.5 M $FeCl_3$ in 0.5 M HCl.
Stirring speed	:	900 rpm.
Particle size	:	-180 + 125 micron
Temperature	:	$90^{o}C$
Sample weight	:	0.2503 gm.
Storage time	:	400 days
		(sample quenched from $420^{o}C$)

Table : B20

Time (Hrs)	% Cu Dissolved
5.00	3.965
18.00	13.414
28.25	21.517
46.00	34.125
68.00	49.473
77.00	55.075
91.00	65.169
101.33	68.610
114.00	75.683
140.00	84.142
162.00	92.662

12. Hydrogen Peroxide Leaching of α -Stannite.

The experimental conditions were :

Solvent	:	150 ml of HCl + 50 ml 20 vol H_2O_2
Stirring Speed	:	900 rpm.
Particle size	:	- 180 + 125 micron
Temperature	:	80°C
Sample weight	:	0.5089 gm.

Table : B21

Time (Hrs)	% Cu Dissolved	% Fe Dissolved	% S As Sulphate
0.25	10.215	9.96	4.61
1.00	9.92	9.22	
3.00	10.41	10.49	
4.00	11.30	10.94	
5.00	11.41	11.21	
6.00	11.68	11.67	13.17
7.00	12.02	11.78	
23.00	14.54	13.79	
27.00	16.05	15.67	
29.00	16.51	13.97	9.22
48.00	19.66	18.79	10.76
119.00	26.01	22.93	13.61
144.00	31.31	27.25	14.27
175.00	42.38	31.29	17.56

.....contd/

Table : B21 contd.....

216.00	50.11	40.88	16.47
290.00	63.65	45.69	16.47
315.00	73.36	55.49	

APPENDIX B.

X-RAY DIFFRACTION DATA

Table : C-1 X-Ray Powder Pattern of the Iron Precipitate

Iron Precipitate		α -Fe_2O_3 [101]		β -FeOOH [101]	
d (A)	I/I_o	d (A)	I/I_o	d (A)	I/I_o
7.48	mw			7.40	100
5.25	w			5.25	40
3.68	w	3.66	25	3.70	10
3.32	mw (br)			3.311	100
3.11	w				
2.695	s	2.69	100	2.616	40
2.545	m			2.543	80
2.505	m	2.51	50		
2.35	hv			2.343	20
2.29	m (br)	2.285	2	2.285	40
2.20	m	2.201	30		
		2.070	2	2.097	20
				2.064	20
1.95	w (br)			1.944	60
1.835	w	1.838	40	1.854	10
				1.746	40
1.692	s	1.690	60	1.719	10
1.639	w (br)	1.634	4	1.635	100
1.595	vw	1.596	16		
1.509	w			1.515	40
1.48	m	1.484	35	1.497	20
1.448	m	1.452	35	1.459	10

s : strong
m : medium
mw : medium weak
w : weak
vw : very weak
hv : hardly visible
br : broad

Table : C-2 X-ray Diffraction Analysis of the Prepared Tin Compound (Section 4.1.c).

Compound		After Heating At 500°C		SnO_2 101		α-Fe_2O_3 101	
d (A)	I/I_o	d (A)	I/I_o	d (A)	I/I_o	d (A)	I/I_o
		3.70	vw			3.66	25
3.37	s(br)	3.36	s	3.351	100		
		2.71	vw			2.69	100
2.63	s(br)	2.63	vs	2.644	81		
		2.53	m			2.51	50
		2.38	w	2.369	24		
		2.299	vw	2.309	5		
		2.212	vw	2.120	2	2.201	30
		1.844	vw			1.838	40
1.764	m(br)	1.760	s	1.765	63		
1.684	br	1.682	br	1.675	63	1.690	60
1.573	br	1.577	br	1.593	8	1.596	16
		1.488	vw	1.498	13	1.484	35
		1.454	m	1.439	17	1.452	35
1.425	br	1.422	br	1.415	15		

Note: Abbreviations are on page 258.

Table : C-3 X-Ray Powder Data for the Leach Residues of Normal Stannite

% Cu Dissolved		1 - 2		13.5		13.8		27.8		41.1		50.7	
d (A)	I/I_o												
5.39	m	5.40	m	5.40	m	5.41	w	5.40	w	5.38	w	5.41	w
3.85	w	3.83	w	3.85	w	3.84	vw	3.83	w	3.82	vw	3.84	w
3.126	vs	3.126	vs	3.127	vs	3.122	vs	3.122	vs	3.126	vs	3.130	vs
2.718	m	2.716	m	2.717	m	2.714	vw	2.710	w	2.712	vw	2.717	m
2.685	m	2.689	w	2.686	w	2.682	vw	2.678	w	2.680	vw	2.684	w
2.429	w	2.424	w	2.424	w	2.420	vw	2.415	vw			2.422	w
2.206	vw	2.204	vw										
1.922	s	1.922	s	1.925	s	1.918	s	1.918	w	1.920	w	1.924	s
1.911	s	1.912	s	1.912	s	1.908	m	1.906	m	1.910	m	1.910	s
1.812	vw												
1.636	s	1.637	s	1.637	s	1.633	m	1.634	m	1.636	m	1.638	s
1.623	s	1.624	m	1.625	m	1.618	m	1.617	w	1.620	w	1.623	m
1.561	m	1.562	w	1.563	m	1.560	vw	1.558	w	1.559	vw	1.563	w

.....contd/

Table :-C-3 contd.....

% Cu Dissolved	57.0		66.5		80.0		85.7		90.0	
	5.37	w	5.40	w	5.43	w	5.39	w	5.41	w
	3.83	w	3.86	w	3.85	w	3.83	w	3.83	hv
	3.133	vs	3.134	vs	3.128	vs	3.126	vs	3.129	vs
	2.723	w	2.724	m	2.719	w	2.720	w	2.721	vw
	2.684	w	2.694	w	2,689	w	2.691	vw	2.686	vw
	2.422	w	2.419	vw	2.428	vw	2.427	vw	2.420	vw
	1.925	m	1.926	s	1.921	s	1.924	m	1.923	m
	1.913	s	1.915	s	1.911	m	1.912	m	1.910	m
	1.638	m	1.640	m	1.636	m	1.638	m	1.640	m
	1.619	w	1.626	w	1.623	w	1.624	w	1.626	w
	1.563	w	1.556	vw	1.559	vw	1.561	vw	1.560	vw

ACKNOWLEDGEMENTS

The author is indebted to his supervisor, Dr.A.R.Burkin for his extraordinary kindness, constant supervision and timely advice, throughout the course of the present work.

Dr.Jim Williamson and Mr.Fred Huggins devoted a lot of their time helping with the X-ray diffraction work. The author is grateful to them.

The model on page 143 was constructed with the assistance of Mr.J.W.P.Gunawardene, B.Sc.(Eng) whose contribution the author greatly appreciates.

So many of the members of the technical staff of the Metallurgy Department were helpful that it is difficult to mention the names individually. The author thanks them all.

Thanks are also due to F.J. for typing the thesis efficiently and fast, and to Sarath for helping with the diagrams.

Finally a word of thanks to Sudath and Nimal for making the life in a distant land less painful.

H.B.Maliyasena
Royal School of Mines
August, 1975

REFERENCES.

1. Sullivan, J.D. Chemistry of Leaching Covellite.
Washington D.C., U.S. Bureau of Mines TP487, 1930

2. Thomas, G. and Ingraham, T.K., Kinetics of Dissolution of Synthetic Covellite in Aqueous Acidic Ferric Sulphate solutions.
Can. Metall. Q., Vol. 6 1967 pp 153-165

3. Dutrizac, J.E. and MacDonald, R.J.C. Ferric Ion as a Leaching Medium.
Min. Sc. Eng. Vol. 6 Nr. 2 1974 pp 59-100

4. King, J.A. Solid State Changes In the Leaching of Copper Sulphides.
Ph.D. Thesis, University of London, 1966.

5. Lowe, D.F. The Kinetics of the Dissolution Reaction of Copper and Copper-Iron Sulphide Minerals Using Ferric Sulphate Solutions.
Ph.D. Thesis, Univ. of Arizona, 1970. (In Ref. 3)

6. Mulak, W. Kinetics of Dissolving Polydispersed Covellite in Acidic Solutions of Ferric Sulphate.
Roczn. Chem. Vol. 45, 1971. pp 1417-1424.
(In ref. 3)

7. Dutrizac, J.E. and MacDonald R.J.C. Kinetics of Dissolution of Covellite in Acidic Ferric Sulphate Solutions.
Can. Metall. Q. Vol. 13 Nr. 3, 1974.pp 423-433

8. Veltman, H., Pellegrini, S. and Mackiw, V.N. J. Metals.
Vol. 19 Nr.2. 1967 pp 21-25.

9. Kakovskii, I.A. and Potashnikov, Yu. M.
Izv. Akad. Nauk, SSSR. Otd. Tekhn,Met.i
Toplivo, No.3, 1962. (from ref.25)

10. Warren, I.A. Aus. J. App. Sc., Vol. 9 (1958)

11. Peters, E. and Loewen, F. Pressure Leaching of Copper
Minerals in Perchloric Acid Solutions.
Met. Trans. Vol. 4 1973 pp 5-11

12. Sullivan, J.D. Chemical and Physical Features of Copper
Leaching. Trans America Inst. Min. Metall.,
Vol. 106 , 1933 pp 515-546

13. Sullivan, J.D. Chemistry of Leaching Chalcocite.
Washington D.C.,U.S. Bureau of Mines, TP-473 (1930)

14. Colombo, A.F. and Frommer, D.W. Leaching Michigan Copper
Ore and Mill Tailings With Acidified Ferric
Sulphate.
Washington D.C., U.S. Bureau of Mines,RI-5924(1962)

15.Tkachenko, O.B. and Tseft, A.L. Kinetics of the Dissolution
of Chalcocite in Ferric Chloride.
Trudy Inst. Metall. Obogaschch, Alma Ata,
Vol. 30 1969 pp 15-23

16. Kopylov, G.A. and Orlov, A.I. Rates of Bornite and
Chalcocite Dissolution in Ferric Sulphate.
Jr. Irkutch. Politckh. Inst. Vol. 46 1969.
pp 127-132

17. Mulak, W. Kinetics of Copper Sulphide Dissolution in
Acidic Solutions of Ferric Sulphate.
Roczn. Chem., Vol. 43. 1969 pp 1387-1394.(In ref.3)

18. Thomas,G., Ingraham,T.R. and MacDonald,R.J.C.
Kinetics of Dissolution of Synthetic Digenite and Chalcocite in Aqueous Acidic Ferric Sulphate Solutions.
Can. Metall. Q.,Vol.6 1967 pp281-291

19.Fisher,W.W. and Roman,R.J.
New.Mex. Inst. of Min. and Tech.,Circular 112(1971)

20. Wadsworth, M.E. Advanves in the Leaching of Sulphide Minerals. Miner. Scic. Eng. Vol.4 No.4 1972, 36-47

21. Subramanium, K.N. and Jennings, P.H. Review of the Hydrometallurgy of Chalcopyrite Concentrate. Can. Metall. Q. Vol.11, 1972 pp387-400

22. Dasher,J. Can. Min. Metall.(CIM) Bull., Vol.66 No.48 1973 p733

23.Roman,R.J. and Benner,B.R.
Miner. Scic. Eng. Vol.5 No.1 1973 pp3-24

24. Corrans, I.J., Harris,B and Ralph,B.J.
Jour. S. African Inst. Min. Met., Vol.72 No.8. 1973 pp221-30

25. Ugarte, G. in "The Future of Copper Pyrometallurgy" (Editor Carlos Diaz) Chilean Institute of Mining and Metallurgy 1973

26. Scheridan, M.J. Leaching of Sulphide Minerals Containing Copper and silver.
Ph.D Thesis University of London 1975

27. Brown, S.L. and Sullivan, J.D. Dissolution of Various Copper Minerals. Washington, D.C., U.S. bureau of Mines RI-3228, 1934

28. Klets, V.E. and Liopo ,Behaviour of Chalcopyrite in Salt Leaching. Trudy-Irkustk. Politech. Inst., Vol.27, 1966 pp123-30

29. Ermilov, V.V., Tkachenko, O.B. and Tseft,A.L. Kinetics of Leaching of Chalcopyrite in Ferric Chloride. Trudy. Inst. Metall., Obogashch., Alma Alta, Vol.30 1969 pp3-14

30. Ichikuni, M. The Dissolution of Sulphide Minerals in Various Media.(III) Factors intervening in the dissolution of synthetic chalcopyrite (Fr) Bull. Chem.Soc. Japan Vol. 33 1960 pp1159-62

31. Dutrizac,J.E., MacDonald, R.J.C. and Ingraham, T.R. The Kinetics of Dissolution of Synthetic Chalcopyrite in Aqueous Acidic Ferric Sulphate Solutions. Trans. Metall. Soc. AIME, Vol.245,1969 pp955-959

32. Haver, F.P. and Wong,M.M. Recovery of Copper,Iron and Sulphur from Chalcopyrite Concentrate using a Ferric Chloride Leach J. Metals. N.Y., Vol.23 No2, 1971 pp25-29

33. Baur,J.P,, Gibbs,H.L, and Wadsworth,M.E. Initial stage Leaching (H_2SO_4) Kinetics of Chalcopyrite using Radiochemical Techniques. U.S.Bureau of Mines. RI-7823 (1974)

34. Ferreira,R.C.H. Leaching of Chalcopyrite Ph.D Thesis, University of London(1972)

36. Stanczyk,M.H. and Rampacek,C
U.S.Bureau of Mines RI-6193 (1963)

37. Yu,P.H., Hansen, C.K and Wadsworth,M.E.
Inter. Symp. on Hydrometallurgy. Chicago 1973

38. Jackson,K.J and Strickland, J.D.H. Dissolution of Sulphide Ores in Acid Chlorine Solutions
Trans. AIMME. Vol.212, 1958 pp373-379

39. Groves,R.D and Smith, P.B. Reactions of Copper Sulphide Minerals with Chlorine in an Aqueous System. U.S.Bureau of Mines RI-7801 (1973)

40. Sullivan, J.D. Chemistry of leaching Bornite
Washington D.C. U.S.Bureau of Mines TP-486(1931)

41. Uchida,T.et al . Leaching of Copper from Copper Bearing Ores with a Dilute Solution of Sulphuric Acid and Ferric Sulphate. Hakko. Kyokaishi.
Vol.25, 1967 pp168-172 (from ref.3)

42. Kopylov,G.A. and Orlov,A.I. Kinetics of Dissolution of Bornite. Izv. Vyssk. Ucheb. Zaved.,Tsvet. Metall., Vol.6,1963 pp68-74 (from ref.3)

43. Dutrizac,J.E., MacDonald,R.J.C.and Ingraham,T.R.
The Kinetics of Dissolution of Bornite in Acidified Ferric Sulphate Solutions
Metall.Trans. Vol. 1, 1970 pp225-231

44. Cabri,L.J. New Data on Phase Relations in the Cu-Fe-S System. Econ.Geol., Vol.68,No.4,1973 pp443-54

45. Ugarte,G. The Leaching of Bornite
Ph.D Thesis University of London, 1971

46. Dutrizac,J.E. et al. Effect of Pyrite, Chalcopyrite and Digenite on the Rate of Bornite Dissolution in Acidic Ferric Sulphate Solutions. Can. Metall. Q. Vol.10, 1971 pp3-7

47. Secco, E.A. Diffusion and Exchange of Zn in ZnS J. Chem. Phys. Vol.29,1958 p406

48. Wagner, C.In 'Atom Movements' American Society for Metals. 1951

49. Symposium Publication." Diffusion " American Society for metals. 1972

50. Richardson,F.D. Physical Chemistry of Melts in Metallurgy.Vol.1 Academic Press 1974

51. Meussner, R.A. and Birchnell, C.E. Corrosion Vol.13,1957 677t

52.Mrowec, S. Rocz. Chem. Vol.42 No,11,1968 pp1913-23 From Chemical Abstracts Vol.70, 99833d.

53. Turkdogan, E.T. Trans.Met. Soc. AIME Vol.242 No.8 1968 pp1665-72

54. Lambertin, M et al. C.R.Acad. Scic. Ser. C. Vol.273 No.3, 1971 pp267-70 From Chemical Abstracts Vol.74, 78870f

55. Pokrovskii, et al. Dokl. akad. nauk. Belorussk SSR. Vol.5,1961 pp499-502 From Chemical Abstracts Vol.57, 8300b.

56. Pavlyuchenko,I.I et al. Vesti.Akad. Nauk.Belorussk SSR. Ser.Khim. Nauk. Vol.4,1965 pp115-117 From Chemical Abstracts Vol.65, 430h

57. Pavlyuchenko, I.I. et al. Dokl. Akad. Nauk. Belorussk SSR Vol.9,No.4, 1967 pp235-237
From Chemical Abstracts Vol. 63,5328h

58. Ibid. Vestsi. Akad. Nauk. Belorussk SSR, Ser. Khim. Nauk. Vol.No.3, 1967 pp35-41
From Chemical Abstracts Vol.69, 7902d

59. Weiss,K. Ber. Bunsenges. Phy. Chem. Vol.73,No4,1969 p338

60. Bartkiewicz,I. et al. Zess. Nauk. Akad.Gorn-Hutn. Krakowie Ceram. Vol.14,1969 pp19-34

61. Sreedhar,A.K. and Sharma, B.L. Radiation Effects Vol.4,(1-2) 1970 pp103-106

62. Kato, Tokio and Oki,Takeo. Nippon Kinzoku Gakkaishi Vol.37 No.6,1973 pp652-658
From Chemical Abstracts Vol.79,60754q

63. Gurvich,A.M. and Shamanov,A.A. Zh. Prikl. Spektrosk. Vol.18 No.3,1973 pp463-468
From Chemical Abstracts Vol.78, 153402t

64. Redington,R.W. Phys. Rev. Vol.87, 1952 pp1066-74

65. Gruner, J.W. and Lin, S.C. Solution of Tin Minerals Studied. Engineering and Mining Journal-Press Vol.121 No.23, 1929 p924

66. Gerlach, J.,Pawler,F. et al. The Influence of the Lattice Structure of Metallic Compounds on Their Leaching Property.
Erzmetall. Bd25 No.9, 1972 pp448-453

67. Spencer, L.I. Crystalline Stannite from Bolivia. Mineral. Mag. Vol.13. 1901 pp54-65

68. Gross,R and Gross, N. Neues. Jahrb. Mineral. Geolo. Beilage. Bd. 48, 1923 pp113-135

69. Brockway. L.O. The Crystal Structure of Stannite. Z. Krist. Vol.89, 1934 pp434-441

69A. Pauling, L. The Nature of the Chemical Bond 3rd Edition, 1960. Cornell UP

70. Ernst-Dieter Franz, Kubicher Zinkies und Tetragonaler Zinkies mit Kuferkies Struktur. Neues.Jahrb.Miner.Monatsh. No5,1971 pp218-223

71. Springer, G. The Pseudobinary System Cu_2FeSnS_4-Cu_2ZnSnS_4 and its Mineralogical Significance. Canadian Mineralogist Vol.11,1972 pp535-41

72. Bernhardt,H.J. Unterschungen in Pseudobinaren Stannin-Kupferkies. N.Jahrb. Miner. H12,1972 pp553-6

73. Lee ,J. Experimental Investigations on Sphalerite-Stannite Solid Solution Series. ibid. pp556-9

74. Bente, K. Unterschungen im Pseudobinaren System Stannin-Briartit.(Cu_2FeGeS_4) ibid. H1, 1974 pp8-13

75. Smith, D.Z. and Zuckermann,J.J. ^{119}Sn Mossbauer Spectra of Tin Minerals. J.Inorg. & Neucl. Chem. Vol. 29 No5,1967 pp1203-10

76. Eibschutz, M., Hermon,E and Shtrikman, S. Determination of Cation Valencies in $Cu_2{}^{57}Fe^{119}SnS_4$ by Mossbauer Effect and Magnetic Susceptibility Measurements. J. Phys. Chem. Solids. Vol.28, 1967 pp1633-36

77. Greenwood,N.N. and Gibb,J.C. Mossbauer Spectroscopy Chapman & Hall 1971

78. Hill,H.A.O. and Day, P.
Physical Methods in Advanced Inorganic Chemistry
Interscience Publishers 1968

79. Greenwood,N.N. and Whitfield,H.J.
Mossbauer Effect Studies on Cubanite and
Related Iron Sulphides.
J. Chem. Soc. A Vol.7,1968 pp1697-99

80. Marfunin, A.S. and Mkrtchyan,A.R.
Geochem. Intern., Vol.4,No.5,1967 p980

81. Marfunin, A.S. et al.,
Investigation of Iron Sulphides by Mossbauer
Spectroscopy. Izv. Akad. Nauk. SSSR Ser. Khim.,
No.6, 1968 pp1267-71

82. Marfunin, A.S. and Mkrtchyan,A.R.
Mossbauer Effect in ^{119}Sn Nuclei in Stannite
Geokhimiya No.4, 1968 pp498-500

83. Goncharov,G.N., Ostanevich, Yu.M.and Tomilov,S.B.
Investigation of Iron Sulphides with aid of
the Mossbauer Effect.
Inter. Geol. Rev. Vol.13, No.4, 1971 pp584-91

84. Vaughan,D.J. and Burns, R.G.
Mossbauer Spectroscopy and Bonding in Sulphide
Minerals Containing Four Coordinated Iron.
24th International Geological Conference,1972
Section 14 pp 159-167

85. Ramdohr, P.
Zum Zinkiesproblem. Abh. Preuss. akad.
Wiss. Maths.Nat. KI - No.4, 1944

86. Ramdohr, P.

The Ore Minerals and Their Intergrowths.

Pergamon, 1969

87. Moh, G.H.

Experimentelle Unterschungen an Zinkiesen und Analogen Germanium Verbindungen

N. Jb.Miner., Abh. Vol.94, 1960 pp1125-46

88. Moh, G.H.and Ottemann,J,

Neue Unterschungen an Zinkiesen und Zinkies--verwandten.

N. Jb. Miner. Abh. Vol.99, 1962 pp1-28

89. Levy,C.

Contribution a la Mineralogie des Sulfures de Cuivre du Type Cu_3XS_4.

Memoir du B.R.G.M. No.54, 1967

90. Markham, N.L. and Lawrence, L.J.

Mawsonite, A New Copper-Iron-Tin-Sulphide from Mount Lyell, Tasmania and Tingha, New South Wales. Amer. Mineralogist, Vol.50,1967 pp900-908

91. Kato, A.

Stannoidite, $Cu_5(FeZn)SnS_8$, a New Stannite-like Mineral. Bull. Nat. Sci. Mus. Tokiyo

Vol 12 No.1, 1969 pp 165-172

92. Springer,G.

Electronprobe Analysis of Stannite and Related Tin Minerals. Mineral. Mag. Vol. 36 No. 284(1968) pp 1045-1051

93. Moh, G.

Carnegie Institution, Washington, Year Book Vol. 62, 1963

94. Nekrasov, I. Ya.

Doka. Akad. Nauk. SSSR(Miner), Vol.206(1),1972 pp 193-196,

95. Nitsche, R., Sargent,D.F. and Wild,P.

Journal of Crystal Growth. Vol.1, 1967 pp52-53

96. Jost,W.

Diffusion in Solids Liquids and Gases Academic Press (N.Y.) 1960

97. Klug,H.E. and Alexander, L.E.

X-Ray Diffraction Procedures. John Wiley, 1974

98. Beryy,L.G. and Thompson, R.M

X-Ray Powder Data for Ore Minerals (Peacock Atlas) Geol.Soc. Amer.Mem. 85, 1962

98. International Tables for X-Ray Crystallography Vol.1

Kynoch Press (Birmingham) 1952

100. Marcel Pourbaix

Atlas of Electrochemical Equilibria in Aqueous Solutions. Pergamon, 1966.

101. A.S.T.M. X-Ray Index Files

α-Fe_2O_3 13-534

β-FeOOH 13-157

SnO_2 5-467